N 69 20281
60 cys

BOEING

LUNAR ORBITER DOPPLER RESIDUAL STUDY

(D2-100817-1)

By Gayle D. Barrow

CASE FILE
COPY

SEATTLE, WASHINGTON

NASA CR-66737

LUNAR ORBITER DOPPLER RESIDUAL STUDY

(D2-100817-1)

By Gayle D. Barrow

Distribution of this report is provided in the interest of information exchange. Responsibility for the contents resides in the author or organization that prepared it.

Prepared under Contract No. NAS1-7954 by
THE BOEING COMPANY
Seattle, Wash.

for

NATIONAL AERONAUTICS AND SPACE ADMINISTRATION

THE BOEING COMPANY

CODE IDENT. NO. 81205

DOCUMENT NO. D2-100817-1

TITLE: LUNAR ORBITER DOPPLER RESIDUAL STUDY

FINAL REPORT

MODEL _____ CONTRACT NO. NAS 1-7954

ISSUE NO.	ISSUED TO

SEE DISTRIBUTION LIMITATIONS PAGE

PREPARED BY	Gayle D. Barrow Gayle D. Barrow	
SUPERVISED BY	W. R. Burr W. R. Burr	
APPROVED BY	L. B. Eldrenkamp L. B. Eldrenkamp	10-16-68
APPROVED BY	J. C. Graves J. C. Graves	10-16-68
APPROVED BY		

2-5145

U3 4287 9000 REV. 7/64

ACTIVE SHEET RECORD

SHEET NUMBER	REV LTR	ADDED SHEETS				SHEET NUMBER	REV LTR	ADDED SHEETS			
		SHEET NUMBER	REV LTR	SHEET NUMBER	REV LTR			SHEET NUMBER	REV LTR	SHEET NUMBER	REV LTR
i ii iii iv v vi vii 1 2 3 4 5 6 7 8 thru 88											

REVISIONS			
LTR	DESCRIPTION	DATE	APPROVAL

LIMITATIONS

DDC DOES NOT APPLY

This document is controlled by 2-5987

All revisions to this document shall be approved by the above noted organization prior to release.

PHOTO SITE ACCURACY ANALYSIS FINAL REPORT DOCUMENTS

TASK A - Photo Support Data

D2-100814-1 - Lunar Orbiter Photo Site Accuracy Analysis - Final Report - Photo Site Analysis

D2-100814-2 - Lunar Orbiter Photo Site Accuracy Analysis - Final Report - Supporting Data

D2-100814-3 - Lunar Orbiter Photo Site Accuracy Analysis - Final Report - Error Analysis

D2-100815-1 - Lunar Orbiter Improved Photo Supporting Data - Final Report - Lunar Orbiter I

D2-100815-2 - Lunar Orbiter Improved Photo Support Data - Final Report - Lunar Orbiter II

D2-100815-3 - Lunar Orbiter Improved Photo Supporting Data - Final Report - Lunar Orbiter III

D2-100815-4 - Lunar Orbiter Improved Photo Supporting Data - Final Report - Lunar Orbiter IV

D2-100815-5 - Lunar Orbiter Improved Photo Supporting Data - Final Report - Lunar Orbiter V

D2-100816-1 - Lunar Orbiter Simple Moon Residuals - Final Report

TASK B - Residual Feedback Study

D2-100818-1 - Application of Residual Feedback to Lunar Orbiter Residual Analysis - Final Report

TASK C - Tracking Data Residuals

D2-100817-1 - Lunar Orbiter Doppler Residual Study - Final Report

USE FOR TYPEWRITTEN MATERIAL ONLY

ABSTRACT AND KEY WORDS LIST

During all Lunar Orbiter missions, significant differences were noticed between the observed and predicted doppler tracking data, especially at the periapsis of the orbit. Various areas including the data acquisition system, computer program operation and physical models have been investigated as possible causes. It is the purpose of this report to document the results of this study.

KEY WORDS

Lunar Orbiter

Residuals

Doppler

USE FOR TYPEWRITTEN MATERIAL ONLY

TABLE OF CONTENTS

USE FOR TYPEWRITTEN MATERIAL ONLY

U3 4802 1434 REV. 8-65

1.0 SCOPE

The investigation concerned with the determination of the cause of Lunar Orbiter doppler residuals was begun under NASA contract NAS1-3800, CCN 157B and was completed under contract NAS1-7954, Task C. This document is a final report covering all the work done on this study from October 1967 through study completion.

USE FOR TYPEWRITTEN MATERIAL ONLY

U3 4802 1434 REV 8-65

2.0 INTRODUCTION

The perilune residual problem first became obvious when the Lunar Orbiter I spacecraft was maneuvered into orbit. As the perilune region of the orbit became visible to the earth-based tracking stations large doppler residuals were found to be present. A doppler residual is simply the difference between the doppler observed by the tracking stations and the doppler computed by the Orbit Determination Program (ODP). To generate a predicted spacecraft ephemeris the ODP uses a trajectory program containing a specified model intended to describe all significant forces acting on the vehicle including a spherical harmonic expansion of the lunar gravitational field.

During the translunar portion of the Lunar Orbiter mission the doppler residuals approached the noise level of the data as shown in Figure 2.1. After the spacecraft achieved lunar orbit the residuals increased by one or two orders of magnitude. The phenomenon is illustrated in Figure 2.2 for the Lunar Orbiter IV mission. The perilune altitude in this case was approximately 2700 km which accounts for the relatively small residuals.

The relationship of residual magnitude to perilune altitude is shown in Figure 2.3. All points are data from Lunar Orbiter missions which include various orbital inclinations, apolune altitudes and tracking station-orbit viewing geometries. The indication that residual magnitude is a function of the inverse square of the perilune altitude is obvious from comparison with the two inverse square curves provided. This phenomenon indicates that perturbation accelerations from lunar surface features could be the cause of the perilune residual problem.

The amount of data included in the arc seriously affects the shape of the perilune residuals. Results of including and deleting data surrounding perilune is shown in Figure 2.4 where the second orbit of a three orbit arc is plotted. A significant difference in the magnitude of the residuals is apparent in the region of perilune. During the first Lunar Orbiter mission doppler data surrounding perilune was deleted from the data arc since the most distinct residual perturbations occurred in that region. The resulting state vector determinations were used for photography prediction. Most photography was accomplished at perilune and it has since been determined that the method was of questionable value since the larger doppler residuals indicate a larger deviation from the predicted trajectory. A more accurate prediction of photo locations will be obtained if all data is included in the OD data arc.

The relative orbit plane-tracking station geometry had a significant effect on the magnitude of the perilune residuals. Figure 2.5 indicates the increase in residual magnitude as the orbit plane rotates edgewise to the line of sight from the tracking stations. Also there is a slight increase in the frequence of the residual function as the orbit changes relative position to the earth. Since information in the doppler data is only available in the line-of-sight direction it is necessary that the residual amplitude exhibit this

USE FOR TYPEWRITTEN MATERIAL ONLY.

tendency if surface features are the major cause of the perilune residual problem. Any significant unmodeled acceleration causing a trajectory perturbation would be more easily detected when the perturbation is in the radial direction from the tracking station.

This document reports the results of various studies performed to determine the cause of the Lunar Orbiter perilune residual phenomenon. The investigations included are:

1) Fourier analysis of Lunar Orbiter tracking data
2) Deep Space Network doppler tracking system
3) One way doppler tracking
4) Lunar atmosphere
5) Surface terrain

USE FOR TYPEWRITTEN MATERIAL ONLY

U3 4802 1434 REV. 8-65

LUNAR ORBITER DOPPLER RESIDUALS

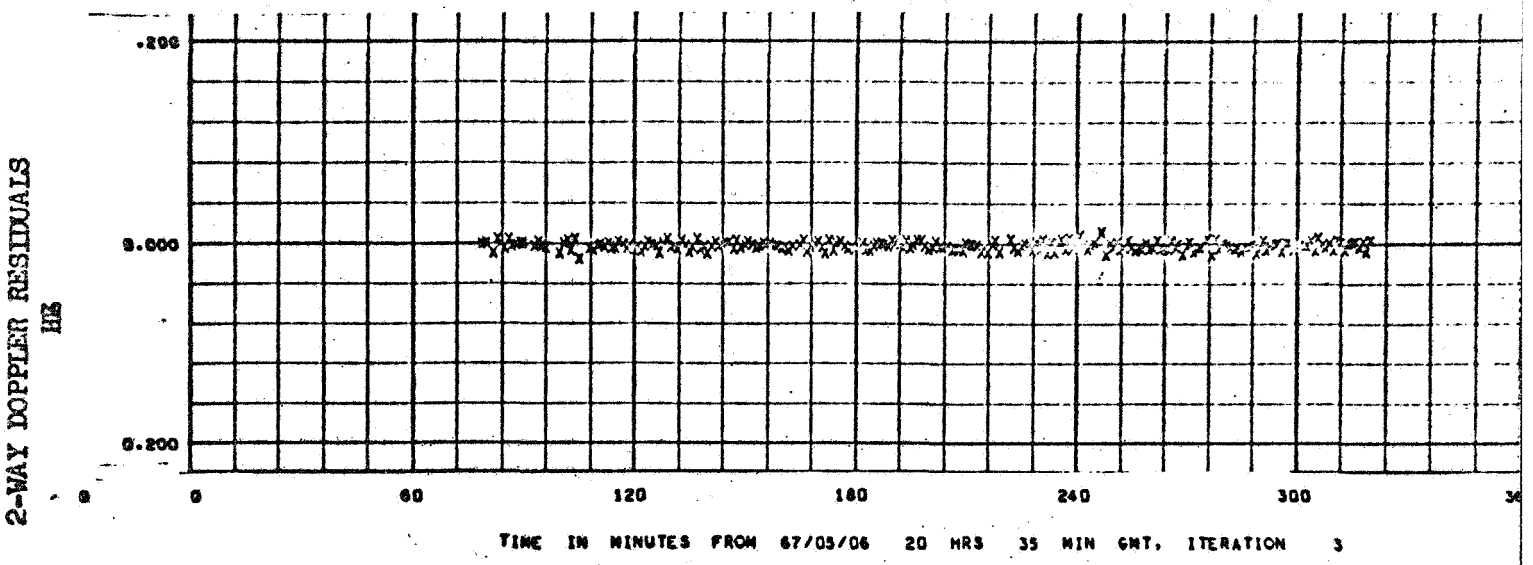

Figure 2.1

TRANSLUNAR PHASE, LO IV MISSION

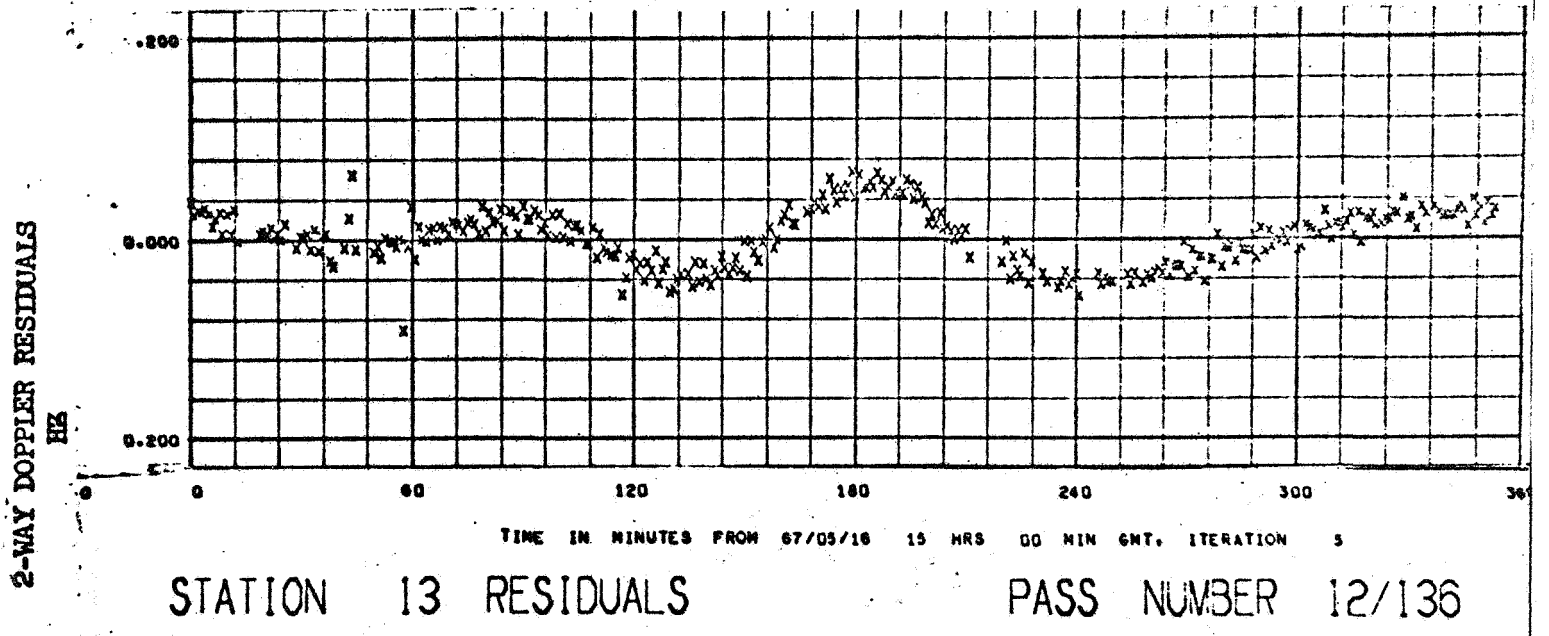

Figure 2.2

LUNAR ORBIT PHASE, LO IV MISSION

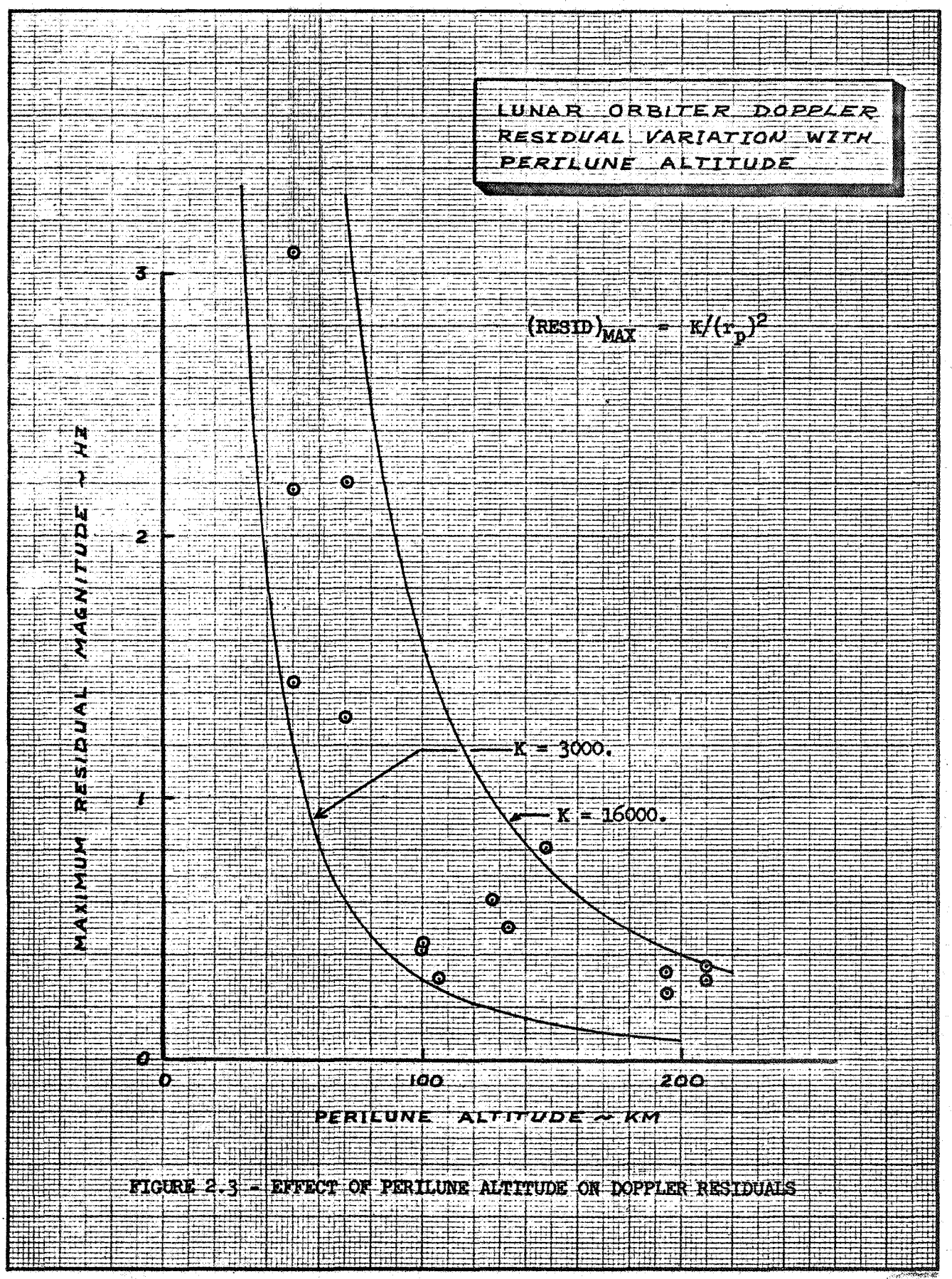

FIGURE 2.3 - EFFECT OF PERILUNE ALTITUDE ON DOPPLER RESIDUALS

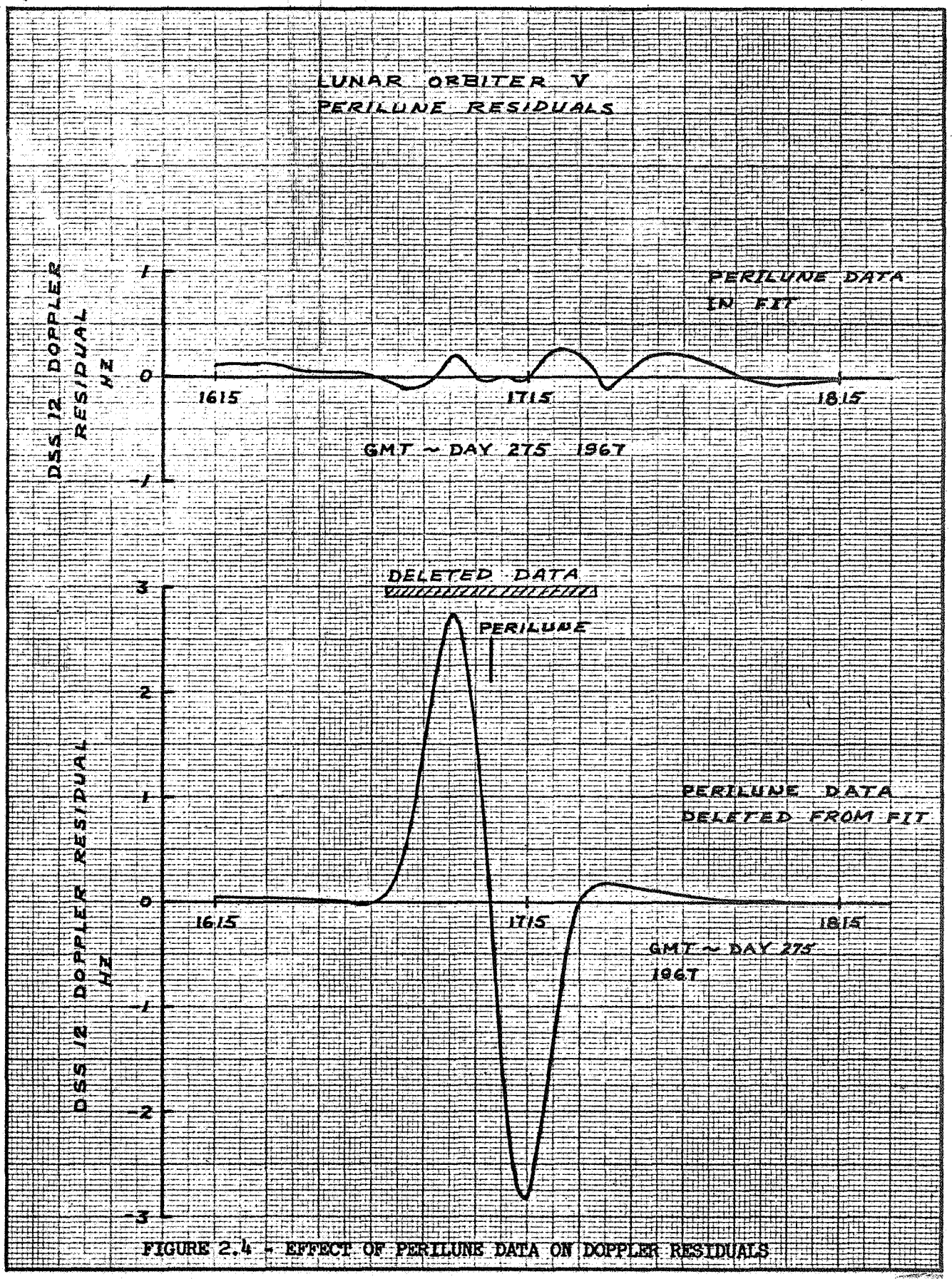

FIGURE 2.4 - EFFECT OF PERILUNE DATA ON DOPPLER RESIDUALS

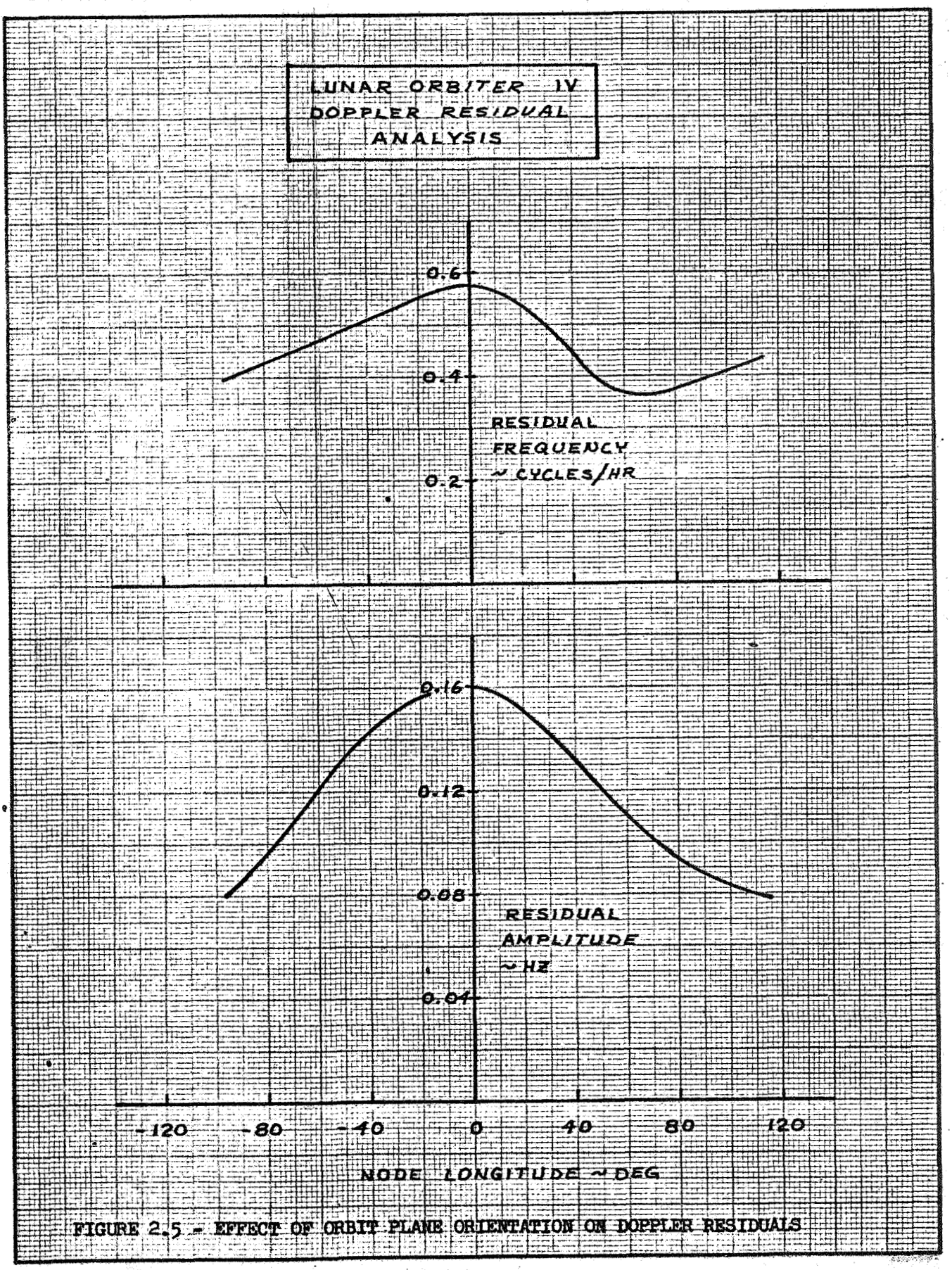

FIGURE 2.5 - EFFECT OF ORBIT PLANE ORIENTATION ON DOPPLER RESIDUALS

3.0 SUMMARY

The results of this study indicate a very distinct correlation between the doppler residual patterns (of orbit determination data arcs involving single orbits) and the ground track of the spacecraft. In some cases the residuals can be directly related to terrain changes on the lunar surface but this was not true in all instances (Reference 11).

An investigation of the simulated and actual doppler tracking data using Fourier transform methods shows a distinct difference between the signatures of the simulated and actual data but no dominant coefficients exist in any frequency range which could consistently account for the residuals.

One way doppler tracking data exhibits similar residual patterns to that of two and three way doppler data verifying that no problem exists in the uplink electronic systems. A thorough study of the complete spacecraft-DSN (Deep Space Net) data acquisition system has led to the conclusion that it in no way could cause the residual phenomenon.

The direct measurement of the orbital period of a Lunar Orbiter spacecraft indicates that the existance of a significant lunar atmosphere above the altitude of 100 km is very unlikely.

It is obvious from this study that there is a serious need for more analysis on the lunar gravitational model. The magnitude of the doppler residuals encountered during this study indicate the deficiency in the currently available lunar models.

USE FOR TYPEWRITTEN MATERIAL ONLY

U3 4802 1434 REV. 8-65

4.0 FOURIER ANALYSIS OF LUNAR ORBITER TRACKING DATA

4.1 INTRODUCTION

This study is specifically concerned with an attempt to determine whether the systematic effect observed in the doppler residuals during the lunar orbit are present in the observed or the predicted doppler shift. This question is significant because :

1) The only symptom of this perilune phenomenon has been from the doppler residual histories, produced by forming:

   Residuals = Observed Doppler - Predicted Doppler

2) It is not clear whether the phenomenon (or phenomena) causing these large perilune residuals are present in the observed data or are induced by the simulation which calculates the predicted doppler.

3) Present selenodetic research is proceeding on the basis that this perilune residual phenomenon is present in the observed doppler and is an exhibition of irregularities in the lunar gravitational field.

The problem posed for study was: is it possible to observe a systematic phenomenon in either the observed or predicted doppler data which could cause the large doppler residuals at perilune?

The problem may be more precisely formulated in the following way:

Let: $R(t)$ = the residual function
$f(t)$ = observed doppler observations
$g(t)$ = predicted doppler observations

then: $R(t) = f(t) - g(t)$

Thus the above question may also be written as: it is possible to detect a systematic phenomenon in either $f(t)$ or $g(t)$ that correlates with the behavior of the residual function $R(t)$ near perilune?

4.2 METHOD OF ATTACK

The basic method of attack chosen was:

1) Assume that the phenomenon causing the perilune residuals is confined entirely to either the observed or predicted data.

USE FOR TYPEWRITTEN MATERIAL ONLY

That is, let:

$$f(t) = h(t) + \psi(t)$$
$$g(t) = h(t) + \phi(t)$$

where:

$h(t)$ = function common to both the observed and predicted doppler observations
$\psi(t)$ = function unique to observed observations
$\phi(t)$ = function unique to predicted observations
$\psi(t) \neq \phi(t)$

therefore:

$$R(t) = \left[h(t) + \psi(t)\right] - \left[h(t) + \phi(t)\right]$$

The assumption is that either $\psi(t) = 0$ or $\phi(t) = 0$.

2) Assume that the Fourier transform of the residual function R(t) would produce a uniformly converging set of coefficients except for a dominant spike over a narrow band of frequencies corresponding to the residual phenomenon.

3) Examine the Fourier coefficients of f(t) and g(t) to determine if a single coefficient or narrow band of coefficients dominates in one set of data and not in the other.

In order to execute the above approach the following specific tasks were performed:

1) One specific Lunar Orbiter (L/O) tracking pass was selected for intensive study.

2) The observed two way doppler shift obtained during this pass was obtained and this data simulated with the L/O real time orbit determination program (ODPL).

3) An existing Fourier analysis computer program was modified to calculate the Fourier coefficients of the Fourier series that fit the data.

4) This program was applied to the observed and simulated two way doppler shift data in the region of perilune.

5) The Fourier coefficients were plotted against their order and the results analyzed.

USE FOR TYPEWRITTEN MATERIAL ONLY

U3 4802 1434 REV. 8-65

4.3 ANALYSIS

4.3.1 Orbit Selected

The specific data selected for this study was a pass of two way coherent doppler data taken from the L/O IV extended mission phase, after the spacecraft had been transferred into a Mission V-like orbit. A specific description of this data is as follows:

ORBIT NUMBERS 98, 99, 100

DATA SPAN 6/16/67-1901 GMT to 6/16/67-2339 GMT

STATIONS 62, 12 (Madrid, Goldstone)

ORBITAL CHARACTERISTICS :

Epoch: 6/16/67 - 19^h 0^m 0^s GMT

Apolune Altitude = 3956.9 km

Perilune Altitude = 69.64 km

Inclination = 85.29 deg.

Nodal Longitude = 334.01 deg.

Argument of Periapsis = 355.99 deg.

Period = 343.63 min.

Time of Perilune Passage = 6/16/67 - 19^h 47^m 31.3^s GMT

This orbit configuration was selected primarily because the high apolune and low perilune altitudes gave almost no residuals at apolune and relatively large residuals at perilune. Also important was:

1) The spacecraft was tracked extensively during the time when both apolune and perilune were visible from the Earth and during a time when no spacecraft maneuvering occurred, other than limit cycling.

2) There were relatively few "blunder" points and/or missing points in the data stream.

3) The doppler resolver was on line during this period of time which substantially reduced the noise level of the time.

USE FOR TYPEWRITTEN MATERIAL ONLY

U3 4802 1434 REV. 8-65

4.3.2 Simulated Data

Two sets of simulated data were used in the study. All elements of the two simulations were common except that two different lunar gravitational models and solution vectors were used:

1) Spherical Moon and state vector solution only.

2) LRC 11/11 Moon Model and state vector plus eight gravitational harmonics.

Both sets of data were produced by fitting the 12 hours of 2-way doppler data described above. The Lunar Orbiter Real Time Orbit Determination Program, ODPL, was used to produce the simulated data. Figures 4.1 and 4.2 show the doppler residual plots that resulted from the spherical moon and LRC 11/11 harmonic moon simulations respectively.

A third set of simulated doppler data was also produced to allow subtraction of station motion and moon motion effects. This data was obtained by making all gravitational constants very small and using an initial state vector for the spacecraft that put it into a circular orbit of large period at 1 km from the moon's center. Subtraction of this simulated doppler data from the observed and simulated data thus results in radial velocity doppler shifts.

4.3.3 Fourier Analysis Computer Program

A Lunar Orbiter Fourier Analysis Program (LOFAP) was written to compute the Fourier coefficients of a set of discrete data. The program consists essentially of input-output coding written around an existing "fast" Fourier transform routine called CTFOUR. This subroutine is a Boeing version of an IBM routine and uses an algorithm due to James W. Cooley and John W. Tukey (Reference 1). The program requires 2^n data points, i.e.; 2, 4, 8, 16, 32, 64, etc. and a typical compilation and run time is 10 seconds. The following capabilities are built into the program:

1) Interpolation between data points.

2) Time shifting of data points by integer numbers of points.

3) Subtraction of a linear function of the end point values to make the data function continuous at the end points.

4) Subtraction of quadratic function of the end point derivatives to make the first derivative of the function continuous at the end points.

5) Reflection of the input data to make the resultant function even or odd.

(text continued on page 25)

USE FOR TYPEWRITTEN MATERIAL ONLY

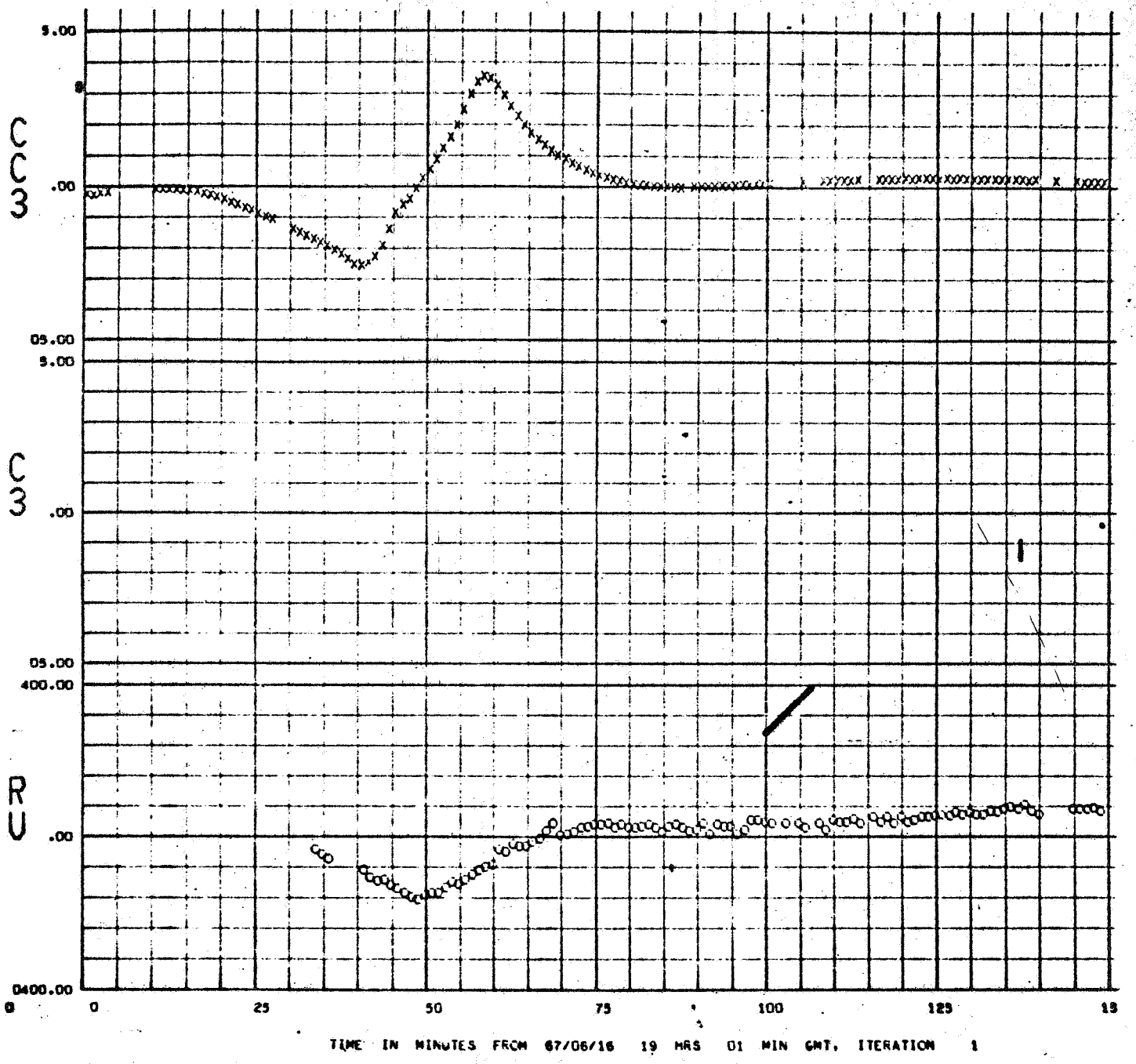
5.00
CC
3
.00
05.00
5.00
C
3
.00
05.00
400.00
R
U
.00
0400.00
0
25
50
75
100
125
15
TIME IN MINUTES FROM 67/06/16 19 HRS 01 MIN GMT, ITERATION 1
STATION 62 RESIDUALS L/O IV
PASS NUMBER NONE
SPHERICAL MOON

FIGURE 4.1

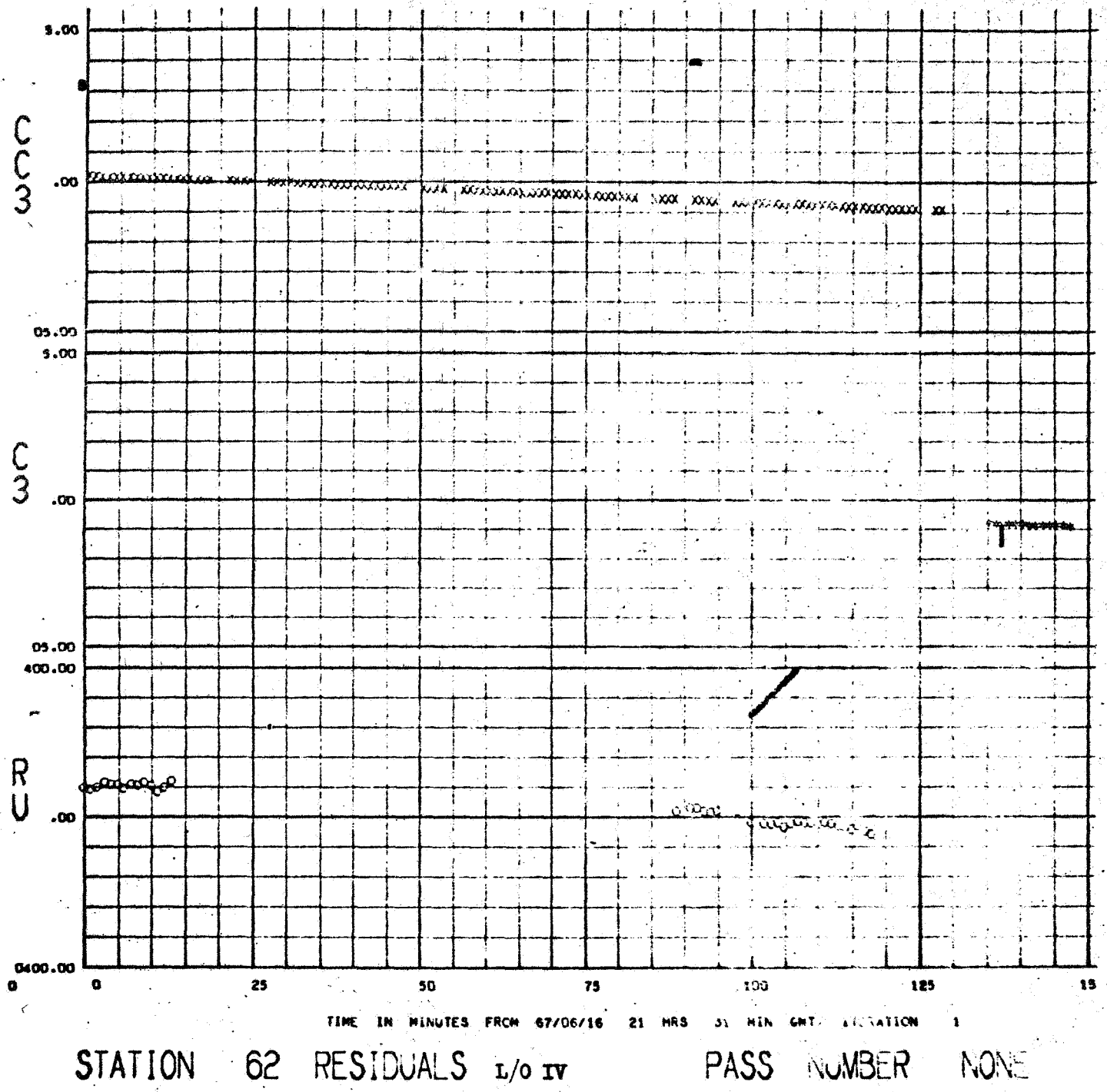

SPHERICAL MOON

FIGURE 4.1 (Continued)

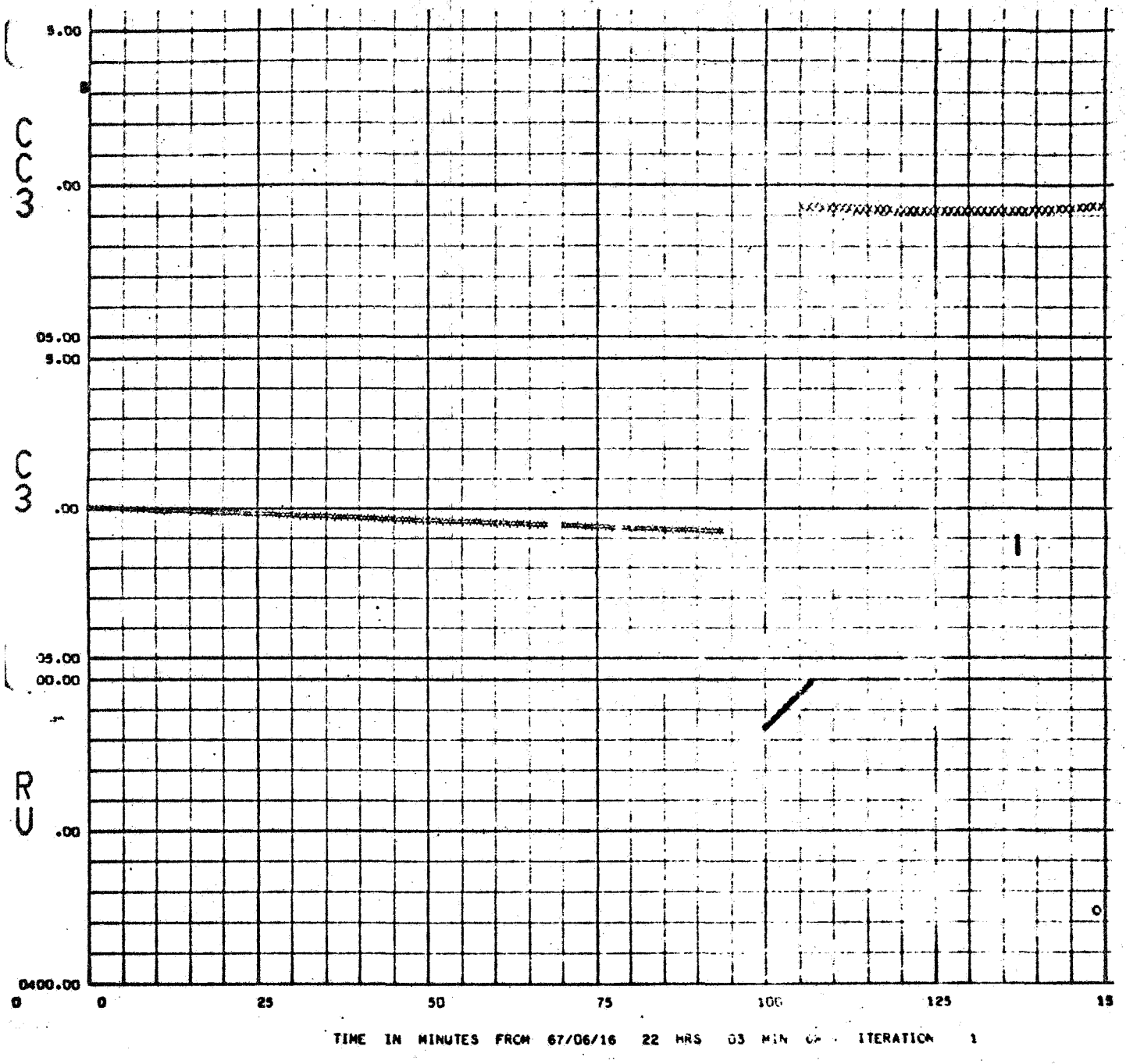

SPHERICAL MOON

FIGURE 4.1 (Continued)

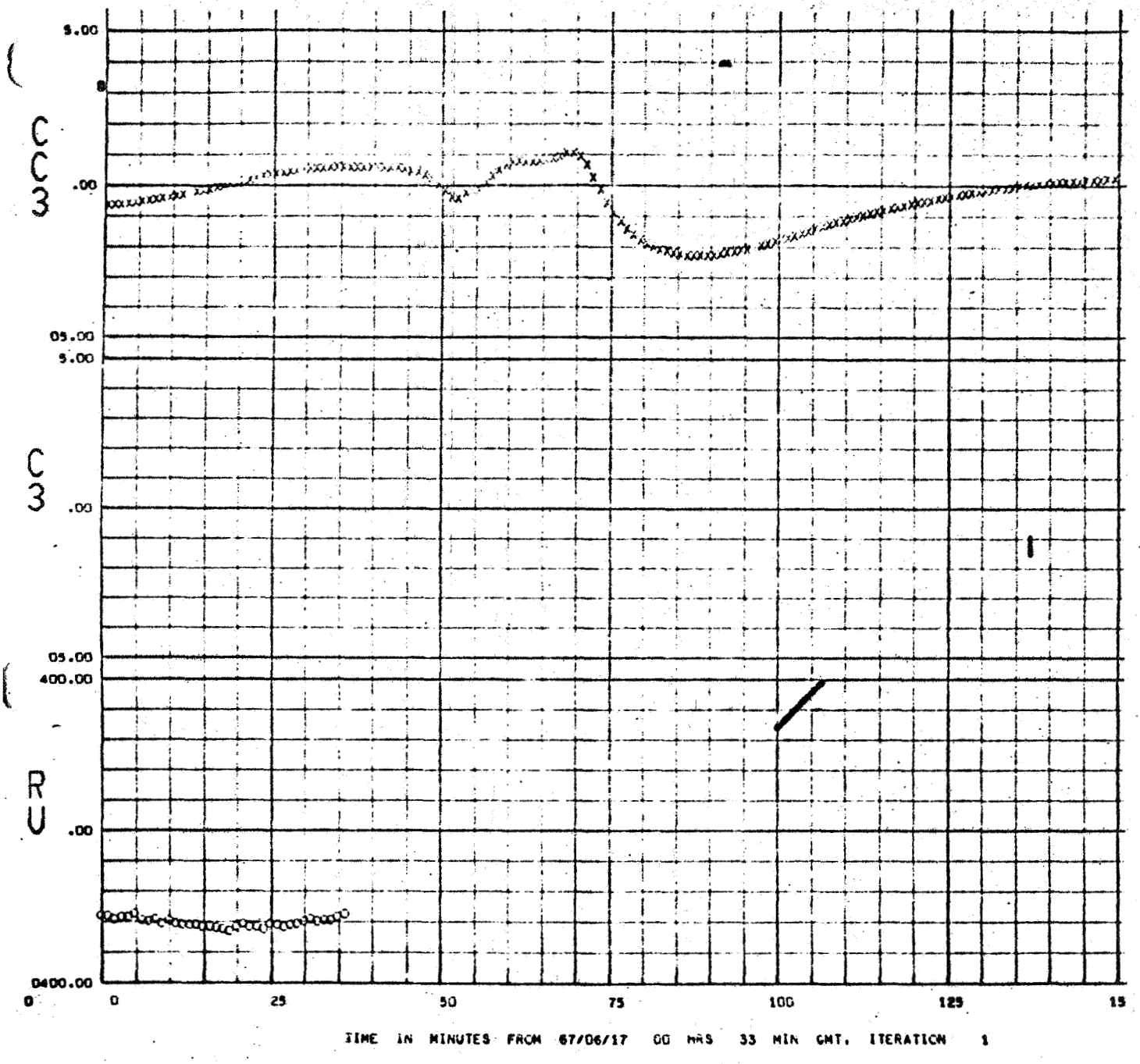

SPHERICAL MOON

FIGURE 4.1 (Continued)

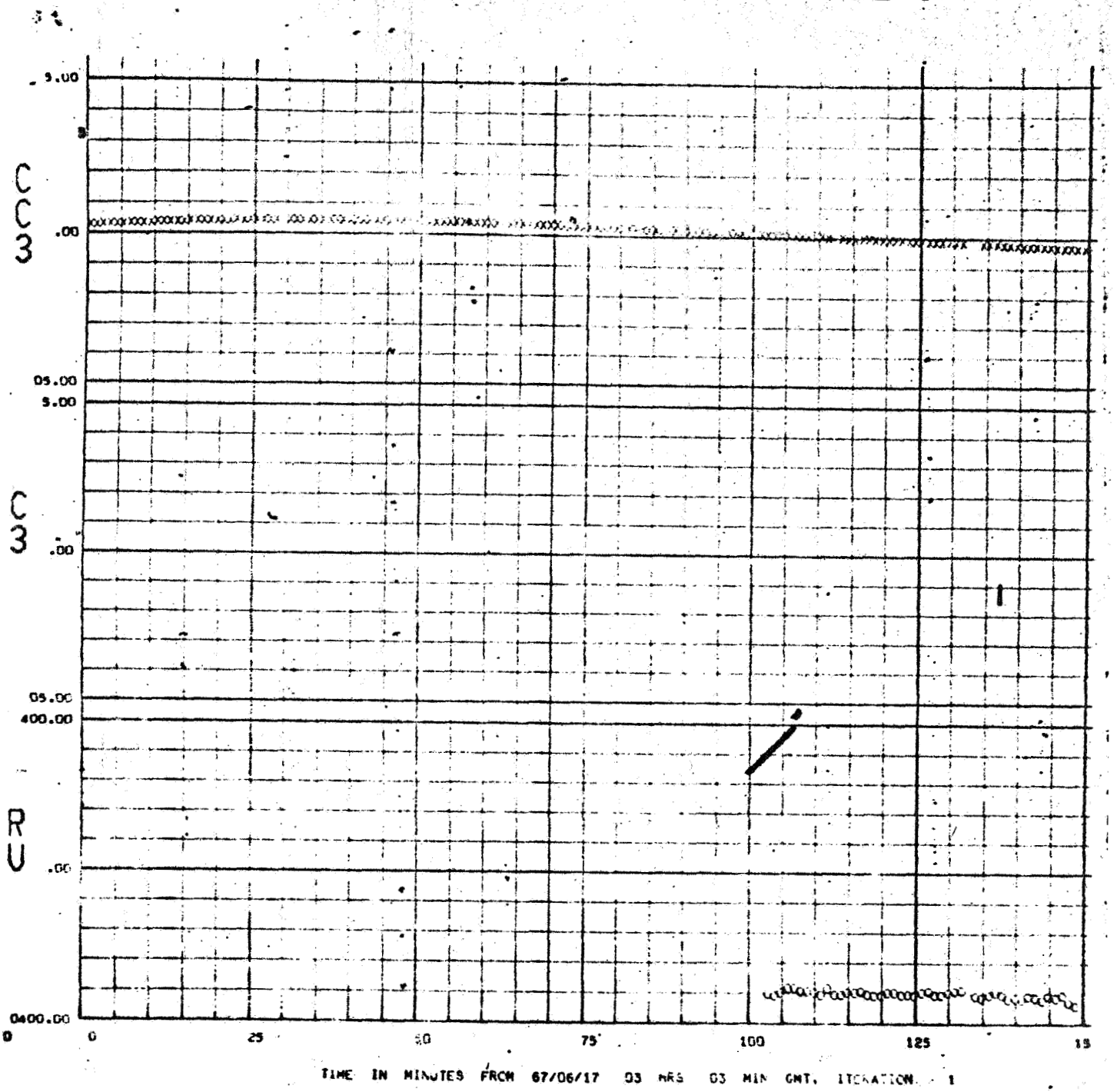

FIGURE 4.1 (Continued)

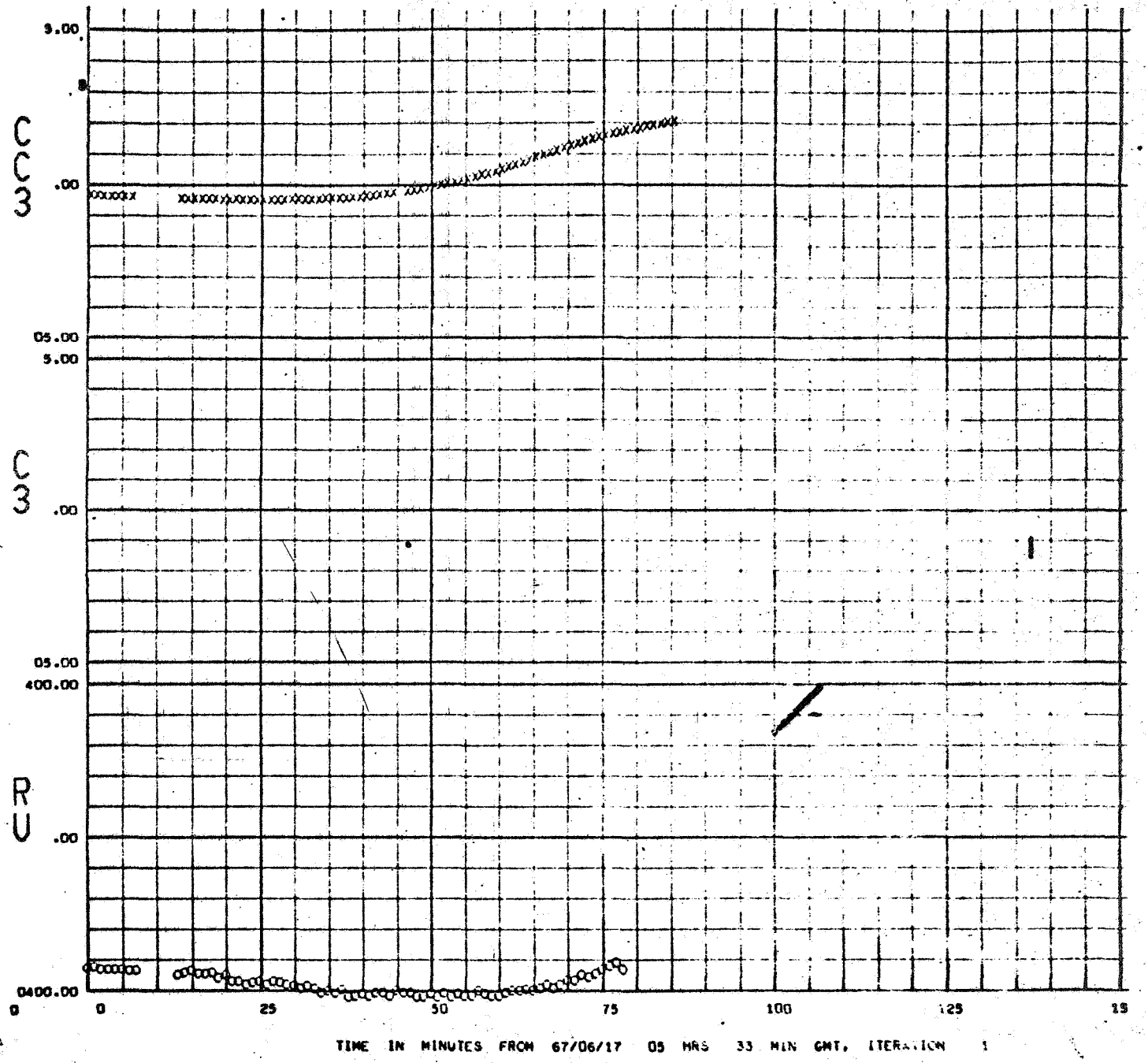

FIGURE 4.1 (Continued)

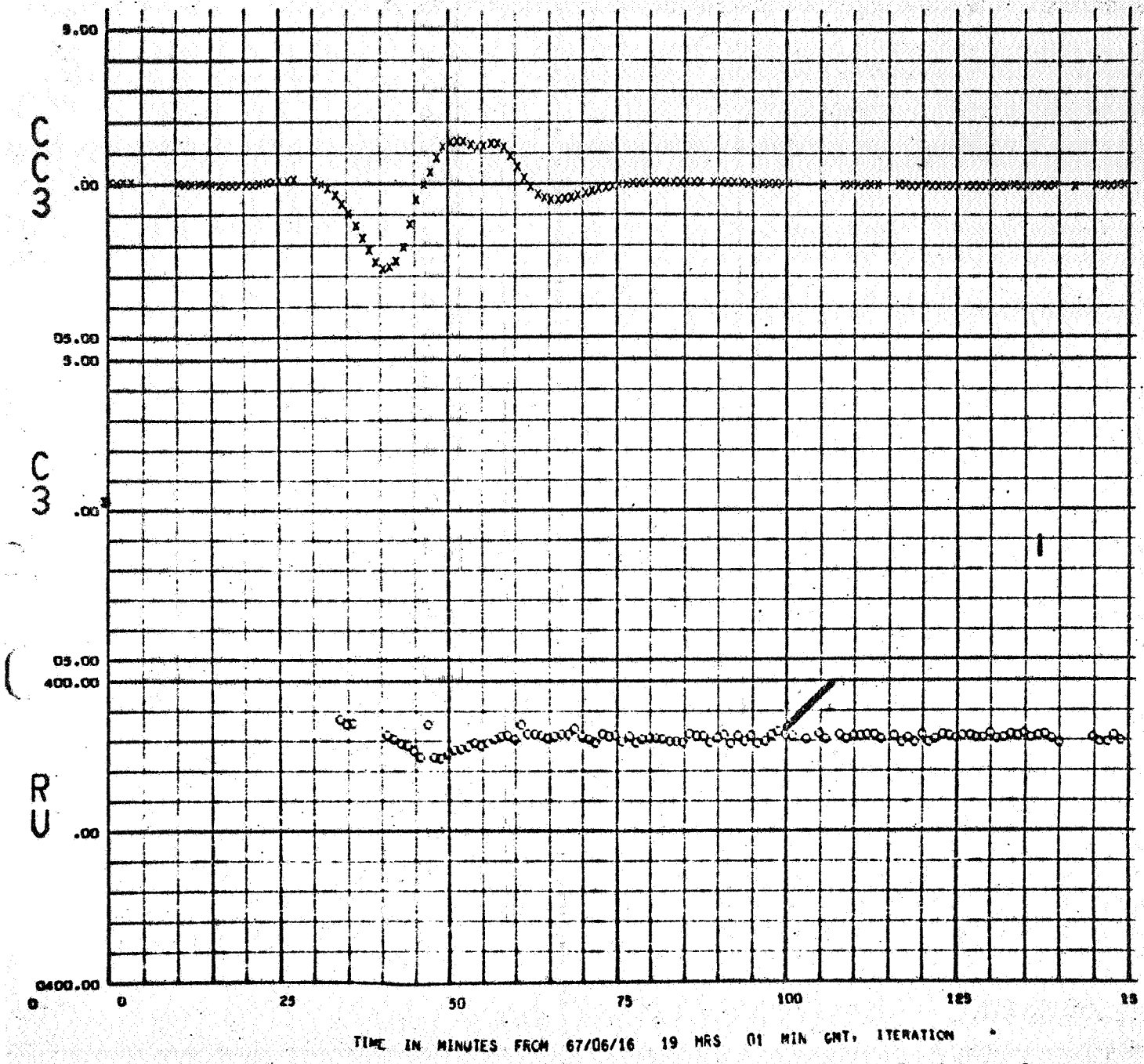
9.00
CC3
.00
05.00
3.00
C3
.00
05.00
400.00
RU
.00
0400.00
0
25
50
75
100
125
TIME IN MINUTES FROM 67/06/16 19 HRS 01 MIN GMT, ITERATION
STATION 62 RESIDUALS L/O IV
PASS NUMBER NONE
LRC 11/11 MODIFIED HARMONICS

FIGURE 4.2

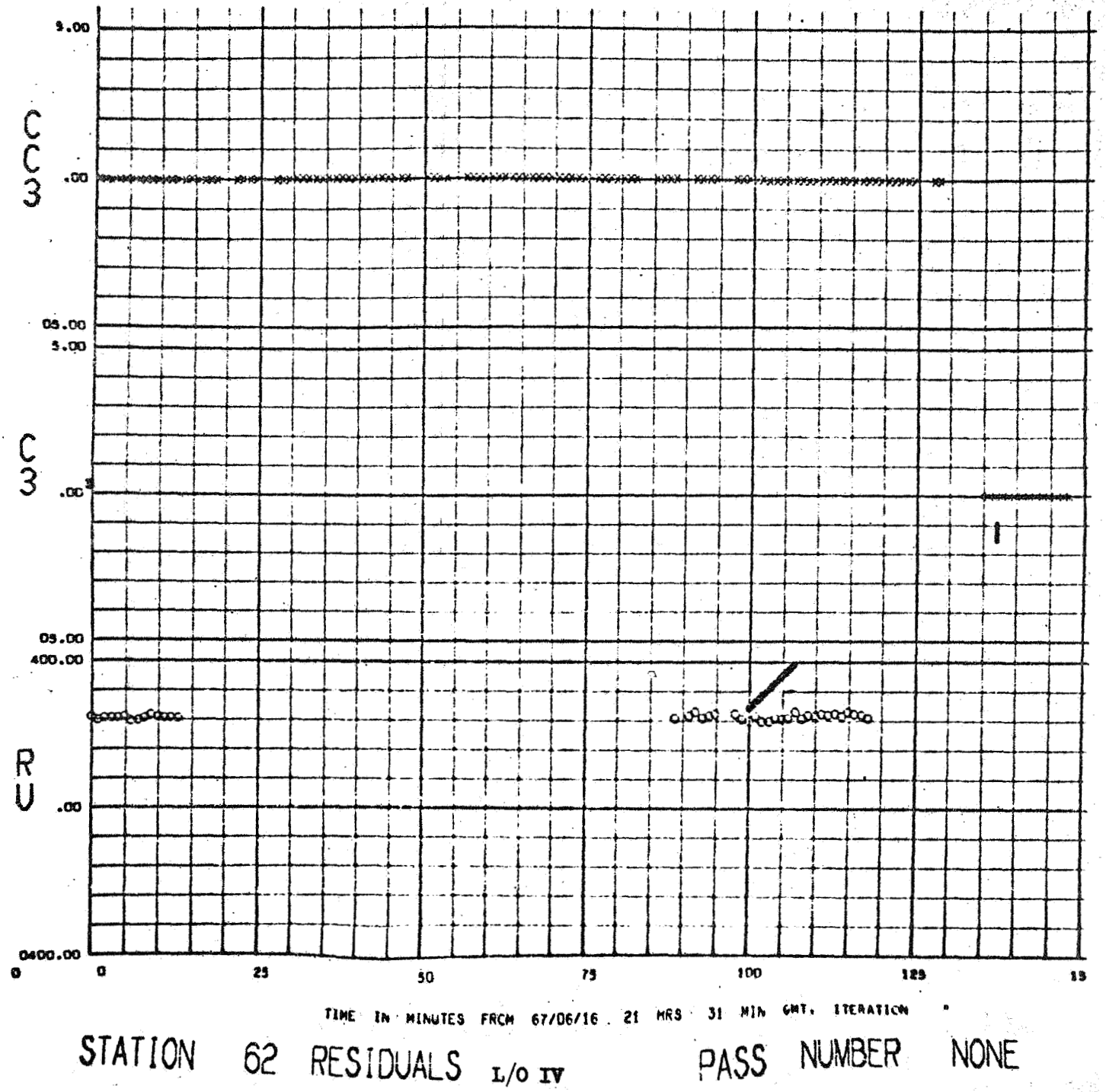

FIGURE 4.2 (Continued)

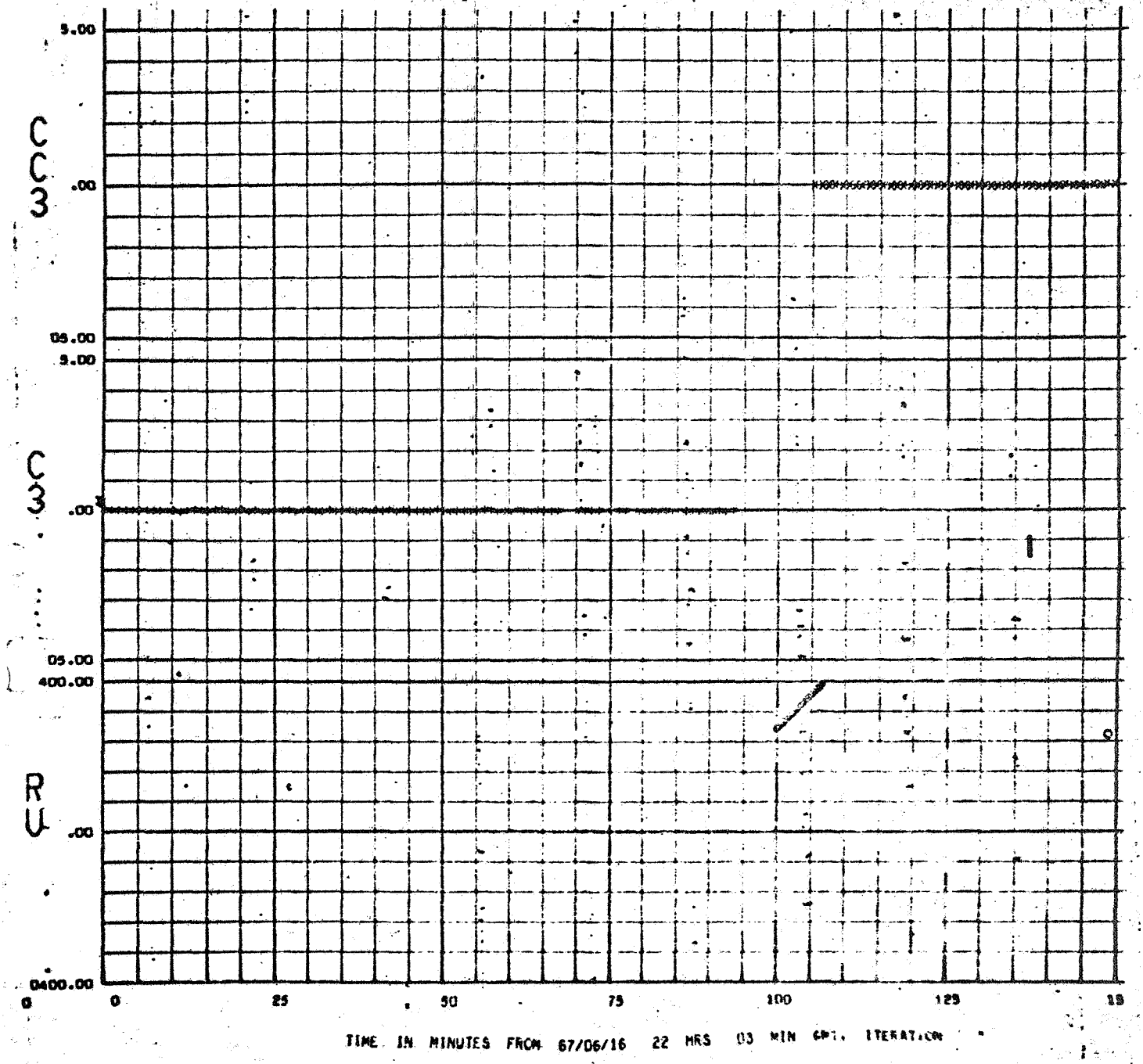

FIGURE 4.2 (Continued)

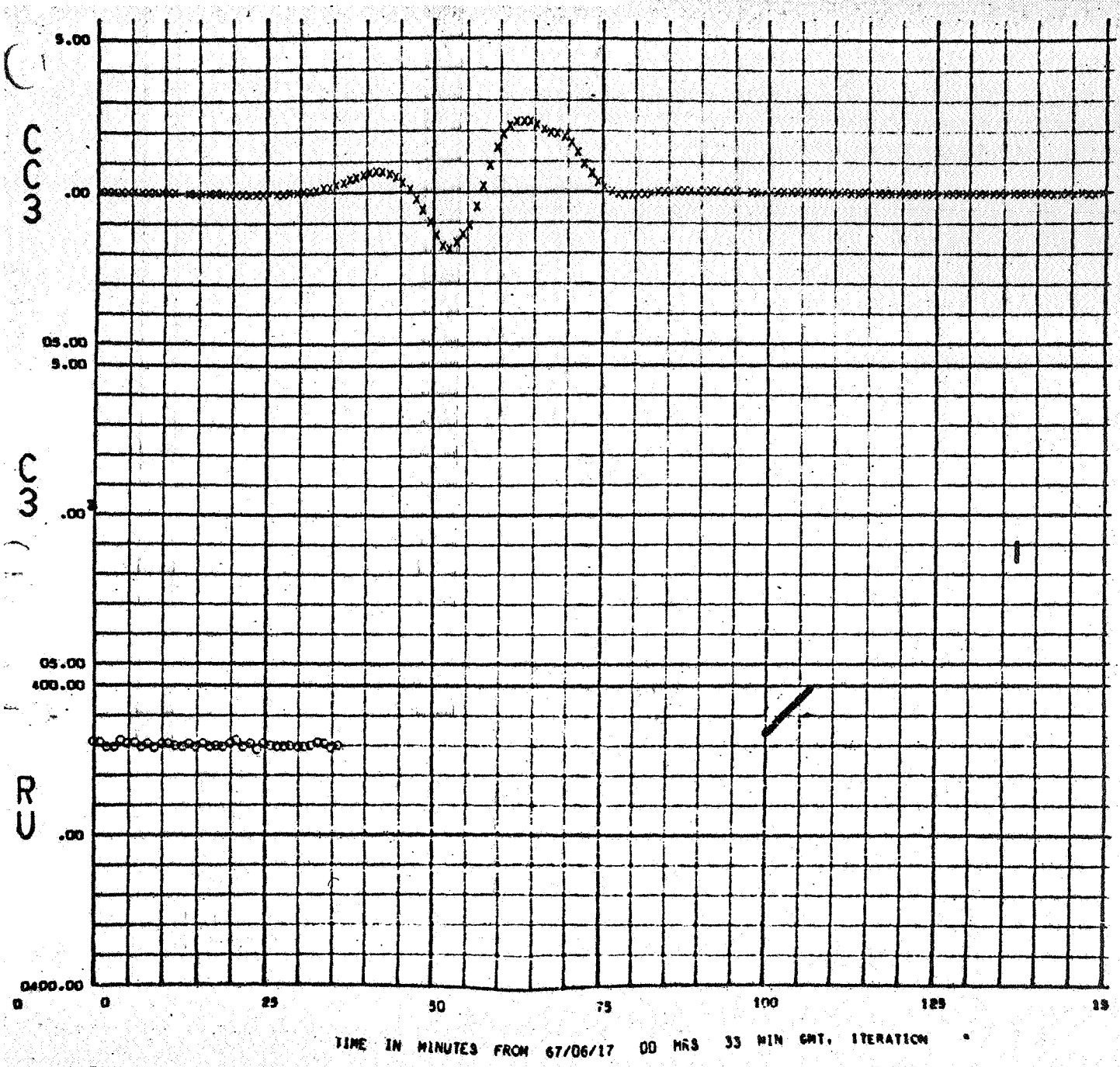

FIGURE 4.2 (Continued)

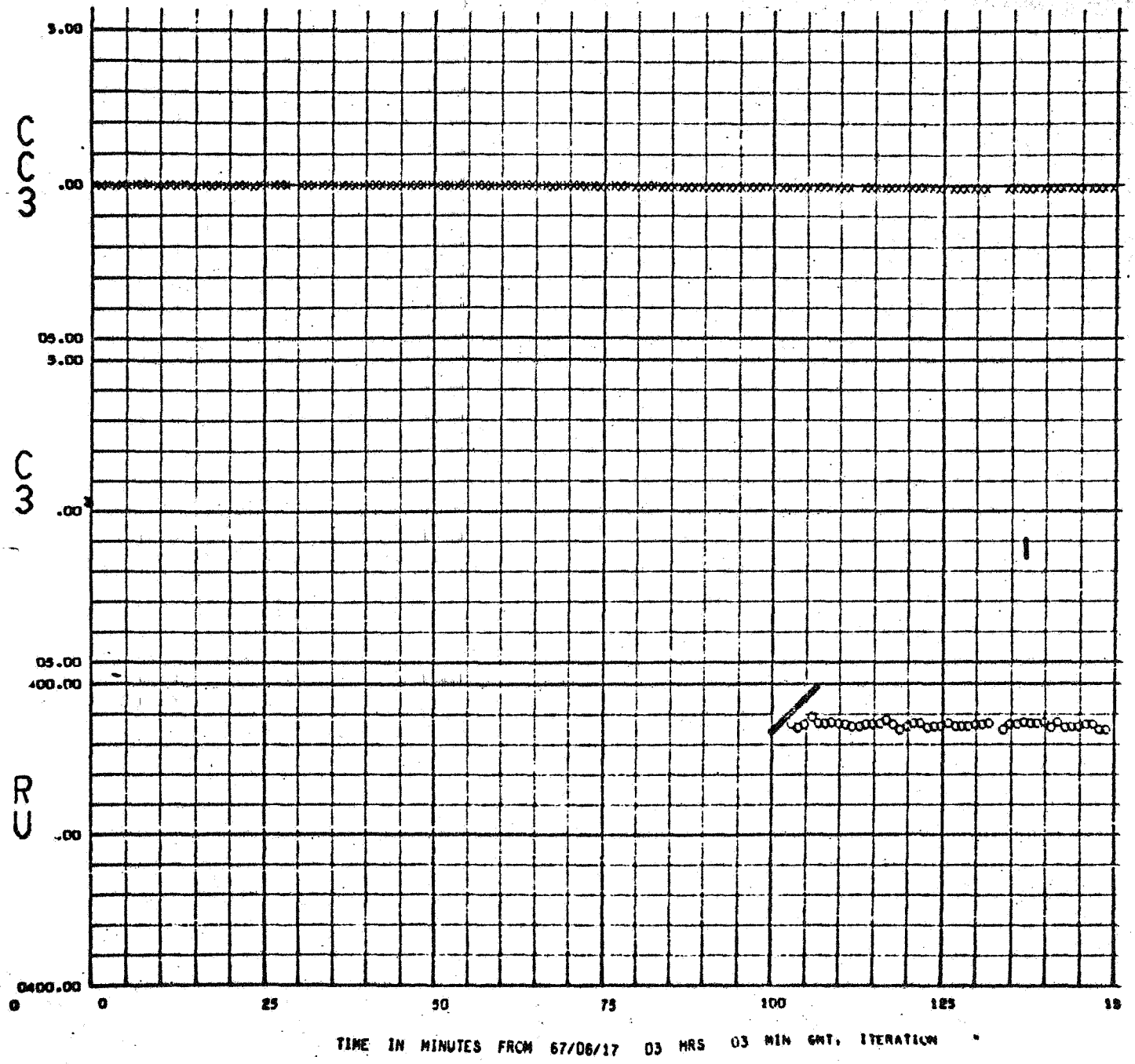

FIGURE 4.2 (Continued)

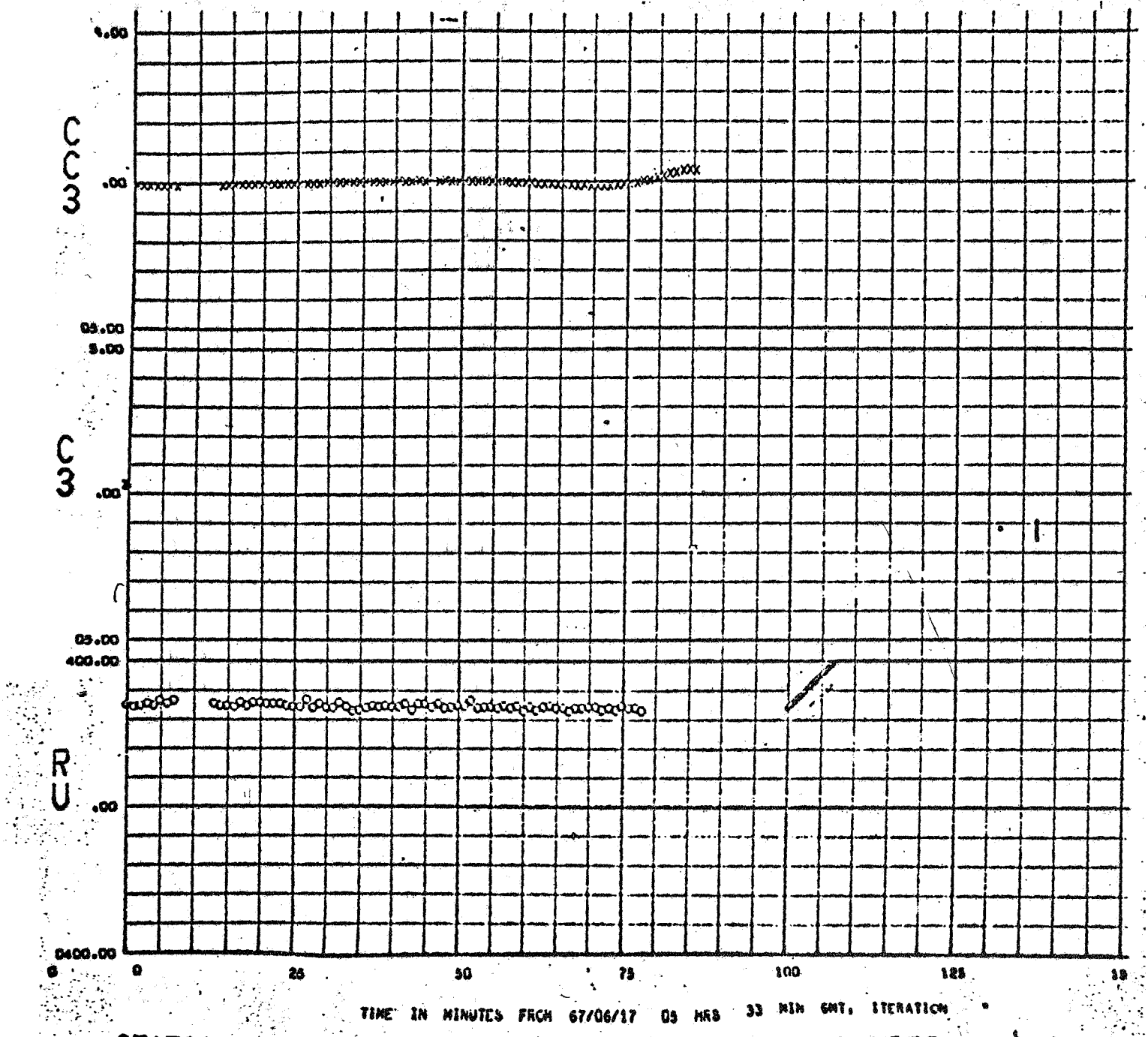

FIGURE 4.2 (Continued)

6) Print out of the frequency, period and order of the coefficients.

It was also necessary to create a separate interpolation program (INTERP) to interpolate between data points whenever a gap existed in the data stream. These gaps were due to blunder points, formats, errors, etc., and data arrays with gaps are not acceptable to LOFAP. The interpolation routine used was TAB, a standard Boeing routine which is in the Univac 1108 library. TAB is a variable order (1 to 5) Aitken's method routine. Fourth order interpolation was selected as most suitable from a series of test runs which showed that the error to be expected from fourth order interpolation between two points is on the order of .01 cps.

4.3.4 Application of LOFAP

Table 4.1 is a summary chart of the runs made with LOFAP. The three sets of observed data used were DSS 62 Perilune, DSS 62 Apolune and DSS 12 Perilune.

The data for the cases involving 129 points were from DSS 12 instead of DSS 62 because it was desirable to have perilune in the center of the data stream and there were not enough points upstream of the DSS 62 perilune. The number of data points was expanded from 33 to 65 to 129 in an attempt to make the period of the perilune oscillations shown in Figures 4.1 and 4.2 small compared to the total span of data used.

The parameters varied in each run (shown by the column headings in Table 4.1) are explained below:

1) First Data Point -- An effort was made to cause the center point of the data stream to coincide with the perilune points, except in cases 3, 6, and 11 where the data were deliberately offset to observe the effect on the Fourier coefficients. Cases 4 and 7 are also offset but for a reason explained below in the Data Interpolation paragraph.

2) Apolune Data -- One case was run with apolune data to see if the Fourier signatures were similar to those produced by the perilune data.

3) Perilune Data -- Self explanatory.

4) First Derivative Made Continuous -- It was recognized from the beginning that it was necessary to make the doppler data a continuous function over the interval considered to obtain any convergence of the Fourier series. This was accomplished by subtracting a linear function of the end point values to force the data to assume values of zero at the end points. After several runs had been made, it was observed that the first derivatives to be continuous by subtracting a quadratic function of the end point derivatives from the data to obtain faster convergence of the Fourier coefficients.

USE FOR TYPEWRITTEN MATERIAL ONLY

33 DATA POINTS (DSS 62 DATA)

CASE	1ST DATA POINT	APOLUNE DATA	PERILUNE DATA	FIRST DERIVATIVE MADE - CONTINUOUS	STATION MOTION SUBTRACTED	DATA INTERPOLATED TO MAKE FUNCTION MORE PERIODIC
1	Day 167 19^h 31^m		X			
2	Day 167 22^h 27^m	X				
3	Day 167 19^h 32^m		X			
4	Day 167 19^h 31.743^m		X			X
5	Day 167 19^h 31^m		X		X	
6	Day 167 19^h 32^m		X		X	
7	Day 167 19^h 31.6875^m		X		X	X
8	Day 167 19^h 31^m		X	X		

TABLE 4.1

SUMMARY OF LOFAP RUNS

65 DATA POINTS (DSS 62 DATA)

CASE	1ST DATA POINT	APOLUNE DATA	PERILUNE DATA	FIRST DERIVATIVE MADE - CONTINUOUS	STATION MOTION SUBTRACTED	DATA INTERPOLATED TO MAKE FUNCTION MORE PERIODIC
9	Day 167 $19^h\ 15^m$		X			
10	Day 167 $19^h\ 15^m$		X	X		

129 DATA POINTS (DSS 12 DATA)

CASE	1ST DATA POINT	APOLUNE DATA	PERILUNE DATA	FIRST DERIVATIVE MADE - CONTINUOUS	STATION MOTION SUBTRACTED	DATA INTERPOLATED TO MAKE FUNCTION MORE PERIODIC
11	Day 168 $00^h\ 21^m$		X			
12	Day 168 $00^h\ 21^m$		X	X		
13	Day 168 $00^h\ 21.584607^m$		X			X
14	Day 168 $00^h\ 21.585623^m$		X			X

TABLE 4.1 (Cont.)

The end point derivatives were computed by interpolating to find values of the function a distance (ϵ = .01) on either side of the end points, differencing these values and dividing by 2.

5) Station Motion Subtracted -- It was postulated that subtraction of the tracking station motion and moon motion effects might cause the resultant data to be more periodic and thus cause the Fourier coefficients to converge more rapidly. Hence the ODPL run described in Section 4.3.2 of this report was made. The data produced by this run represented the doppler shift a station would observe by tracking the center of the moon. Subtraction of this data from the total spacecraft doppler data then produced a moving plane-of-the-sky radial velocity doppler shift history, which was used in Cases 5, 6, and 7.

6) Data Interpolated to Make Function More Periodic -- Examination of the data produced by subtracting the linear trend from the original doppler shift values, in Case 1, showed that the resultant function was basically sinusoidal in nature but was aperiodic in the sense that the value of the function was not zero at $\pi/2$ but had a small negative value. The same effect was noted in Case 3 except that the value of the function at $\pi/2$ was now a small positive value. This suggested that if interpolation was used to time shift the data a fractional part of a minute so that the value of the function went to zero $\pi/2$, convergence of the Fourier coefficients might be hastened.

4.4 RESULTS

Results obtained are shown in Figures 4.3 through 4.18, which are plots of the higher order Fourier coefficient magnitudes vs. their order in the expansion for the cases shown in Table 4.1.

4.5 CONCLUSIONS

1) There are detectable differences between the Fourier signatures of the observed and simulated doppler shift data near perilune but there is no one dominant coefficient or narrow band of coefficients in either data source of sufficient magnitude to account for the residuals shown.

2) To the same scale, there are no detectable differences between the Fourier coefficients of the observed and simulated doppler shift data near apolune, except in the vicinity of the noise level.

3) To the same scale as (1), there is no detectable difference between the Fourier coefficients of the data created with a simple moon model

USE FOR TYPEWRITTEN MATERIAL ONLY

US 4802 1434 REV. 8-65

(spherical moon) and the data created with a more complex moon model (LRC 11/11 model modified by orbit determination solution for 8 harmonics).

4) Time shifting and interpolation on the observed and simulated data significantly changes the Fourier coefficient signatures, but does not concentrate the coefficients into one or a narrow band of frequencies.

5) Subtraction of the doppler shift due to station motion and moon motion from the observed and simulated data (reduction to radial velocity data), produces Fourier signatures that are very similar to those obtained from the data with station motion and moon motion included. Thus there is a physical effect present in the observed data which is not due to station motion, moon motion, or lunar harmonic model.

6) There are several orders of magnitude difference between the even and odd Fourier coefficients when the first derivatives are not forced to be continuous at the end points.

7) Forcing the first derivatives of the data to be zero at the end points reduces the difference between the even and odd Fourier coefficients.

8) There is no significant increase in the rate of convergence of the smallest coefficients when the first derivatives are made continuous.

9) Comparison of the magnitudes of the lower order coefficients (i.e. 0—5) in the LOFAP runs shows differences between the coefficients of the observed and simulated data large enough to account for the perilune residuals in Figures 4.3 and 4.4; however, these differences are spread through a range of coefficients and not concentrated at any one frequency.

10) The LOFAP printout for Cases 1 and 4 show that time shifting the data by a Δt to cause the data function to be zero at $\pi/2$ for the observed data does not also cause the simulated data function to be zero at $\pi/2$; in all cases, the simulated data function still had a small value at $\pi/2$.

11) The LOFAP printout for Cases 13 and 14 show that the spherical moon simulated data must be time shifted by 60 milliseconds more than the observed data to null the function at $\pi/2$.

USE FOR TYPEWRITTEN MATERIAL ONLY

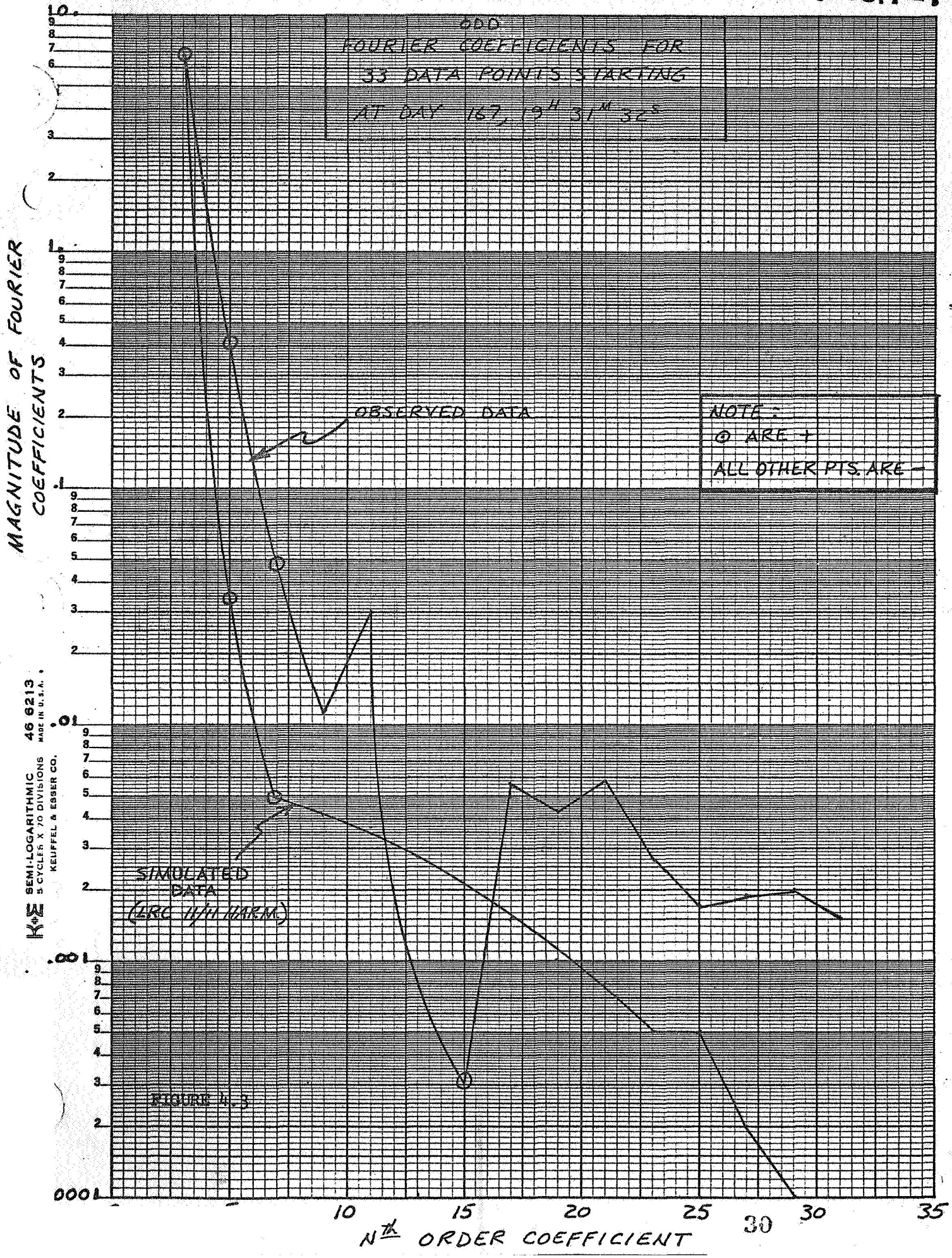
600
FOURIER COEFFICIENTS FOR
33 DATA POINTS STARTING
AT DAY 167, 19H 31M 32S
NOTE:
① ARE +
ALL OTHER PTS. ARE −
OBSERVED DATA
SIMULATED DATA
(ARC 11/11 HARM.)
MAGNITUDE OF FOURIER COEFFICIENTS
Nth ORDER COEFFICIENT
10
15
20
25
30
35
SEMI-LOGARITHMIC
5 CYCLES X 70 DIVISIONS
KEUFFEL & ESSER CO.
46 6213
MADE IN U.S.A.

FIGURE 4.3

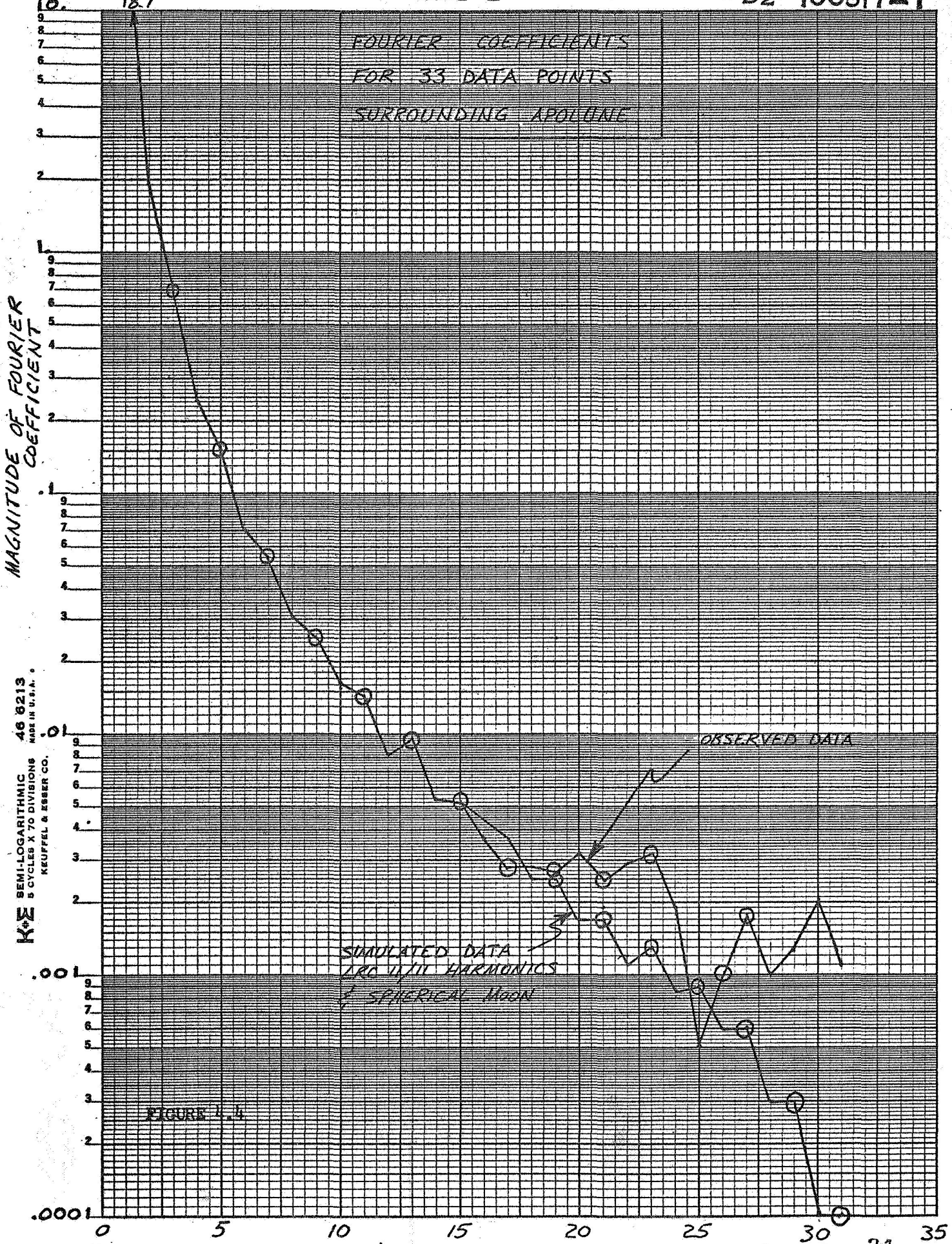
FOURIER COEFFICIENTS
FOR 33 DATA POINTS
SURROUNDING APOLUNE
18.7
OBSERVED DATA
SIMULATED DATA
IRC II/III HARMONICS
& SPHERICAL MOON
MAGNITUDE OF FOURIER COEFFICIENT
10.
1.
.1
.01
.001
.0001
0
5
10
15
20
25
30
35
Nth ORDER FOURIER COEFFICIENT
SEMI-LOGARITHMIC
5 CYCLES X 70 DIVISIONS
KEUFFEL & ESSER CO.
46 6213
MADE IN U.S.A.

FIGURE 4.4

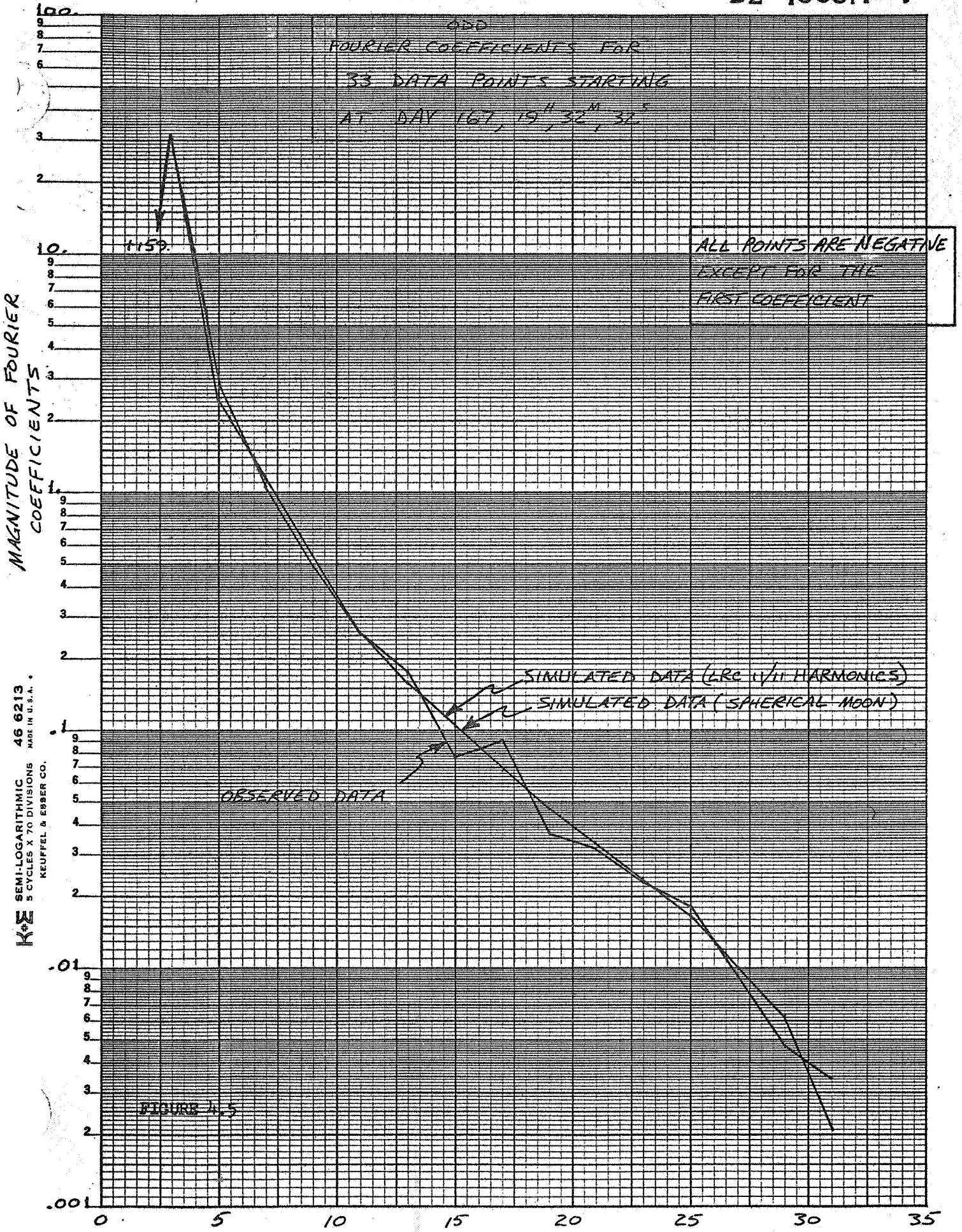
ODD
FOURIER COEFFICIENTS FOR
33 DATA POINTS STARTING
AT DAY 167, 19H, 32M, 32S
ALL POINTS ARE NEGATIVE
EXCEPT FOR THE
FIRST COEFFICIENT
1159.
SIMULATED DATA (LRC I/II HARMONICS)
SIMULATED DATA (SPHERICAL MOON)
OBSERVED DATA
MAGNITUDE OF FOURIER COEFFICIENTS
100.
10.
1.
.1
.01
.001
0
5
10
15
20
25
30
35
Nth FOURIER COEFFICIENT
SEMI-LOGARITHMIC
5 CYCLES X 70 DIVISIONS
KEUFFEL & ESSER CO.
46 6213
MADE IN U.S.A.

FIGURE 4.5

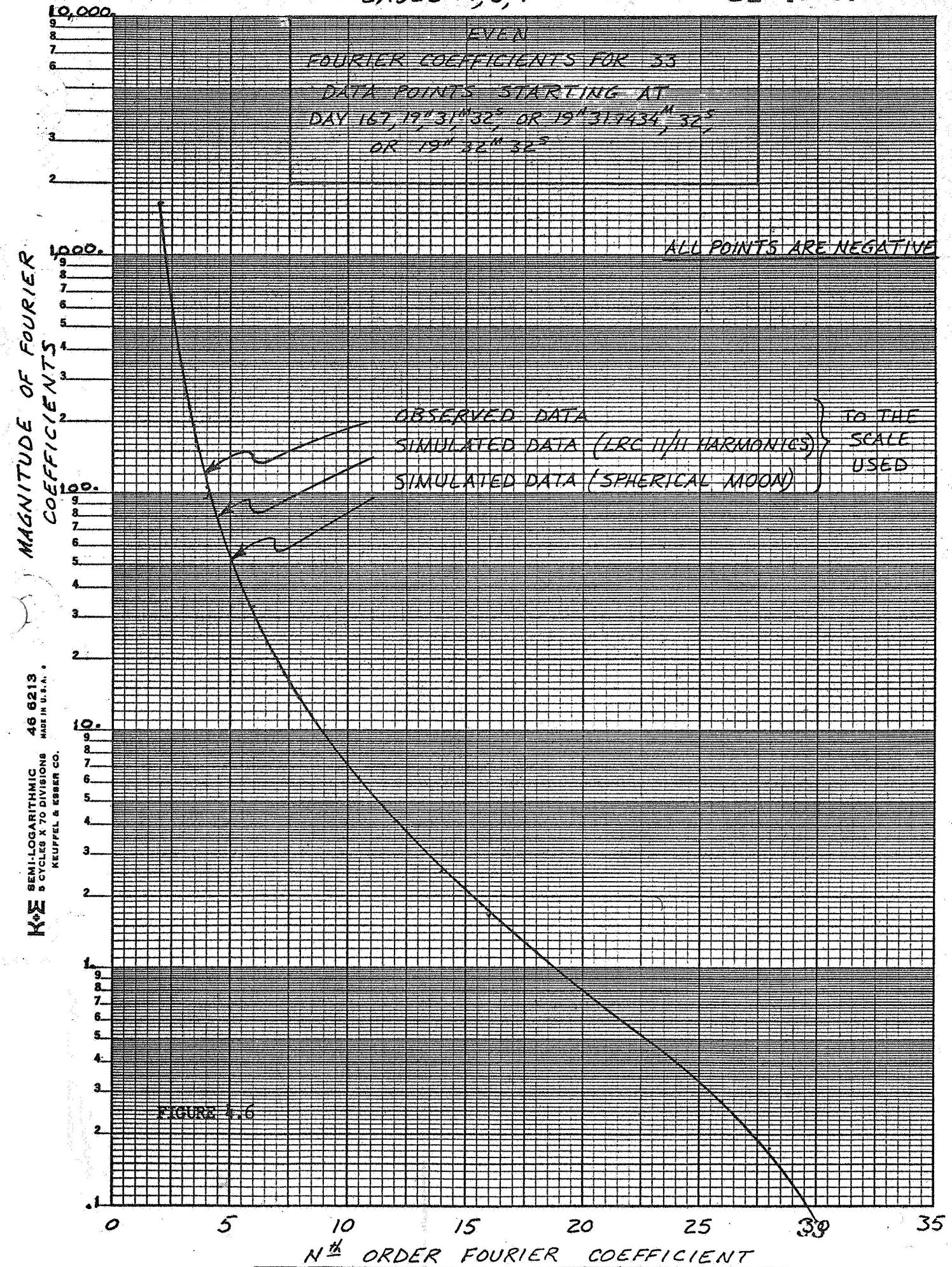
EVEN
FOURIER COEFFICIENTS FOR 33
DATA POINTS STARTING AT
DAY 167, 19H 31M 32S OR 19H 31.1434M 32S
OR 19H 32M 32S
ALL POINTS ARE NEGATIVE
OBSERVED DATA
SIMULATED DATA (LRC II/II HARMONICS)
SIMULATED DATA (SPHERICAL MOON)
TO THE SCALE USED
MAGNITUDE OF FOURIER COEFFICIENTS
10,000.
1000.
100.
10.
1.
.1
0
5
10
15
20
25
30
35
Nth ORDER FOURIER COEFFICIENT
K&E SEMI-LOGARITHMIC 5 CYCLES X 70 DIVISIONS KEUFFEL & ESSER CO. 46 6213 MADE IN U.S.A.

FIGURE 4.6

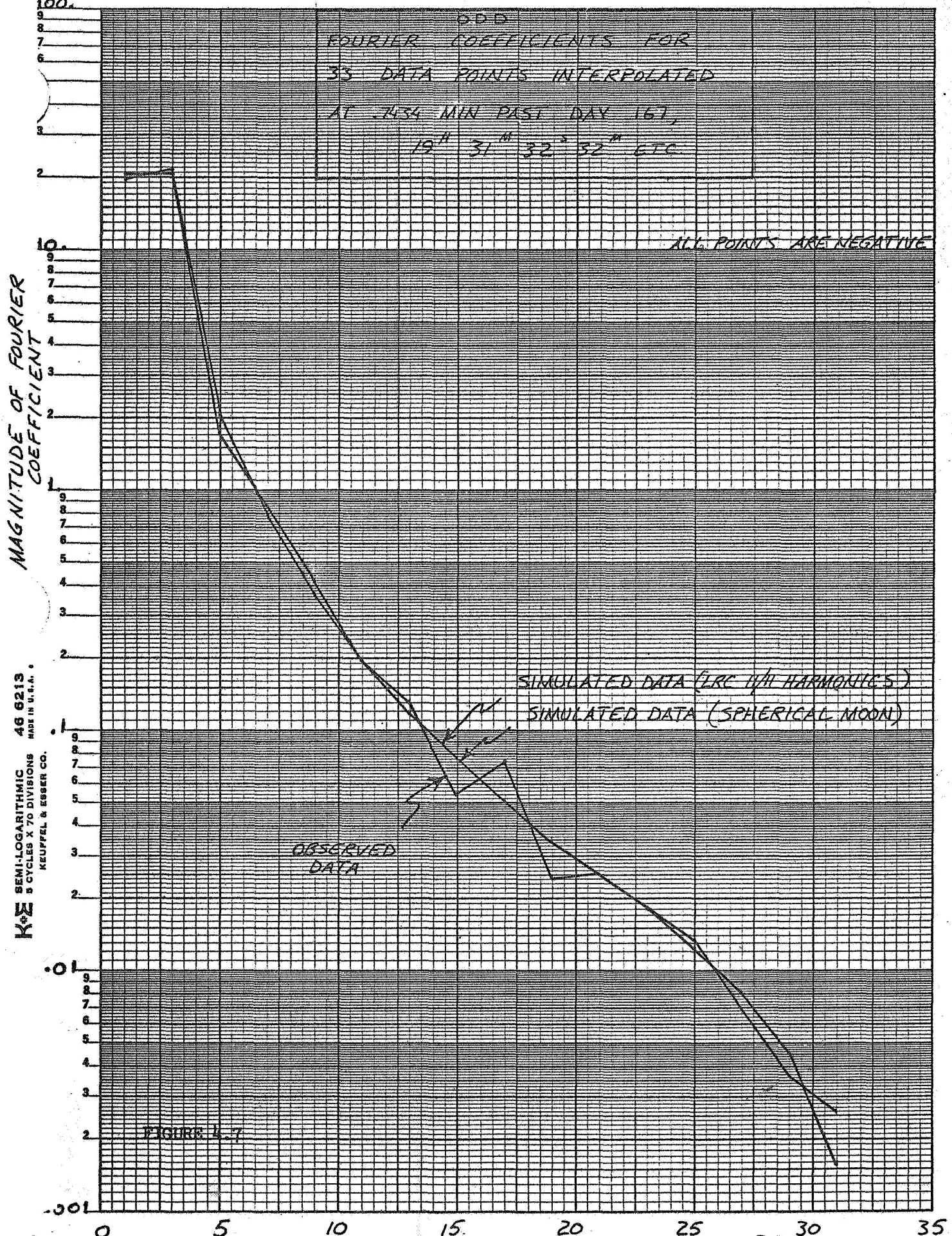
DDD
FOURIER COEFFICIENTS FOR
33 DATA POINTS INTERPOLATED
AT .434 MIN PAST DAY 167,
19H 31M 32S 32M ETC
ALL POINTS ARE NEGATIVE
SIMULATED DATA (LRC 11/11 HARMONICS)
SIMULATED DATA (SPHERICAL MOON)
OBSERVED DATA
MAGNITUDE OF FOURIER COEFFICIENT
100.
10.
1.
.1
.01
.001
0
5
10
15
20
25
30
35
Nth ORDER FOURIER COEFFICIENT
SEMI-LOGARITHMIC
5 CYCLES X 70 DIVISIONS
KEUFFEL & ESSER CO.
46 6213
MADE IN U.S.A.

FIGURE 4.7

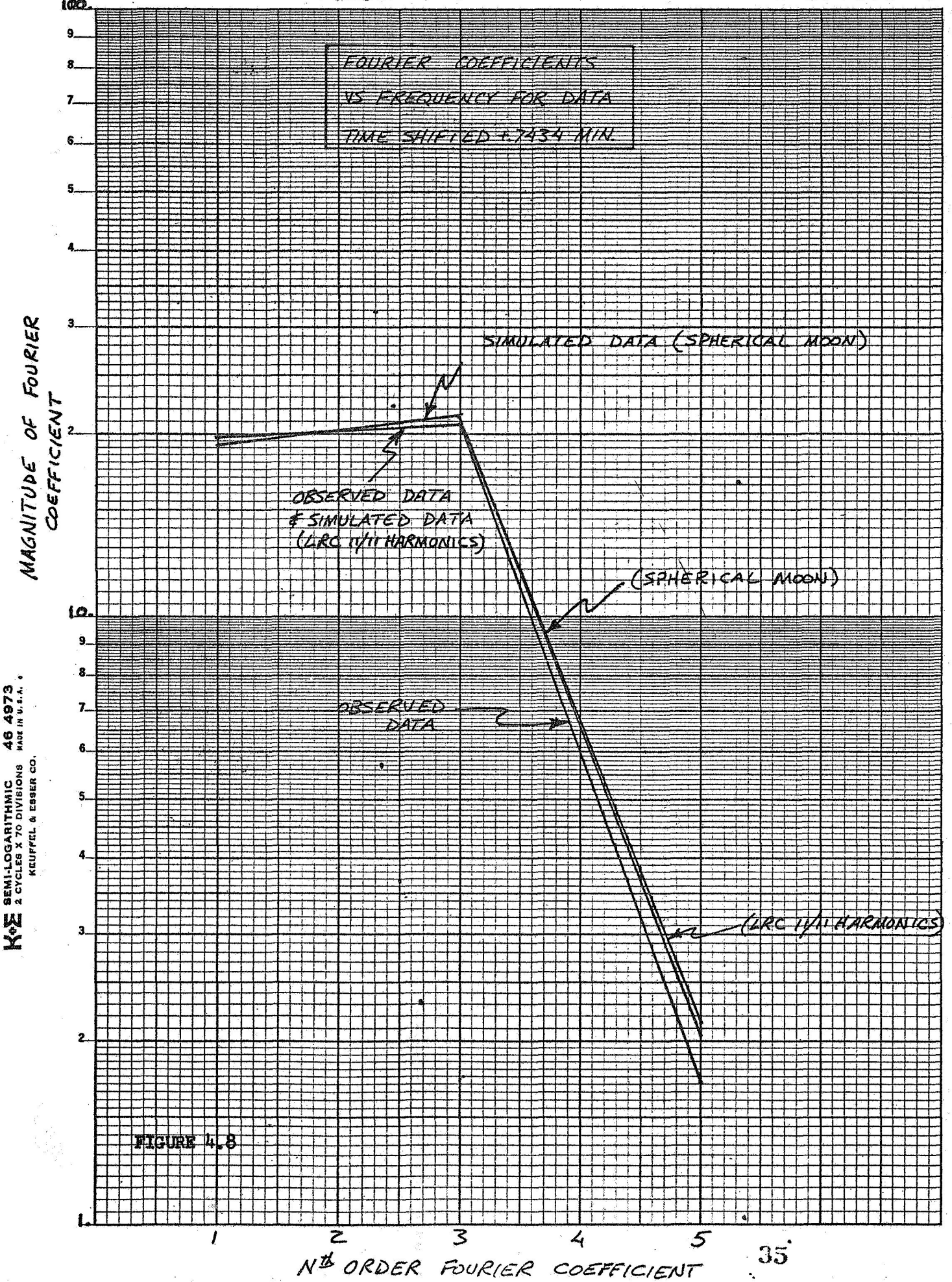
FOURIER COEFFICIENTS
VS FREQUENCY FOR DATA
TIME SHIFTED +.7434 MIN.
MAGNITUDE OF FOURIER COEFFICIENT
SIMULATED DATA (SPHERICAL MOON)
OBSERVED DATA & SIMULATED DATA (LRC 1/11 HARMONICS)
(SPHERICAL MOON)
OBSERVED DATA
(LRC 1/11 HARMONICS)
100.
9
8
7
6
5
4
3
2
10.
9
8
7
6
5
4
3
2
1.
1
2
3
4
5
Nth ORDER FOURIER COEFFICIENT
K&E SEMI-LOGARITHMIC 46 4973
2 CYCLES X 70 DIVISIONS MADE IN U.S.A.
KEUFFEL & ESSER CO.

FIGURE 4.8

CASE 5

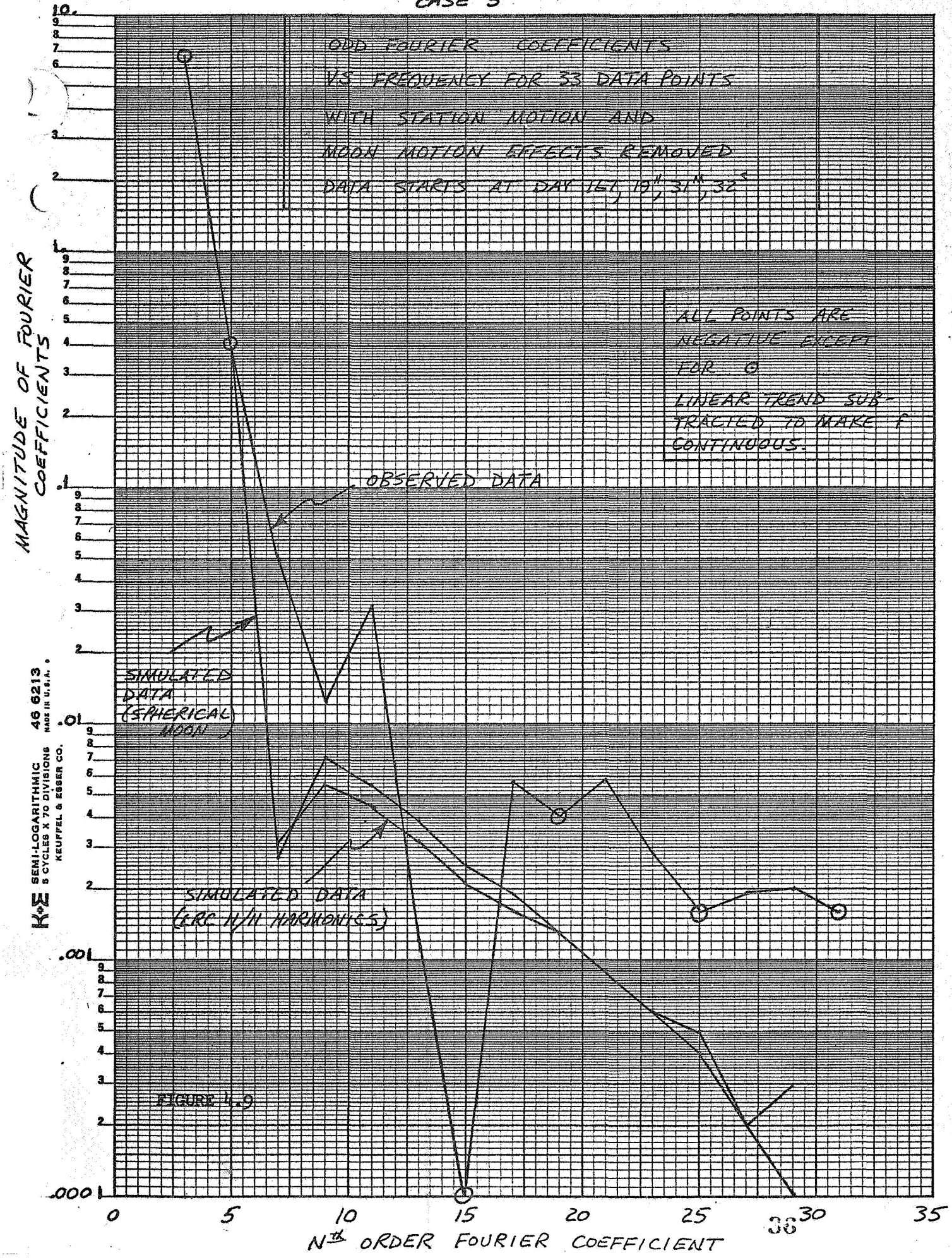

FIGURE 4.9

CASE 5

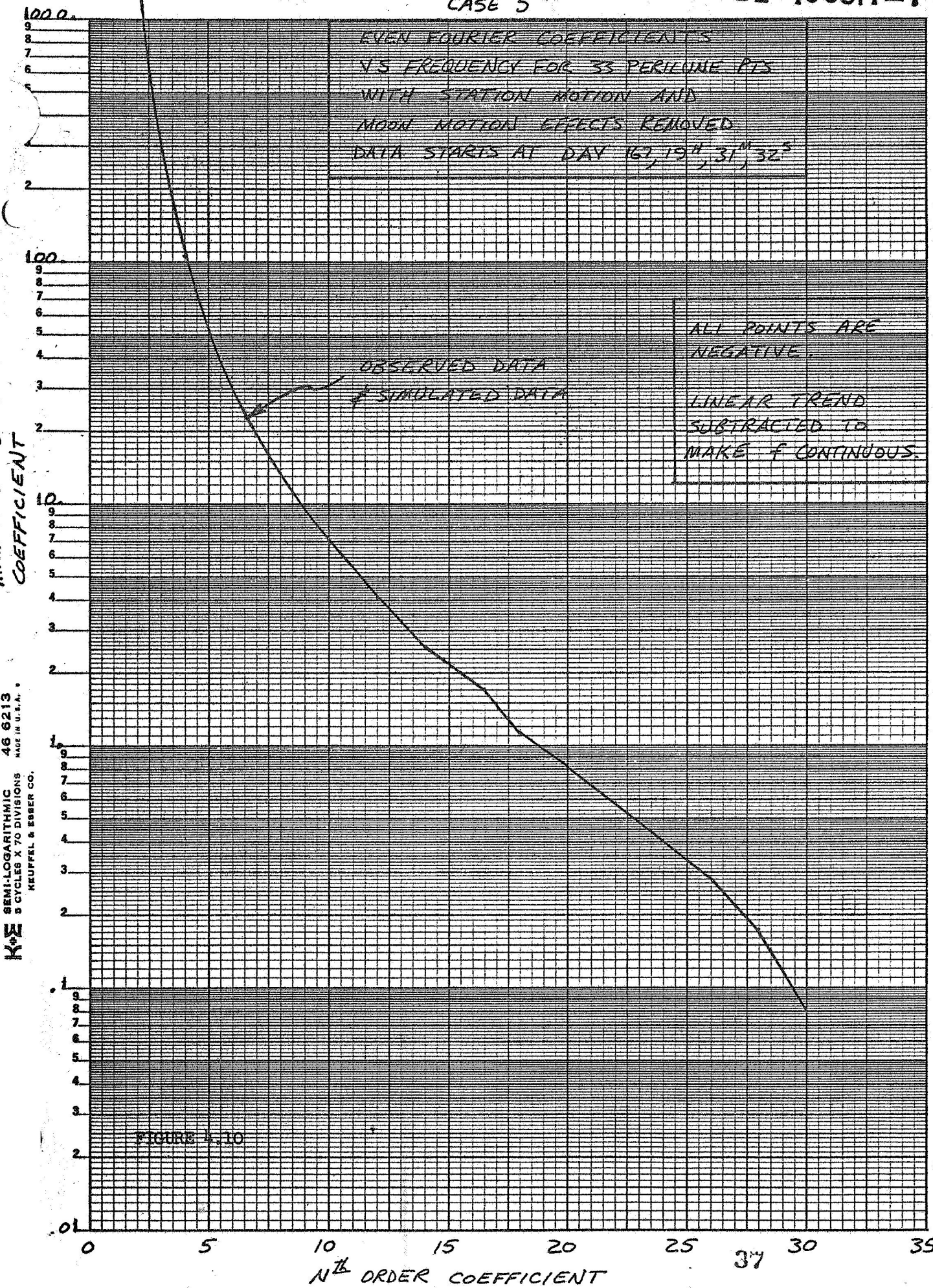

FIGURE 4.10

CASE 6

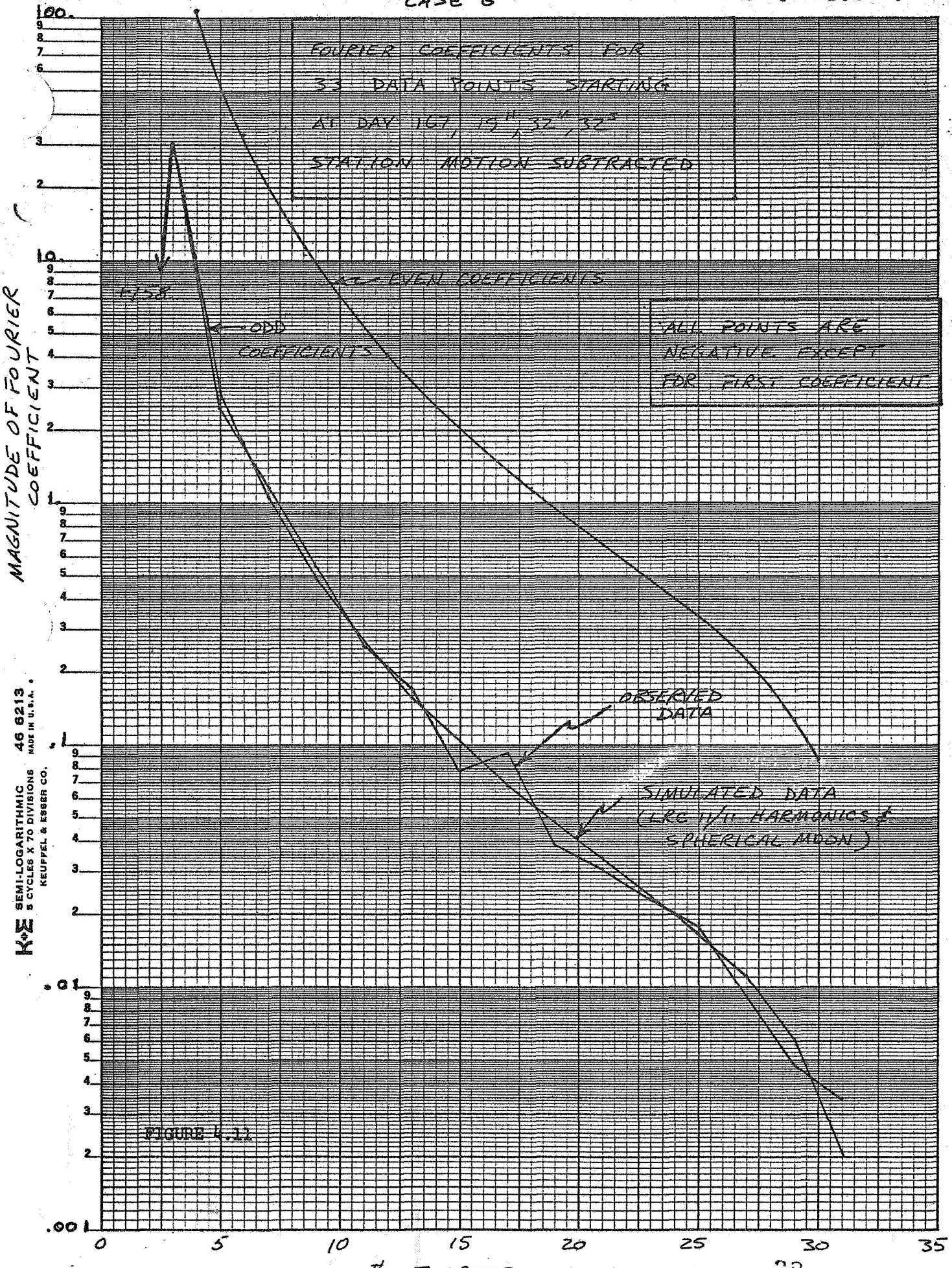

FIGURE 4.11

CASE 7

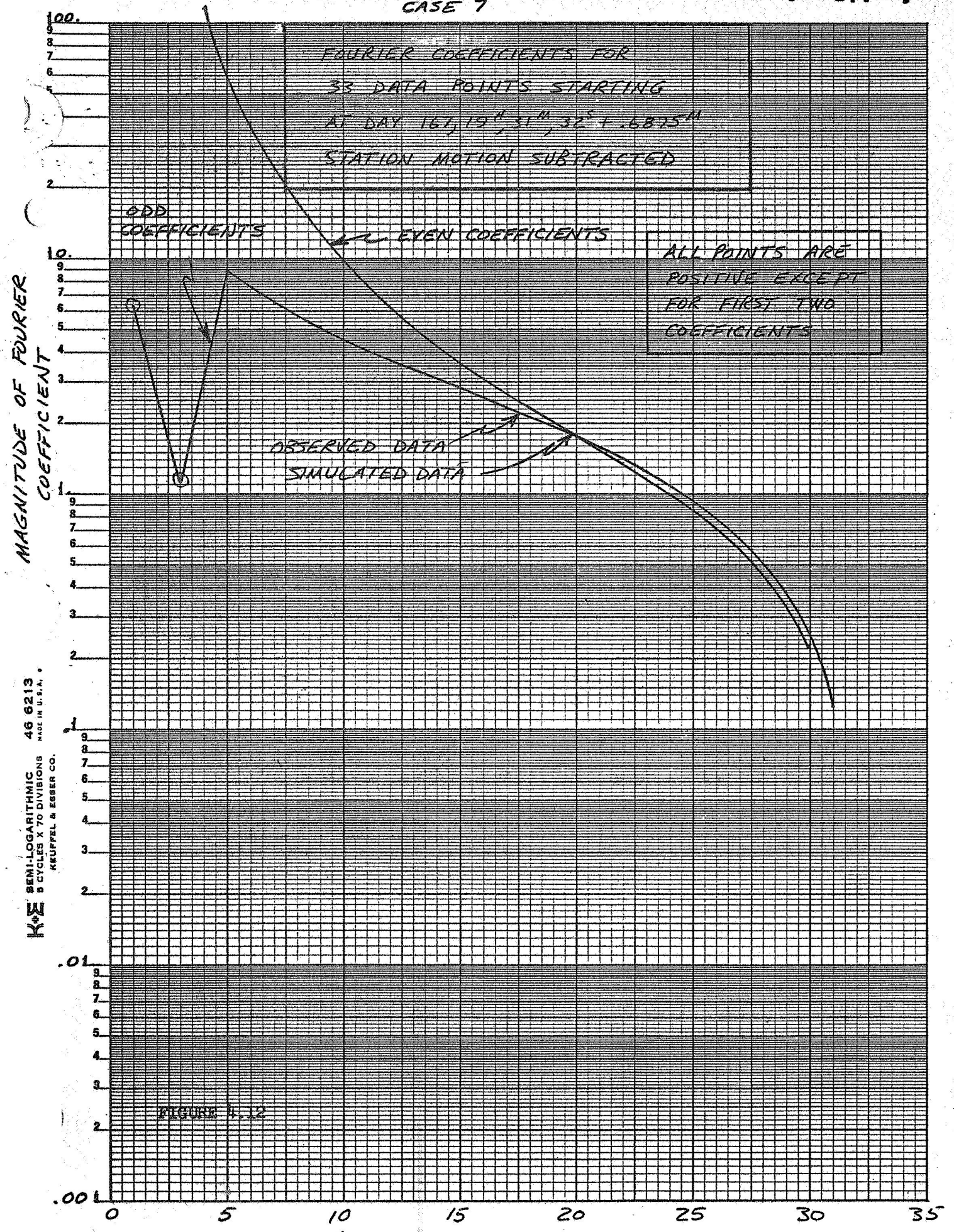

K+E SEMI-LOGARITHMIC 46 6213 MADE IN U.S.A.
5 CYCLES X 70 DIVISIONS
KEUFFEL & ESSER CO.

FIGURE 4.12

CASE 8

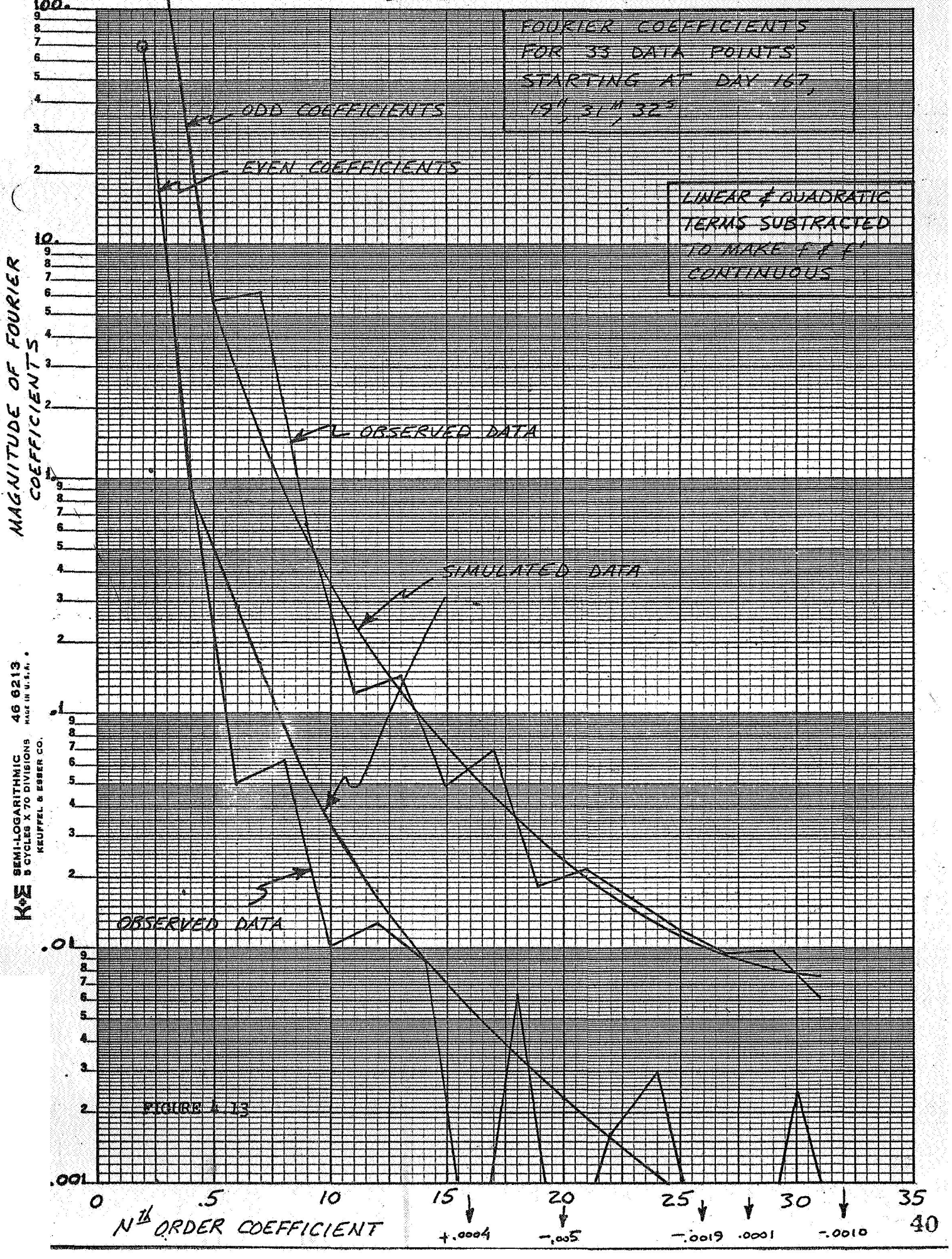

FIGURE 4.13

K&E 46 6213 SEMI-LOGARITHMIC 5 CYCLES X 70 DIVISIONS KEUFFEL & ESSER CO. MADE IN U.S.A.

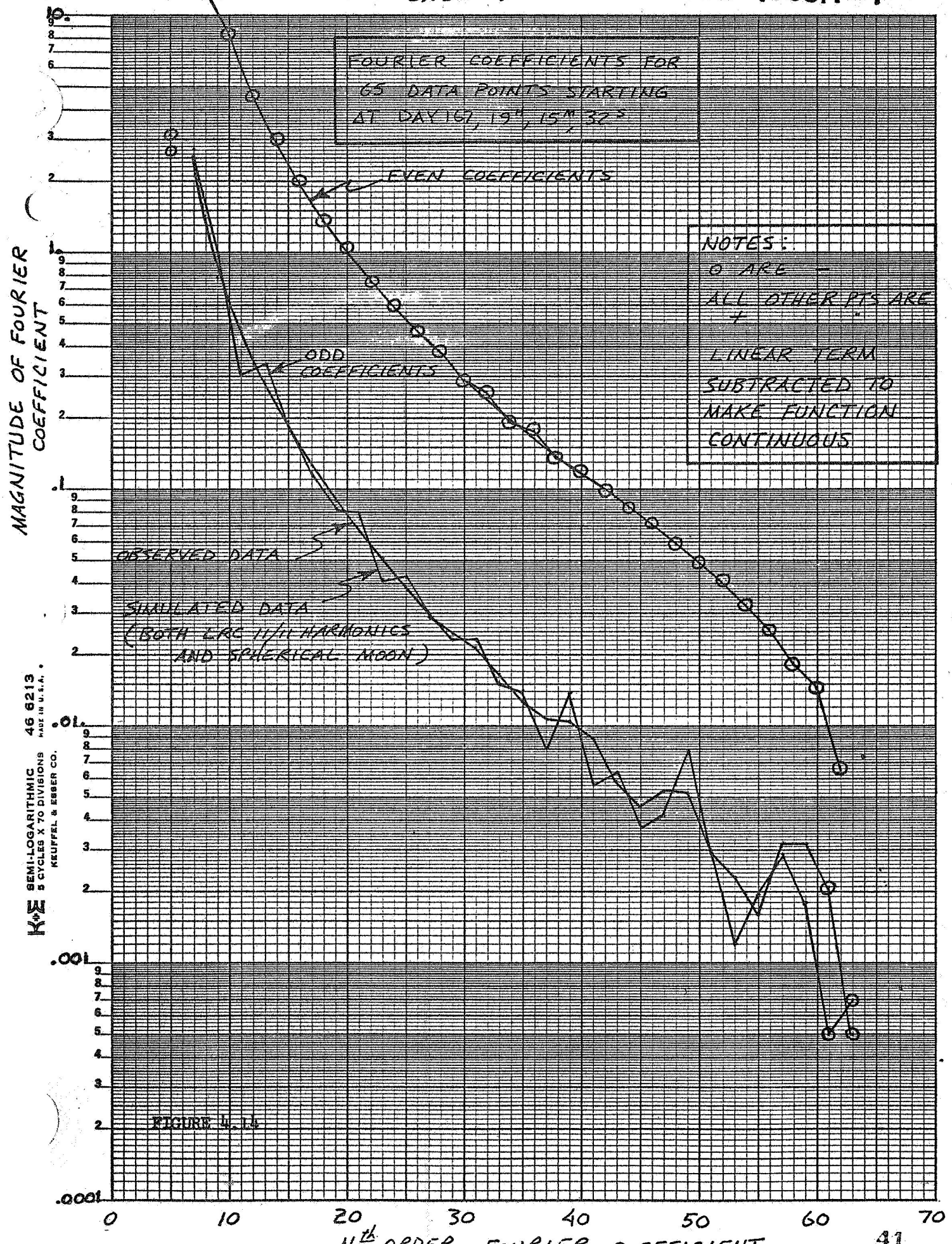
FOURIER COEFFICIENTS FOR 65 DATA POINTS STARTING AT DAY 167, 19ʰ, 15ᵐ, 32ˢ
EVEN COEFFICIENTS
ODD COEFFICIENTS
NOTES:
O ARE −
ALL OTHER PTS ARE +
LINEAR TERM SUBTRACTED TO MAKE FUNCTION CONTINUOUS
OBSERVED DATA
SIMULATED DATA (BOTH LRC 11/11 HARMONICS AND SPHERICAL MOON)
MAGNITUDE OF FOURIER COEFFICIENT
10.
1.
.1
.01
.001
.0001
0
10
20
30
40
50
60
70
Nth ORDER FOURIER COEFFICIENT
K+E SEMI-LOGARITHMIC 5 CYCLES X 70 DIVISIONS KEUFFEL & ESSER CO. 46 6213 MADE IN U.S.A.

FIGURE 4.14

CASE 10

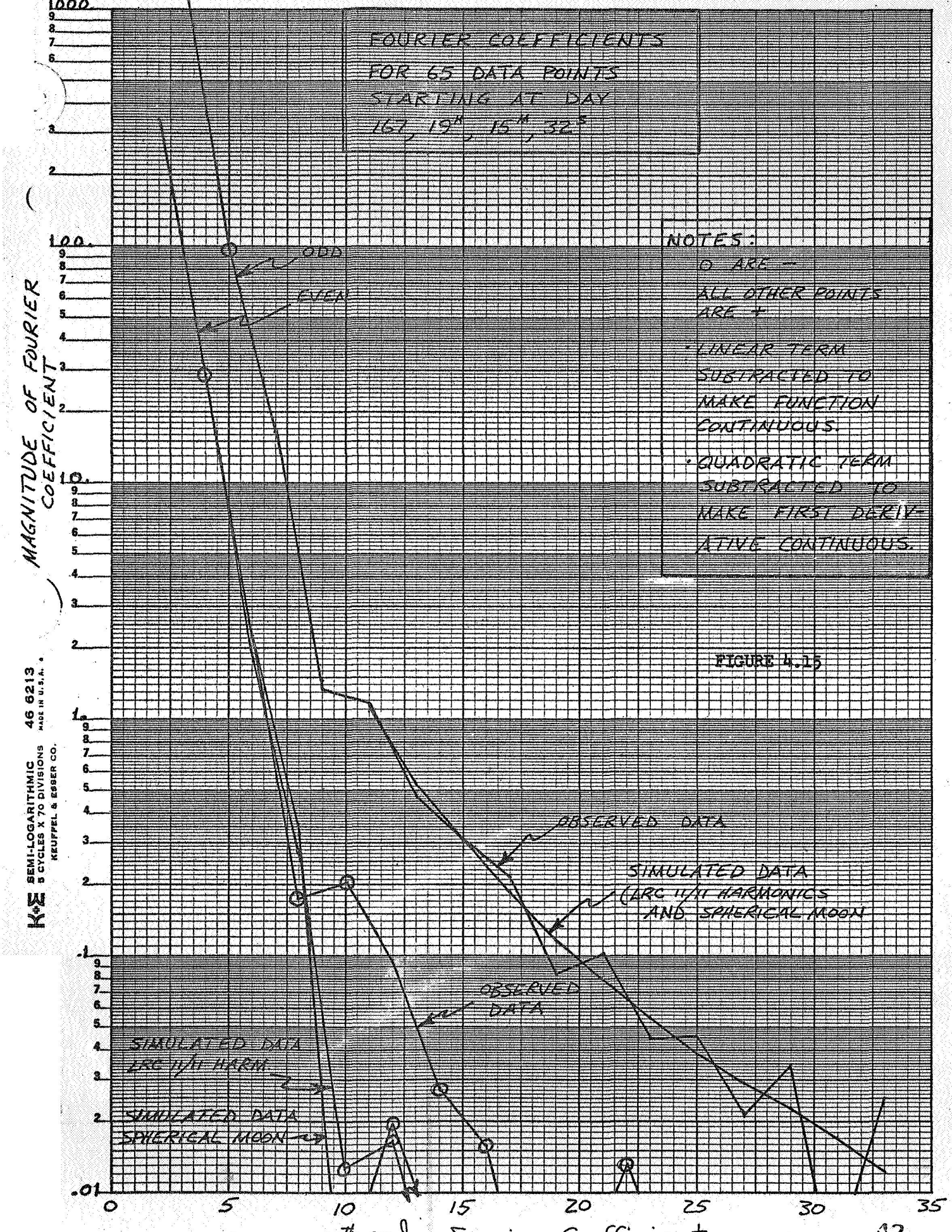

FIGURE 4.15

K+E 46 6213 MADE IN U.S.A.
SEMI-LOGARITHMIC
5 CYCLES X 70 DIVISIONS
KEUFFEL & ESSER CO.

CASE 11

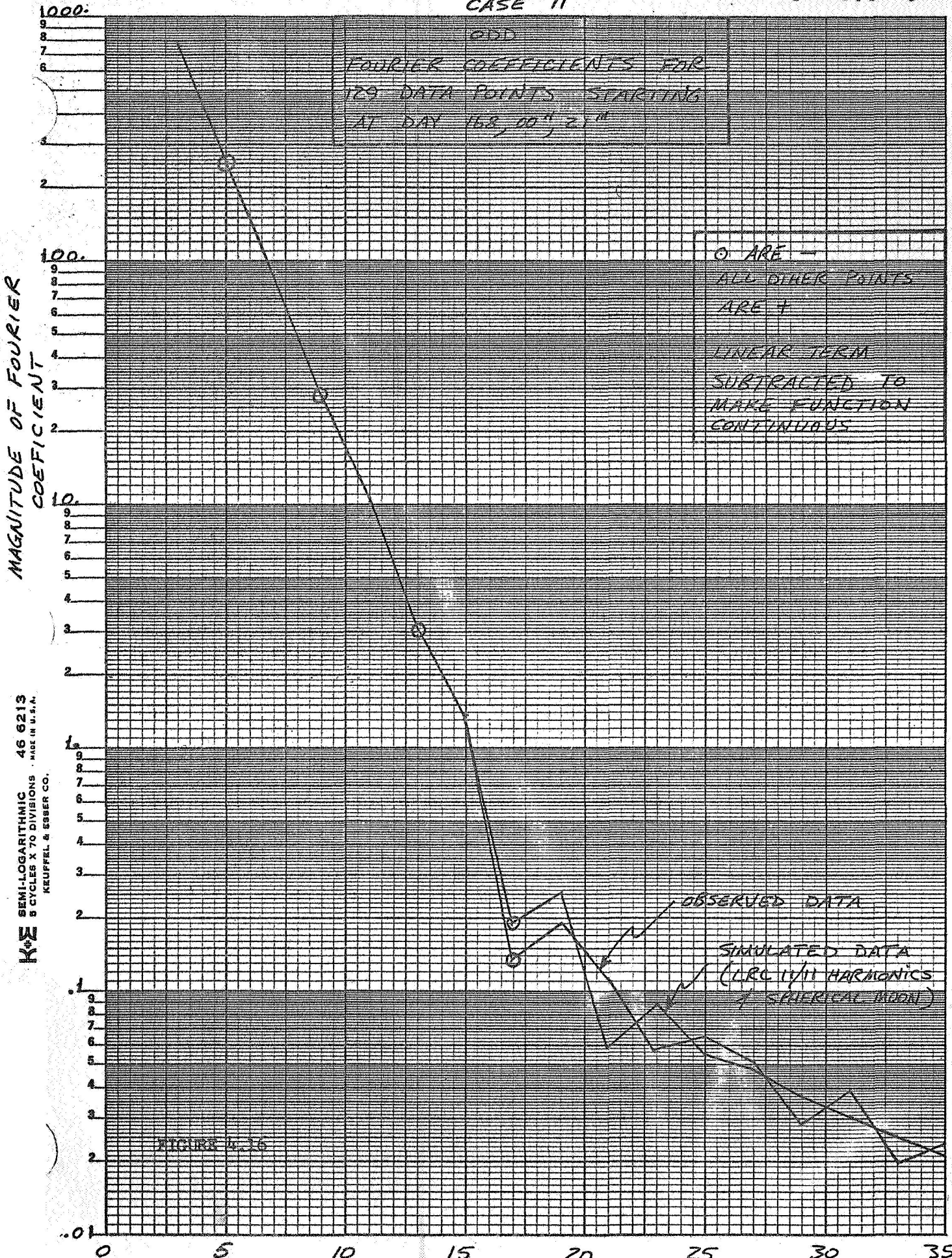

FIGURE 4.36

K&E SEMI-LOGARITHMIC 46 6213
5 CYCLES X 70 DIVISIONS MADE IN U.S.A.
KEUFFEL & ESSER CO.

CASE 11

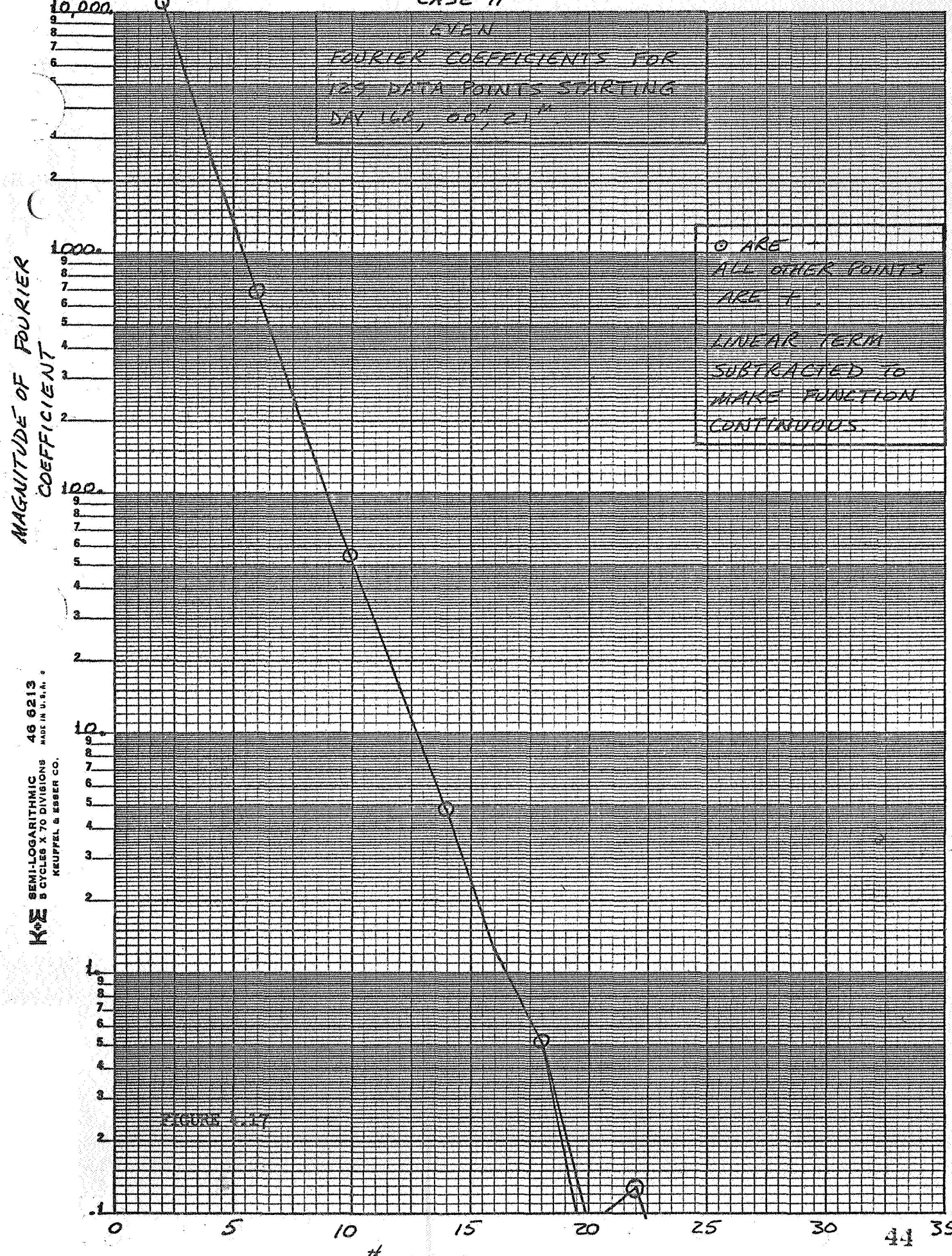

FIGURE 4.27

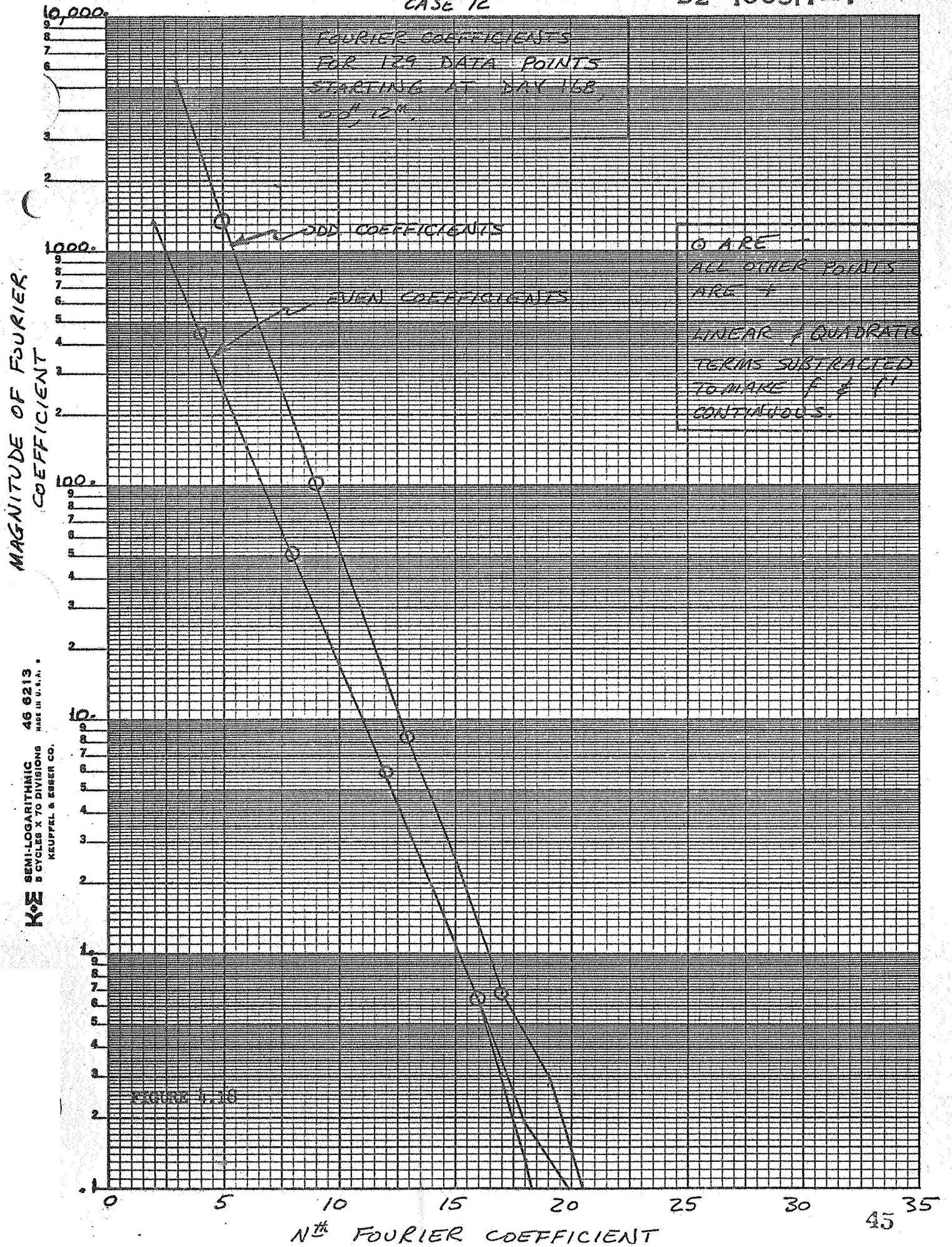
FOURIER COEFFICIENTS FOR 129 DATA POINTS STARTING AT DAY 168, Δt, 12 hr.
ODD COEFFICIENTS
EVEN COEFFICIENTS
⊙ ARE
ALL OTHER POINTS ARE +
LINEAR & QUADRATIC TERMS SUBTRACTED TO MAKE f & f' CONTINUOUS.
MAGNITUDE OF FOURIER COEFFICIENT
10,000.
1000.
100.
10.
1.
0
5
10
15
20
25
30
35
Nth FOURIER COEFFICIENT
K&E SEMI-LOGARITHMIC 46 6213
5 CYCLES X 70 DIVISIONS
KEUFFEL & ESSER CO.

FIGURE 4.18

5.0 DEEP SPACE NETWORK DOPPLER TRACKING SYSTEM

5.1 INTRODUCTION

This investigation examines the possibility that the perilune doppler residual phenomenon observed during the Lunar Orbiter flights may have been caused by hardware discrepancies in the Spacecraft-DSN doppler tracking system. The possible discrepancies examined are the tracking capabilities of the phase lock loops (Spacecraft and DSN) and multipath interference with the up-link signal.

Under conditions of large frequency offsets (ΔF) and/or large doppler rates ($\dot{\Delta F}$), it is possible to stress a phase lock loop to the point where it will begin to unlock or "skip cycles". If the loop isn't stressed to the point where it will unlock, the cycle skipping will be passed on and result in an incorrect doppler count. Also, if the loop signal-to-noise ratios (SNR's) become small enough, the loop will begin to unlock--again resulting in cycle skipping. (References 2, 3, and 4). Either or both of these conditions may then result in a case of cycle skipping which would cause an incorrect reading in the doppler count at the DSIF.

Up-link multi-path had been ruled out previously (Reference 5), the reasoning being that residuals still were present even when perilune occurred at the edge of the moon's disc and the line of sight from the DSIF antenna did not intersect the moon--hence minimal reflections from the lunar surface. However, since the main beam of the DSIF antenna has a 0.3° beamwidth, half of the antenna beam (.15°) is still intersecting the moon when the spacecraft is at the disc edge. Therefore, up-link multipath still remains a possible cause for the doppler residuals.

5.2 METHOD OF ATTACK

In an attempt to investigate the effects of up-link multipath in more detail, a post mission experiment was conducted with Lunar Orbiter V in which the spacecraft was tracked one-way during perilune. Data from this experiment is analyzed to see if the residuals are still present and, if so, whether or not the tracking system was responsible for their presence.

5.3 ANALYSIS

5.3.1 Tracking System Capabilities

1) Spacecraft -- The tracking capability of the phase lock loop in the spacecraft transponder is highly dependent upon the magnitude of the received signal strength. The tracking loop bandwidth varies with the magnitude of the signal strength, having its minimum bandwidth at threshold and its maximum bandwidth at strong signal conditions.

USE FOR TYPEWRITTEN MATERIAL ONLY

US 4802 1434 REV. 8-65

The received signal levels experienced by the spacecraft during the five Lunar Orbiter missions ranged between -90 dbm and -100 dbm. For the phase lock loop in the spacecraft transponder this corresponded to strong signal conditions. Table 5.1 lists some of the loop parameters for the transponder and their relation to received signal strength.

PARAMETER		VALUE
	Threshold	-142 dbm
Phase-locked loop equivalent noise bandwidth	$2B_{LO}$ (-142 dbm)	100 dbm
	$2B_{L}$ (-110 dbm)	540 Hz
Frequency Offset	ΔF_{max} (-142 dbm)	± 3.6 KHz
	ΔF_{max} (-110 dbm)	± 63.5 KHz
Doppler Rate	$\Delta \dot{F}_{max}$ (-142 dbm)	149 Hz/sec
	$\Delta \dot{F}_{max}$ (-110 dbm)	5.76 KHz/sec

TABLE 5.1
TRANSPONDER LOOP PARAMETERS

Since the signal received by the transponder was always greater than -110 dbm, the loop was capable of tracking an incoming signal offset in frequency by as much as 63.5 KHz and having a frequency rate of change up to 5.76 KHz/sec. With the spacecraft experiencing one way doppler shifts (frequency offsets) on the order of 15 KHz and doppler rates of change of 17 Hz/sec, the loop could easily track all incoming signals. During Missions III through V, the uplink frequency was offset by as much as (96)(420) ≈ 40 KHz (S-band); with this offset the total frequency shift was 15 KHz + 40 KHz = 55 KHz, still well within the capability of the loop. It may appear that the loop is beginning to be stressed at a frequency offset of 55 KHz (it is still more than 8 KHz within its capability, however), but it should be remembered that during Missions I and II there was no offset at the DSIF transmitter, yet residuals were present during those missions as well as during the last three.

With the transponder operating at strong signal levels, the signal-to-noise ratios in the loop are:

USE FOR TYPEWRITTEN MATERIAL ONLY

US 4802 1434 REV. 8-68

$2 B_{LO}$ = 100 Hz = 20 db

Threshold = -142 dbm

Noise Density = -142 -20 = -162 dbm · Hz

$2 B_L$ (> -110 dbm) = 540 Hz = 27.3 db

Loop Noise Power (> -110 dbm) = -162 + 27.3 = -134.7 dbm

SNR (- 90 dbm) = - 90 + 134.7 = 44.7 db

SNR (-100 dbm) = -100 + 134.7 = 34.7 db

With loop signal-to-noise ratios ranging from 34.7 db to 44.7 db the transponder was essentially operating in a clean signal mode (no noise). With the loop operating in a clean signal mode and well within its tracking capability, the possibility that any discrepancies in doppler tracking arose in the transponder phase lock loop must be discounted.

2) DSIF -- The tracking capability of the DSIF phase lock loop is dependent not only on received signal strength, but also on the choice of the loop bandwidth setting. Table 5.2 lists some of the loop parameters for the DSIF receiver. Reference 6 contains a more detailed listing of the loop parameters.

Parameter	$2 B_{LO}$ (Threshold)		
	12 Hz	48 Hz	152 Hz
Threshold*	-166 dbm	- 160 dbm	- 155.8 dbm
$2 B_L$ (Strong Signal)	132 Hz	274 Hz	518 Hz
Δ °F (Strong Signal)**	160 Hz/sec.	1500 Hz/sec.	7500 Hz/sec

TABLE 5.2

DSIF LOOP PARAMETERS

The nominal setting for the loop bandwidth was 12 Hz when tracking (doppler) data was being extracted by the receiver system. During the Lunar Orbiter missions the received signal strength at the DSIF ranged between -135 dbm and -145 dbm when the spacecraft was in the low power mode. With a threshold of -166 dbm, this corresponded to loop signal-to-noise ratios of 21 db to 31 db over design threshold. Table 5.3 lists

* For T_s = 165°K (System noise temperature with antenna pointed at the moon)

** Frequency offset = $\pm 30/10^6$ Hz

USE FOR TYPEWRITTEN MATERIAL ONLY

the tracking capabilities of the loop for these SNR's.

Parameter	db over Design Threshold	Value
ΔF	21	$30/10^6$ Hz
$\Delta^{\bullet}F$	21	95 Hz/sec
ΔF	31	$3/10^6$ Hz
$\Delta^{\bullet}F$	31	150 Hz/sec

TABLE 5.3

LOOP PARAMETERS – 21 DB AND
31 DB SNR OVER DESIGN THRESHOLD

USE FOR TYPEWRITTEN MATERIAL ONLY

The maximum 2-way doppler rates experienced in lunar orbit were on the order of 30 KHz maximum. (See Figure 5.1 for a typical example.) With the SNR's that existed in the loop, this doppler rate was well within the capability of the tracking loop. To investigate the effects of the loop bandwidth setting on the doppler residuals an experiment was conducted in which the spacecraft was tracked two-way in the high power mode (received signal = -100 dbm) for two consecutive passes, the first with the loop bandwidth set at 152 Hz andthe second with it set at 12 Hz (Reference 5). It was thought that the greater amount of filtering in the 12 Hz bandwidth may be causing some lag effects in the tracking data. The results of the experiment showed an agreement in residuals within .02 Hz thereby eliminating the possibility that the filters in the 12 Hz bandwidth may be causing some lag effects in the tracking data. The results of the experiment showed an agreement in residuals within .02 Hz thereby eliminating the possibility that the filters in the 12 Hz loop were responsible for the residuals.

The loop SNR's at the -135 dbm to -145 dbm received signal levels can be calculated as follows:

$2 B_{LO}$ = 12 Hz = 10.8 db

Threshold = -166 dbm

Noise Density = -166 - 10.8 = -176.8 dbm. Hz

$2 B_L$ (-135 dbm) = 120 Hz = 20.8 db (Reference 5)

$2 B_L$ (-145 dbm) = 78 Hz = 18.9 db (Reference 5)

Loop Noise Power (-135 dbm) = -176.8 + 20.8 = -156 dbm

Loop Noise Power (-145 dbm) = -176.8 + 18.9 = -157.9 dbm

U3 4802 1434 REV. A_RR

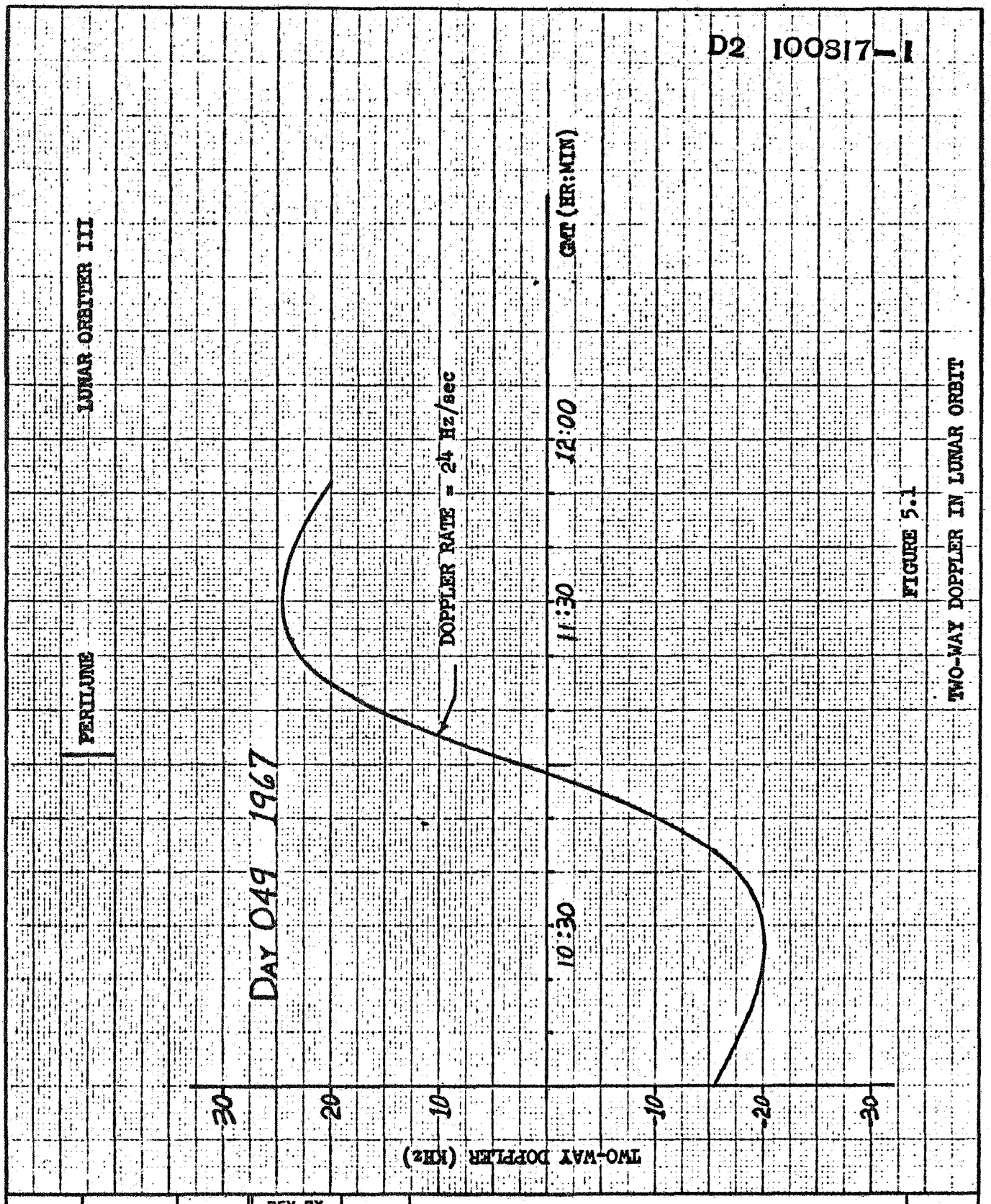

FIGURE 5.1 TWO-WAY DOPPLER IN LUNAR ORBIT

	INITIALS	DATE	REV BY INITIAL	DATE	TITLE	MODEL
CALC						
CHECK						
APPD.						
APPD.						

U3 4013 8000 REV. 1/66

REV LTR_____

BOEING NO. 50

SH.

SNR (-135 dbm) = 21.0 db

SNR (-145 dbm) = 12.9 db

With the loop operating at SNR's ranging from 12.9 db to 21 db, the probability of the loop beginning to unlock and skip cycles is essentially zero (References 2, 3 and 4). Also, since the doppler rates are well within the tracking capability of the loop, the possibility that the DSIF data acquisition system is introducing errors into the doppler extraction must be discounted.

5.3.2 Multipath Interference

Since the Lunar Orbiter spacecraft came at times within 40 km of the moon's surface at perilune, the possibility exists that the doppler residuals might have been caused by interference of the reflected signals with the direct signal, i.e., multipath.

Multipath on the down-link signal had been ruled out previously because residuals were still found to exist even when the spacecraft was tracked in the high power mode. The high power mode utilizes the travelling wave tube and the directional antenna for transmission to Earth. In this mode the direct signal is at least 37 db larger than the reflected signal from the lunar surface and for all practical purposes "swamps" out the reflected signal.

For the case of up-link multipath the reflected signal must be considered in more detail. The geometry that would exist for a maximum reflected signal is shown in Figure 5.2. In this case the entire beam intersects the moon and perilune occurs at the center of the moon's disc.

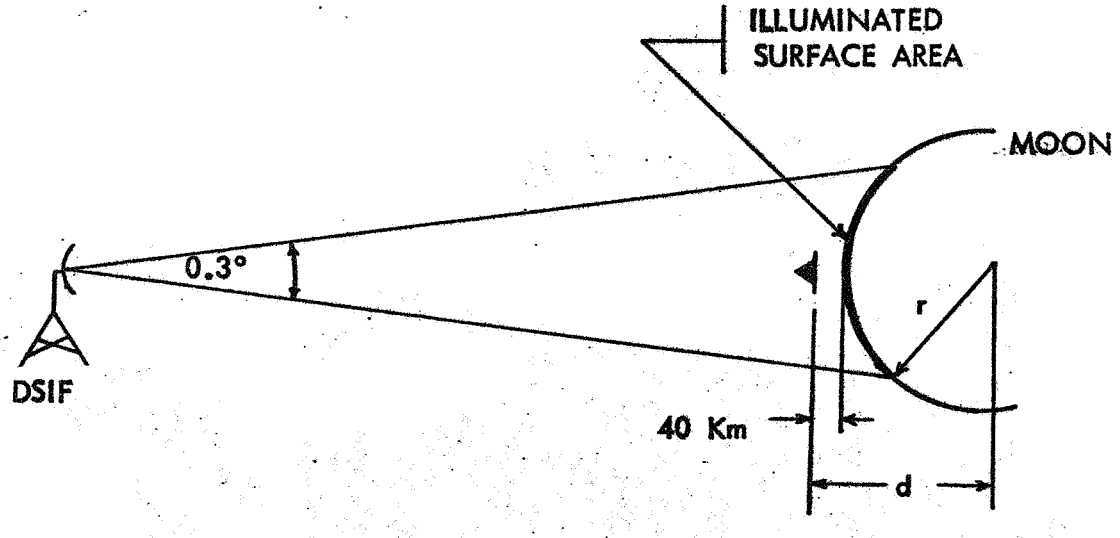

FIGURE 5.2

GEOMETRY FOR WORST CASE MULTIPATH

USE FOR TYPEWRITTEN MATERIAL ONLY

US 4802 1434 REV. 8-65

The power density at the moon resulting from the DSIF transmitter may be determined from the radar equation.

$$P_d = \frac{P_t G_t}{4 R^2} \quad \frac{w}{km^2}$$

P_d = power density at the moon

P_t = transmitted power = 10 KW

G_t = transmitting antenna gain = 57 db = 1.26×10^5

R = range to the moon = 384,000 km

$$P_d = \frac{(10^4)\ (1.26 \times 10^5)}{(3.84 \times 10^5)^2}$$

$$P_d = 6.82 \times 10^{-4}\ w/km^2$$

The system losses involved in the transmitting system amount to 0.7 db. Taking this factor into account yields a power density at the moon of 5.8×10^{-4} w/km^2.

The amount of energy reflected by the moon is dependent upon an efficiency factor, E

$$E = \eta \rho G_M$$

where

η = reflectivity

ρ = directivity

G_M = gain of the moon

For purposes of analysis, the moon will be considered as an isotropic radiator ($G_M = 1$), and the value of $\eta \rho$ will be taken as 0.075 (Reference 7). The reflected power density is then

$$P_{dR} = (0.075)\ P_d$$

$$P_{dR} = 4.34 \times 10^{-5}\ w/km^2$$

Since a major portion of the reflected energy comes from the center of the illuminated moon disc (References 7 and 8), the reflected power density may be approximated by a source (P_{eq}) at the center of the moon whose power density at the surface is 4.34×10^{-5} w/km^2.

When the spacecraft is 40 km above the surface, the distance from the center of the moon in terms of the moon's radius, r, is as follows:

USE FOR TYPEWRITTEN MATERIAL ONLY

US 4802 1434 REV. 8-65

$$d = 40 \text{ km} + r \qquad r = 1738 \text{ km}$$

$$\frac{d}{r} = \frac{1778}{1738} = 1.023$$

$$d = 1.023\, r$$

$$d^2 = 1.0465\, r^2$$

The power density at the spacecraft is

$$P_{d\text{-s/c}} = \frac{P_{eq}}{4\pi} \frac{1}{d^2}$$

$$= \frac{P_{eq}}{4\pi} \frac{1}{1.0465\, r^2}$$

$$= \frac{P_{eq}}{4\pi r^2} \frac{1}{1.0465}$$

$$= (4.34 \times 10^{-5})\ (0.95554)$$

$$P_{d\text{-s/c}} = 4.15 \times 10^{-5} \text{ w/km}^2$$

The effective area, A_{eff}, of the omnidirectional antenna (assuming a gain of unity) is

$$A_{eff} = \frac{\lambda^2}{4\pi}$$

$$A_{eff} = \frac{(1.42 \times 10^{-4})^2}{(1.256 \times 10^{1})}$$

$$A_{eff} = 1.6 \times 10^{-9} \text{ km}^2$$

The power received at the spacecraft is:

1) Direct Link $= \frac{P_t G_t}{4\pi R^2} (A_{eff})$

$$= (5.8 \times 10^{-4})\ (1.6 \times 10^{-9})$$

$$= 9.28 \times 10^{-13} \text{ watts}$$

$$= -90.3 \text{ dbm}$$

USE FOR TYPEWRITTEN MATERIAL ONLY

US 4802 1434 REV. 8-65

2) Multipath $= (P_d - s/c)\,(A_{eff})$

$= (4.15 \times 10^{-5})\,(1.6 \times 10^{-9})$

$= 6.64 \times 10^{-14}$ watts

$= -101.8$ dbm

For a worst case analysis at apolune--where apolune occurs at the center of the disc--the distance of the spacecraft from the center of the moon in terms of the moon's radius r, is

$$d = 1800 \text{ km} + r$$

$$\frac{d}{r} = \frac{1800 + 1738}{1738} = 2.04$$

$$d^2 = 4.15\, r^2$$

The power in the multipath signal can be calculated as before. For this value of d^2, the power in the multipath signal at the spacecraft is 1.67×10^{-14} watts or -107.8 dbm.

From these calculations the difference between the direct and multipath signals may be determined. Table 5.4 lists the differences at perilune and apolune.

	SIGNAL POWER (DBM)		
	DIRECT	MULTIPATH	DIFFERENCE (DB)
Perilune	-90.3	-101.8	11.5
Apolune	-90.3	-107.8	17.5

TABLE 5.4
DIRECT AND MULTIPATH SIGNAL POWERS

Since the signal in the carrier tracking loop is sinusoidal, the interference of the two signals-direct and multipath may be represented by the phasor diagram of Figure 5.3.

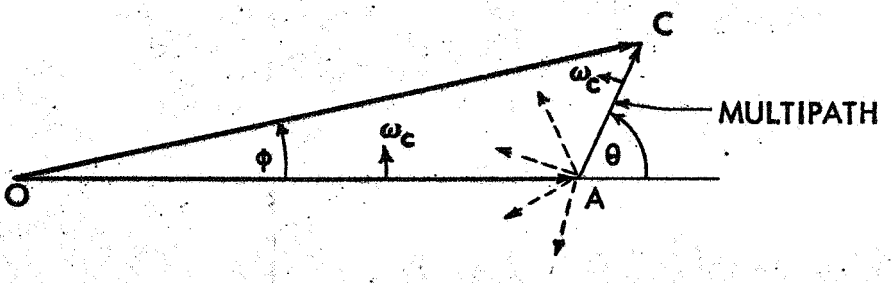

FIGURE 5.3
SUPERPOSITION OF TWO SINUSOIDAL SIGNALS

USE FOR TYPEWRITTEN MATERIAL ONLY

U3 4802 1434 REV. A--65

Assuming that the magnitude of the direct signal, OA, is unity, the magnitude of the interferring signal, AC, varies between .071 (-11.5 db) and .018 (-17.5 db). It is immediately apparent that the interferring signal can never cause the instantaneous resulting phase, ϕ, to even approach 90° which is the condition required for the loop to skip a cycle. The interferring signal will, however, cause some residual phase modulation. The frequency of the multipath signal, AC, is the same as the direct signal, but the amplitude will change as a function of time along with the phase (θ in Figure 5.3). The amplitude will be changing as a function of time because the altitude or distance to the moon is changing as the spacecraft moves through its orbit and also because the irregularities in the lunar surface preclude a uniform reflected signal. The direct signal, OA (Figure 5.3), may be represented as a constant, unity, and the reflected signal, AC, by a(t) since both signals have the same frequency. The resultant signal, OC, may then be expressed as

$$e(t) = \left[(1 + a(t) \cos \theta)^2 + (a(t) \sin \theta)^2\right]^{1/2} \cos (\omega_c t + \phi)$$

where

$$\phi = \tan^{-1}\left[\frac{a(t) \sin \theta}{1 + a(t) \cos \theta}\right]$$

θ = Phase of reflected signal with respect to the direct signal.

The resultant signal contains both amplitude and phase modulation.

The amplitude modulation represented by $\left[(1 + a(t) \cos \theta)^2 + (a(t) \sin \theta)^2\right]^{1/2}$ is removed by the limiter in the spacecraft transponder. However, the phase angle, ϕ, results in the presence of an additional frequency component, $\Delta\omega$, in the tracking loop.

$$\omega_{INST} = \frac{d}{dt} (\omega_c t + \phi) = \omega_c + \frac{d\phi}{dt}$$

$$\Delta\omega = \frac{d\phi}{dt}$$

Since a(t) is small with respect to unity, the expression for the phase, ϕ, becomes

$$\phi = \tan^{-1}\left[\frac{a(t) \sin \theta}{1 + a(t) \cos \theta}\right] \approx \tan^{-1} (a(t) \sin \theta)$$

$$\phi \approx a(t) \sin \theta$$

The above phase modulation then is responsible for the frequency of the resultant signal received by the spacecraft to be continually varying about a mean value equal to the frequency of the direct up-link signal. Since the wavelength of the S-band signal is very small compared to the altitude of the spacecraft, the phase of the multipath signal with respect to the direct signal will essentially be random. This is to say that the reflected signal will have gone through many revolutions (cycles) before it reaches the spacecraft--hence the probability that reflected signal leads the direct signal (θ positive in Figure 5.3) is roughly the same as the probability that the reflected signal lags

USE FOR TYPEWRITTEN MATERIAL ONLY

US 4802 1434 REV. A-65

the direct signal (θ negative in Figure 5.3). Thus over a period of time, the leading and lagging reflected signals would average out and would not produce any net effect on the direct signal. Therefore, the possibility that up-link multipath is responsible for the doppler residuals must also be ruled out. This conclusion can be further substantiated by tracking data from LO III where perilune occurred at the edge of the lunar disc. In this circumstance the line of sight to the spacecraft did not intersect the moon and only half of the DSIF antenna beam intersected the moon. The part of the moon that is illuminated under these conditions is the edge portion where the moon's curvature will produce more diverse scattering of the up-link signal. In this case the reflected signal to the spacecraft would be minimal and the effects of multipath significantly reduced. Even under these conditions residuals were still found to exist. (See Figure 5.4).

5.3.3 One-Way Tracking Experiment - L.O. V

A post mission experiment was conducted with Lunar Orbiter V in which the spacecraft was tracked one way through perilune and apolune in a further attempt to investigate the possibility that up-link multipath may be responsible for the doppler residuals.

Figure 5.5, illustrates the one-way doppler and doppler rates which existed during this experiment. The signal strength at the DSIF receiver was -142 dbm during the track. For the tracking loop of the DSIF receiver, this corresponded to a SNR of -142-(-166) = 24 db over design threshold (for $2 B_{LO}$ = 12 Hz). At this SNR the loop is capable of tracking a doppler rate of 115 Hz/sec with a frequency offset up to ± 70 KHz (Reference 5). The maximum frequency offset during the experiment was approximately 43 KHz with a peak doppler rate of 2 Hz/sec. This is well within the tracking capabilities of the loop so it is extremely unlikely that any errors were introduced into the tracking data by the doppler extraction system.

5.4 RESULTS

The spacecraft received signal strength during all Lunar Orbiter missions was of sufficient magnitude that the transponder phase lock loop was always operating under strong signal conditions. Under these conditions the loop was always operating well within its capability to track the received ground signal.

The largest stress which the transponder loop experienced was the frequency offset introduced in Missions III through V. During these missions the total frequency offset--DSIF transmitter bias and doppler shift--approached 55 KHz; this still was more than 8 KHz within the capability of the loop.* Missions I and II did not have any frequency bias introduced by the DSIF transmitter, and the stress experienced by the loop was an offset on the order of 15 KHz--more than 48 KHz within the capability of the loop.* Since residuals occurred through all missions, there is no reason to believe that the loop performed any less satisfactorily during the last three missions than during the first two.

* (For a received signal level -110 dbm)

USE FOR TYPEWRITTEN MATERIAL ONLY

US 4802 1434 REV 8-65

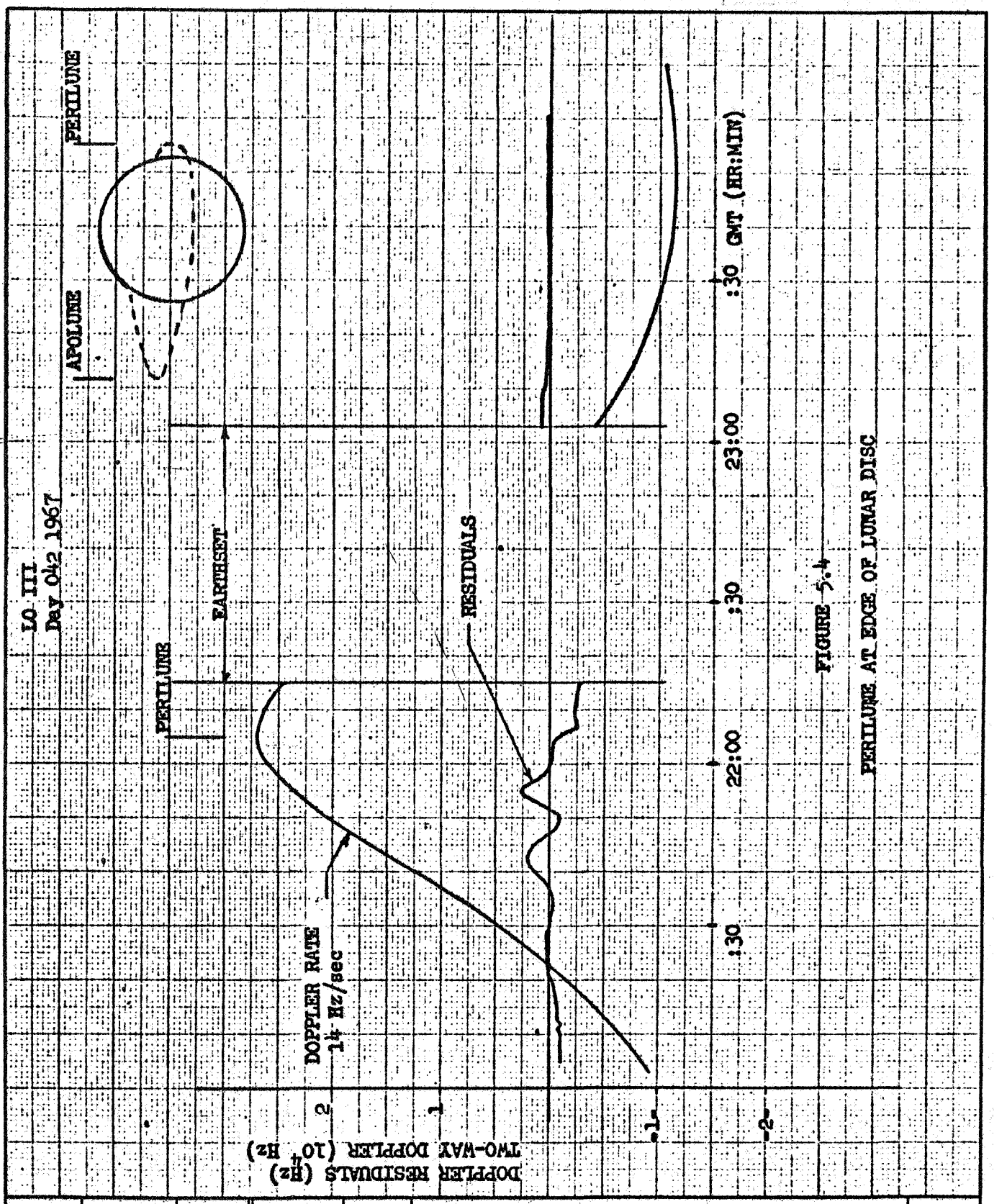

FIGURE 5.4
PERILUNE AT EDGE OF LUNAR DISC

	INITIALS	DATE	REV BY INITIAL	DATE	TITLE	MODEL
CALC						FIG 5.4
CHECK						
APPD.						
APPD.						

U3 4013 8000 REV. 1/66

REV LTR_____

BOEING NO.

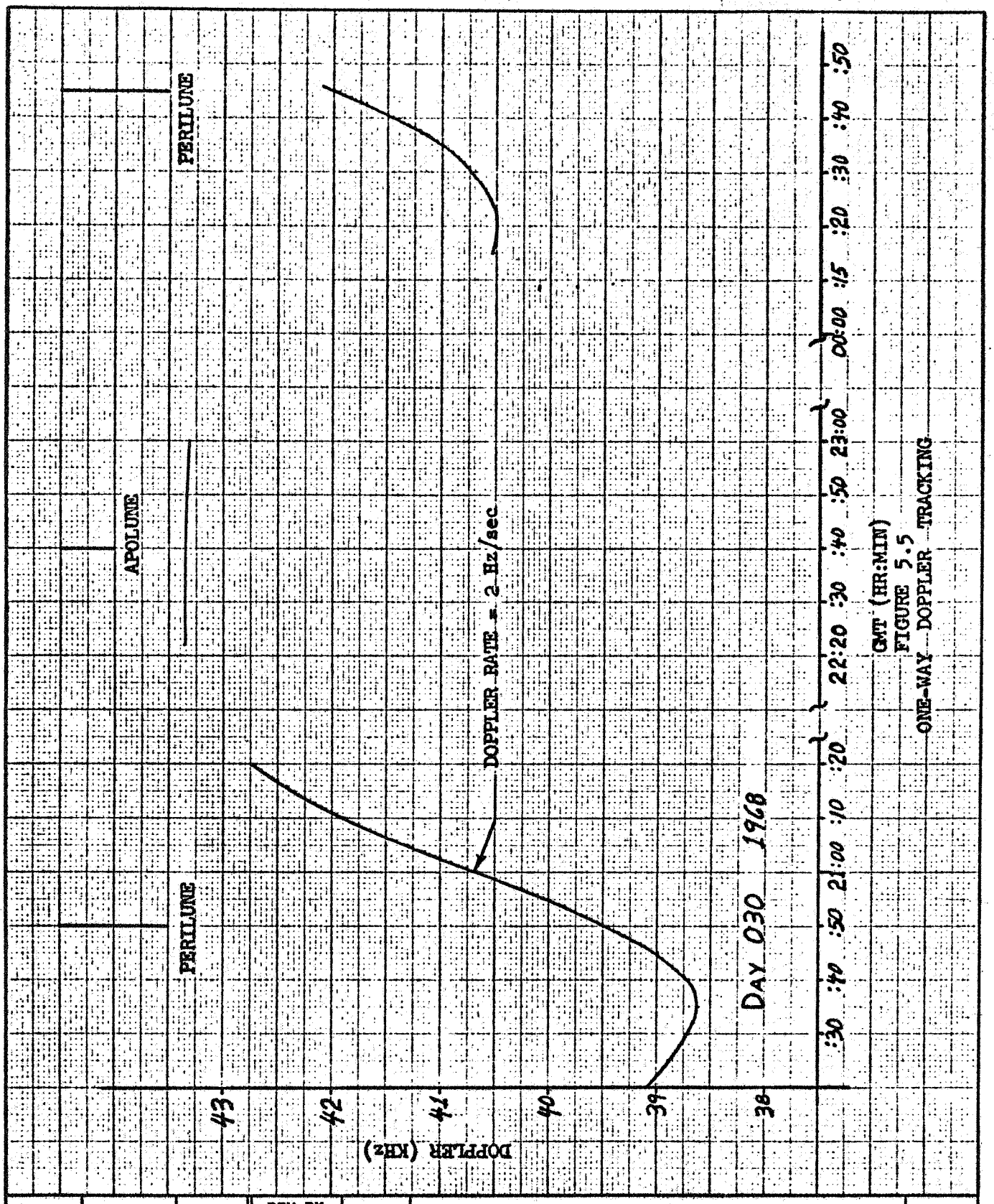

FIGURE 5.5
ONE-WAY DOPPLER TRACKING

	INITIALS	DATE	REV BY INITIAL	DATE	TITLE	MODEL
CALC						Fig 5.5
CHECK						
APPD.						
APPD.						

U3 4013 8000 REV. 1/66

REV LTR

BOEING NO.

SH.

The DSIF received signal strength during all missions was of sufficient magnitude that the signal-to-noise ratios which existed in the receiver phase lock loop were 21 db to 31 db over design threshold for the $2 B_{LO} = 12$ Hz noise bandwidth. At these SNR's the loop was always well within its tracking capabilities by a substantial margin so there is little reason to believe that any discrepancies were introduced into the doppler extraction by the DSIF receiving system.

Multipath has also been investigated as a possible cause for the doppler residuals. Downlink multipath had already been ruled out because previous experiments had shown that residuals were still present even when tracking was conducted with the spacecraft in a high power mode. The directional antenna used by the spacecraft for transmission in this mode results in the direct signal being at least 37 db larger than the reflected signal.

Analysis of uplink multipath has shown that the reflected signal is on the order of 11.5 db less than the direct signal for a worst case condition (maximum reflected signal). For this value of reflected signal strength, and because of the special phase relationships required for multipath interference, there is little reason to believe that uplink multipath is responsible for the doppler residuals.

5.5 CONCLUSION

The conclusion of this study is that the doppler residuals were not caused by the Spacecraft-DSIF data acquisition system.

USE FOR TYPEWRITTEN MATERIAL ONLY

US 4802 1434 REV. A-AR

6.0 ONE-WAY DOPPLER TRACKING

6.1 INTRODUCTION

An experiment involving one-way doppler tracking of the Lunar Orbiter V spacecraft was accomplished to determine if one way data exhibits residual oscillations similar to that prevalent in two and three way doppler data. One way tracking involves the use of an oscillator on-board the spacecraft as a frequency reference for the doppler tracking. This is in comparison to the normal two-way doppler tracking where the frequency reference is at the tracking station and the spacecraft acts mainly as a signal reflector. The experiment was conducted to eliminate uplink electronics and multipath effects as a possible cause of the residual phenomenon.

6.2 METHOD OF ATTACK

On Days 30 and 31 of 1967 Lunar Orbiter V was tracked one-way during perilune passage on two orbits and the included apolune region. Analysis of the data obtained during this period was accomplished for the major purpose of determining if the perilune residuals are present in the one-way tracking data. The data at apolune was analyzed to verify that variations in doppler residuals were only present at perilune.

The orbital geometry at the time of the experiment is indicated in Table 6.1.

Epoch: Day 30 20^h 49^m 25.18^s

Semi-major axis	2831.57 km
Eccentricity	0.328267
Argument of periapsis	6.45 deg
Longitude of ascending node	283.38 deg
Inclination	84.68 deg
Perilune radius	1902.1 km
Apolune radius	3761.1 km
Sun longitude	170.45 deg. E
Sun latitude	1.44 deg. S
Earth longitude	5.30 deg. E
Earth latitude	5.40 deg. N
Perilune longitude	76.03 deg. W
Perilune latitude	6.42 deg. N

ORBITAL ELEMENTS SELENOGRAPHIC OF DATE COORDINATES
TABLE 6.1

USE FOR TYPEWRITTEN MATERIAL ONLY

A pictorial representation of the geometry is presented in Figure 6.1.

6.3 ANALYSIS

Analysis of Lunar Orbiter V one-way tracking data required a period of two and three-way tracking in order to obtain an accurate state vector solution. The lack of temperature control of the spacecraft's auxiliary oscillator caused frequency drifts which would not allow the use of one-way doppler data for orbit determination.

The change in transponder temperature during the experiment period is shown in Figure 6.2, based on spacecraft telemetry data. The overall downward trend in temperature is due to the gyro drift which is increasing the off-sun angle. The small oscillations are due to limit cycling within the IRU*(Inertial Reference Unit) dead-band (±2 degrees). This limit cycling can be seen in Figure 6.3 during the time period of interest. The yaw position error is most significant since the off-sun angle was predominantly about the yaw axis and changes in yaw position will have the greatest effect on transponder temperature.

Telemetry acquired during the experiment period also provided data on solar array current as plotted in Figure 6.4. There is a direct relation between array current and the spacecraft off-sun angle which is the dominant factor causing changes in transponder temperature. The combined effects of gyro drift and limit cycling are obvious from the figure where an increase in off-sun angle is indicated by a decrease in array current. From this data it is obvious that a partial solar eclipse of the spacecraft occurred about 2050 GMT on Day 30 during perilune passage. The rapid increase of solar array current and transponder temperature (Figure 6.2) after 0100 GMT Day 31 is due to a yaw maneuver back to the sun line in preparation for the impact maneuver of Lunar Orbiter V.

6.4 RESULTS

Processing of the one-way tracking data involved an initial solution for a state vector using two and three-way doppler data surrounding the experiment period. Using this as the best estimate of the spacecraft trajectory it was possible to remove the doppler shift due to tracking station, lunar and spacecraft relative motion. Removal of this doppler shift resulting in Figures 6.5, 6.6 and 6.7 which are plots of one-way doppler residuals for the three experiment periods. Transponder frequency changes caused by temperature variations are the obvious cause of the large doppler residuals in the one-way data.

The orbit determination program (ODPL) has the capability of removing a linear frequency drift from the one-way doppler data. In order to analyze this data it was necessary to determine regions of linear temperature change in which to apply the correction.

(text continued on page 69)

USE FOR TYPEWRITTEN MATERIAL ONLY

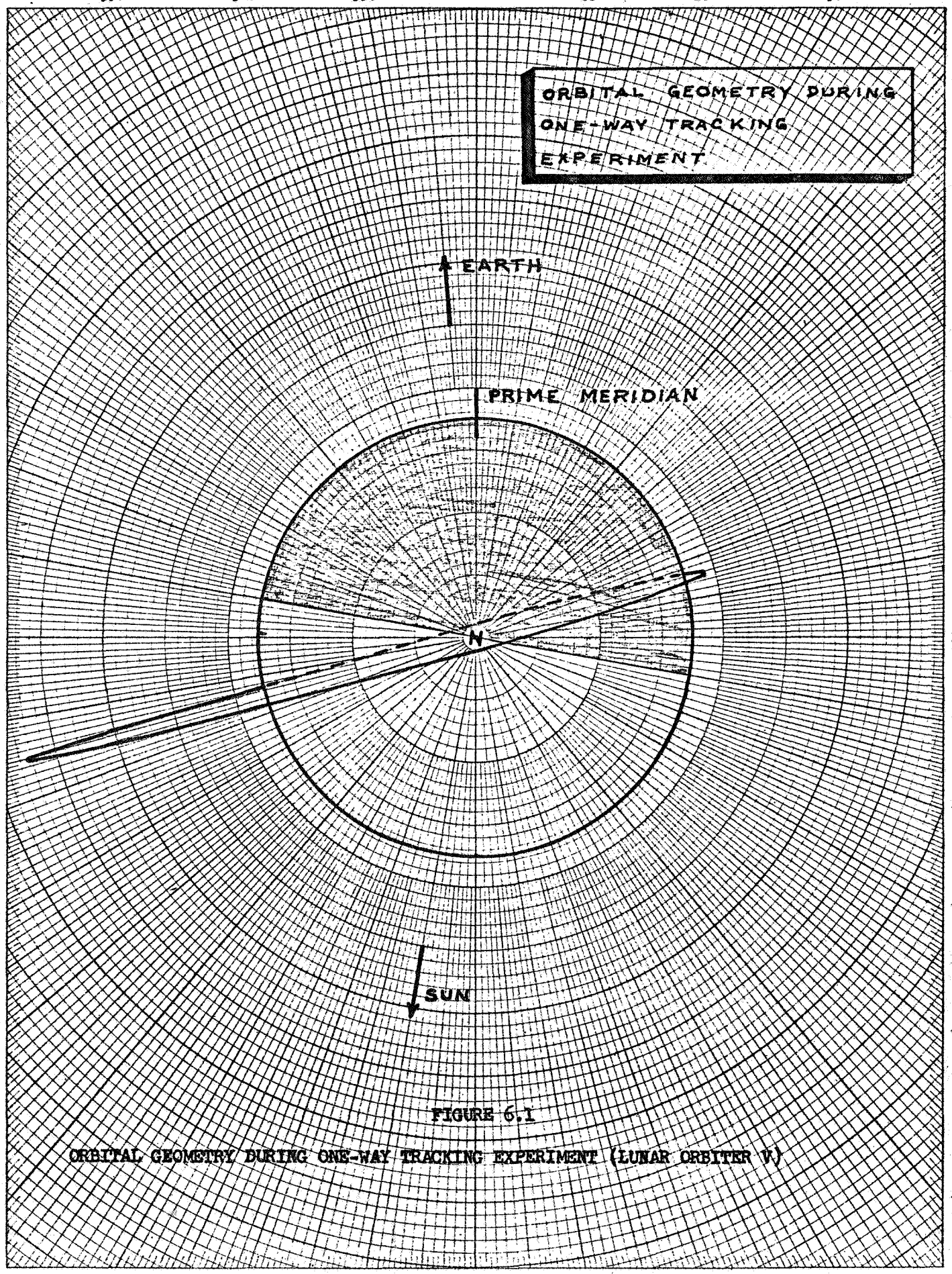

FIGURE 6.1

ORBITAL GEOMETRY DURING ONE-WAY TRACKING EXPERIMENT (LUNAR ORBITER V)

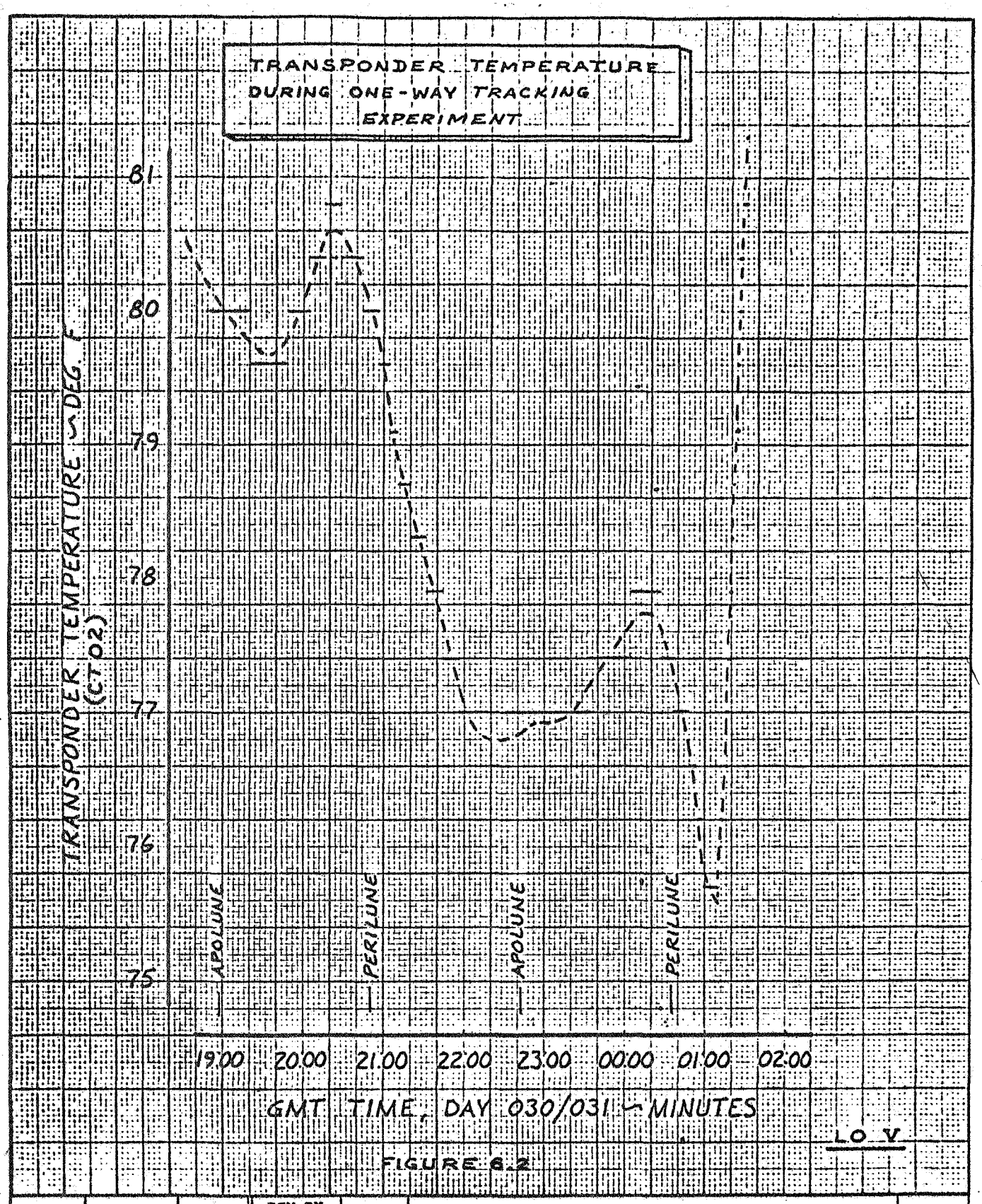

LO V

FIGURE 6.2

	INITIALS	DATE	REV BY INITIAL	DATE	TITLE	MODEL
CALC	GMD	3/7/68			LO V TRANSPONDER TEMPERATURE	FIG 6.2
CHECK						
APPD.						
APPD.						

U3 4013 8000 REV. 1/66

REV LTR

BOEING NO. D2 100817-1

SH.

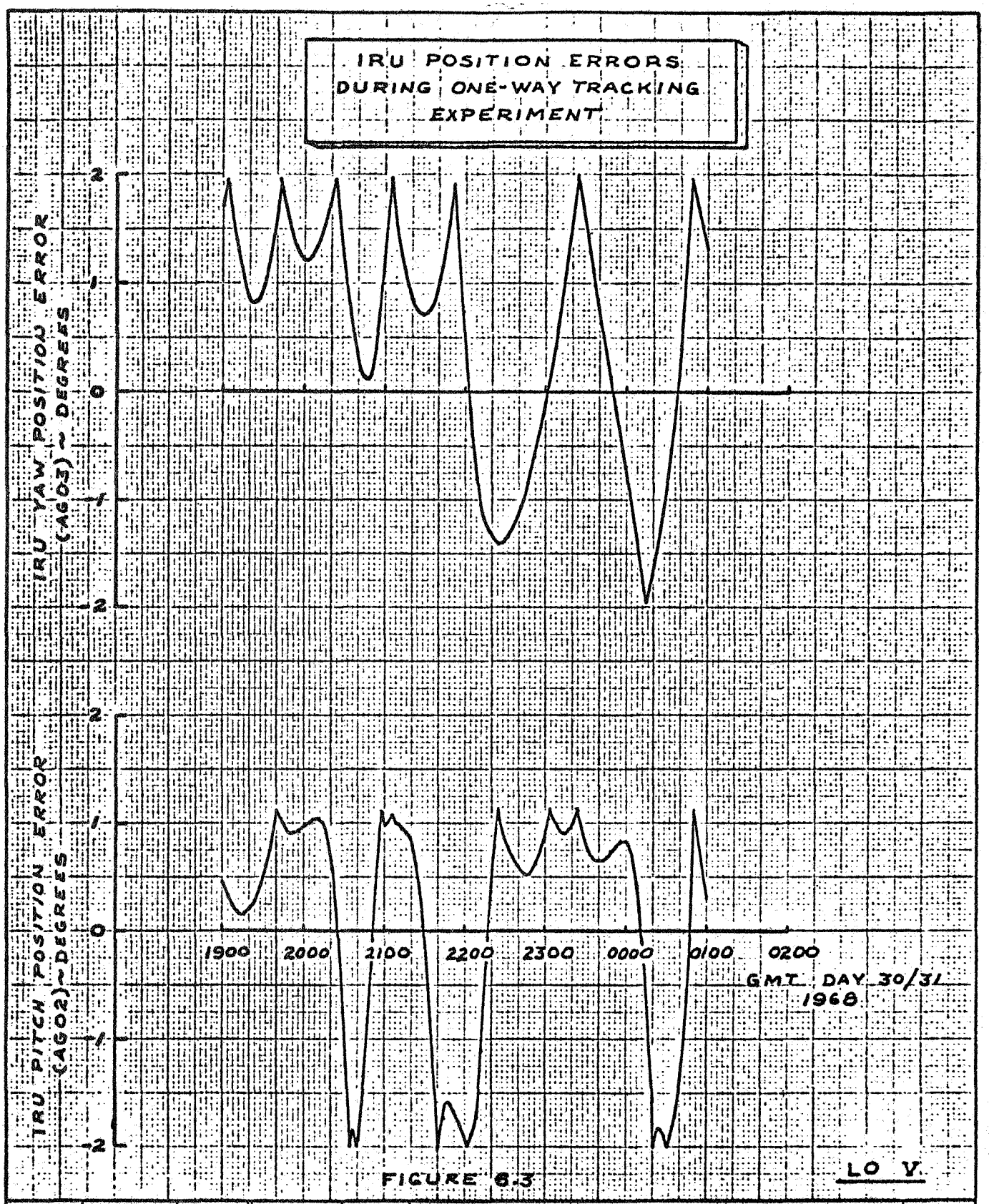

FIGURE 6.3

LO V.

	INITIALS	DATE	REV BY INITIAL	DATE	TITLE	MODEL
CALC	[illegible]	3-12-68				FIG 6.3
CHECK						
APPD.						
APPD.						

US 4013 8000 REV. 1/66

REV LTR

BOEING NO. D2 100817-1

SH. 61

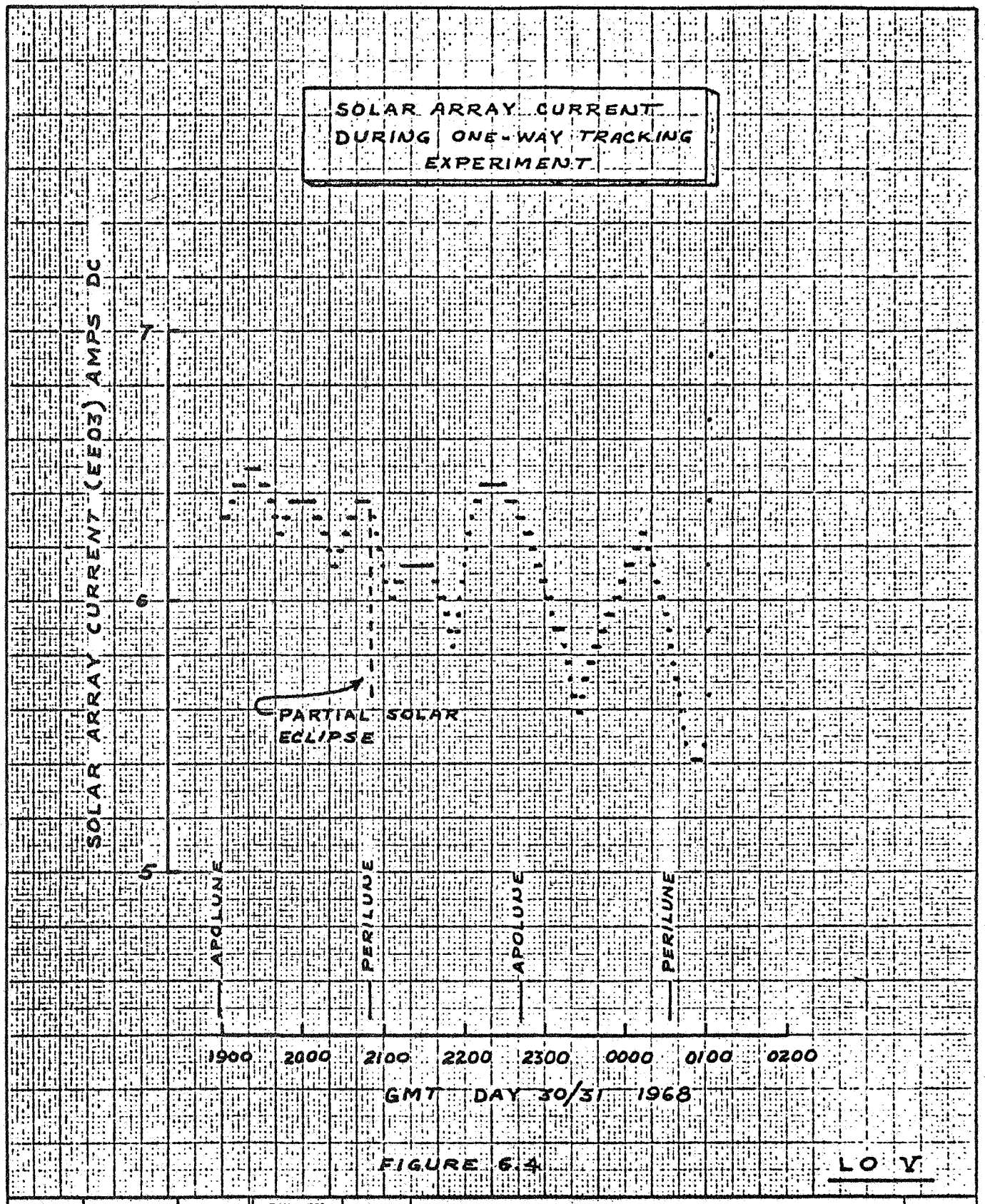

FIGURE 6.4

LOV

	INITIALS	DATE	REV BY INITIAL	DATE	TITLE	MODEL
CALC	YB	3-22-68				FIG 6.4
CHECK						
APPD.						
APPD.						

U3 4013 8000 REV. 1/66

REV LTR

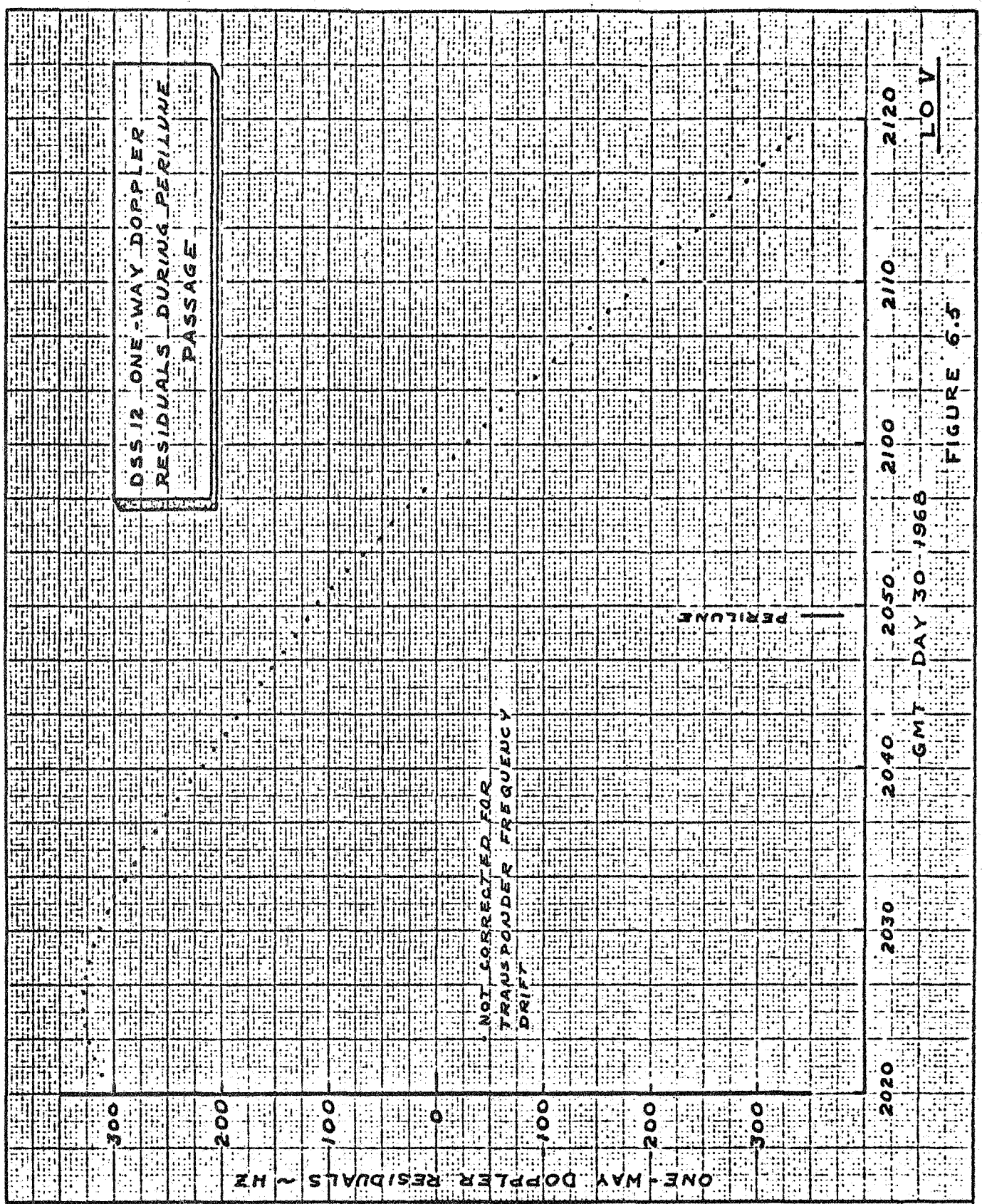

FIGURE 6.5

	INITIALS	DATE	REV BY INITIAL	DATE	TITLE	MODEL
CALC	YB	3-15-68				FIG 6.5
CHECK						
APPD.						
APPD.						

U3 4013 8000 REV. 1/66

REV LTR

BOEING NO. D2 100817-1

SH.

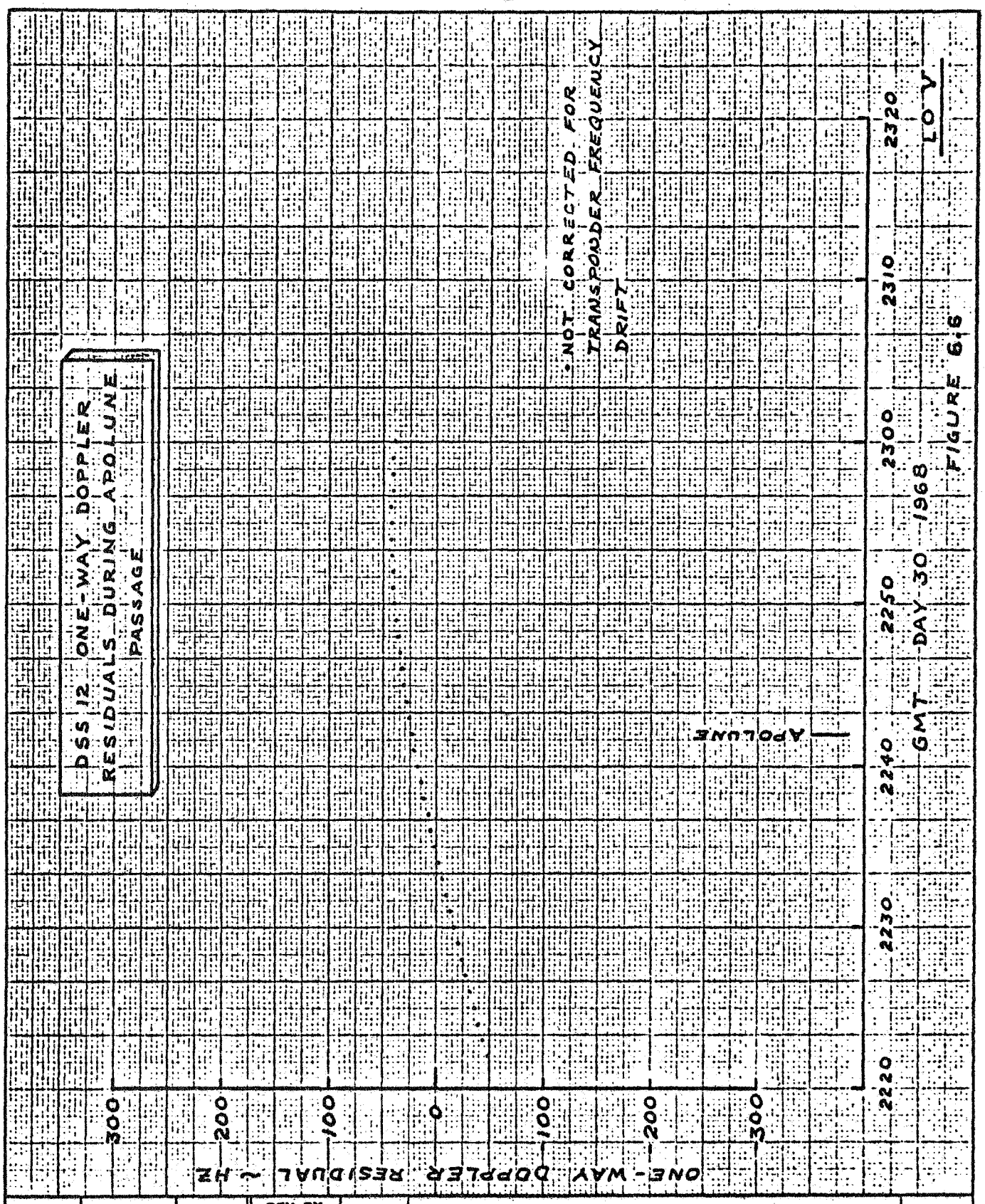

FIGURE 6.6

	INITIALS	DATE	REV BY INITIAL	DATE	TITLE	MODEL
CALC	HB	2-15-68				FIG 6.6
CHECK						
APPD.						
APPD.						

U3 4013 8000 REV. 1/66

REV LTR

	INITIALS	DATE	REV BY INITIAL	DATE	TITLE	MODEL
CALC	YB	7-12-68				FIG. 6.7
CHECK						
APPD.						
APPD.						

U3 4013 8000 REV. 1/66

REV LTR

The processing of doppler data during apolune passage required little initial analysis since the transponder temperature remained relatively constant during the time period (Figure 6.8). The solar array current plotted from telemetry data in Figure 6.9, indicates the gradual drift of the spacecraft off the sun line. The orbit determination program was then used to removed the linear frequency drift which resulted in the doppler residual curve shown in Figure 6.10. The noise level on the data has been attributed to the inaccuracy of the frequency standard on board the spacecraft.

Processing the doppler data during perilune passage required a more thorough analysis of the transponder temperature variations. Figure 6.11 indicates the temperature changes during this time period. The solar array current plotted in Figure 6.12 indicates the reason for the non-linear temperature variation. In order to process this data it was necessary to select time intervals where the temperature change was linear. Three of these intervals were found and the results are shown in Figure 6.13. Also included in this figure is an example of two-way doppler residuals occurring in the tracking data two orbits prior to the experiment period. The general shapes of the two curves indicate very good agreement. It appears that the doppler noise level is directly proportional to the doppler rate since at apolune the rate is 0.25 Hz/sec and at perilune the rate is 2 Hz/sec.

6.5 CONCLUSIONS

Based on the results of this study it can be stated that cyclic residuals exist in the one-way doppler data at perilune which are similar to the two and three-way doppler residuals in evidence during all Lunar Orbiter missions. Also the absence of such an effect at apolune is obvious.

This study, in effect, removes as a possible cause of perilune doppler residuals the station and spacecraft uplink electronics and also the uplink multipath effect (interference of reflected and direct signals to the spacecraft).

A secondary effect of this study is the obvious poor quality of one-way tracking data for use in the orbit determination process due to its sensitivity to temperature variations.

USE FOR TYPEWRITTEN MATERIAL ONLY

US 4802 1434 REV. 8-65

TRANSPONDER TEMPERATURE DURING APOLLUNE PASSAGE

TRANSPONDER TEMPERATURE
DEG F (CTO2)

78
77
76

APOLLUNE

GMT DAY 30 1968

2320
2310
2300
2250
2240
2230
2220

LOY

FIGURE 6.8

	INITIALS	DATE	REV BY INITIAL	DATE	TITLE	MODEL
CALC	HB	4-1-68				F16
CHECK						6.8
APPD.						
APPD.						

US 4013 8000 REV. 1/66

REV LTR

FIGURE 6.9

	INITIALS	DATE	REV BY INITIAL	DATE	TITLE	MODEL
CALC	LB	4-1-68				FIG 6.9
CHECK						
APPD.						
APPD.						

U3 4013 8000 REV. 1/66

REV LTR

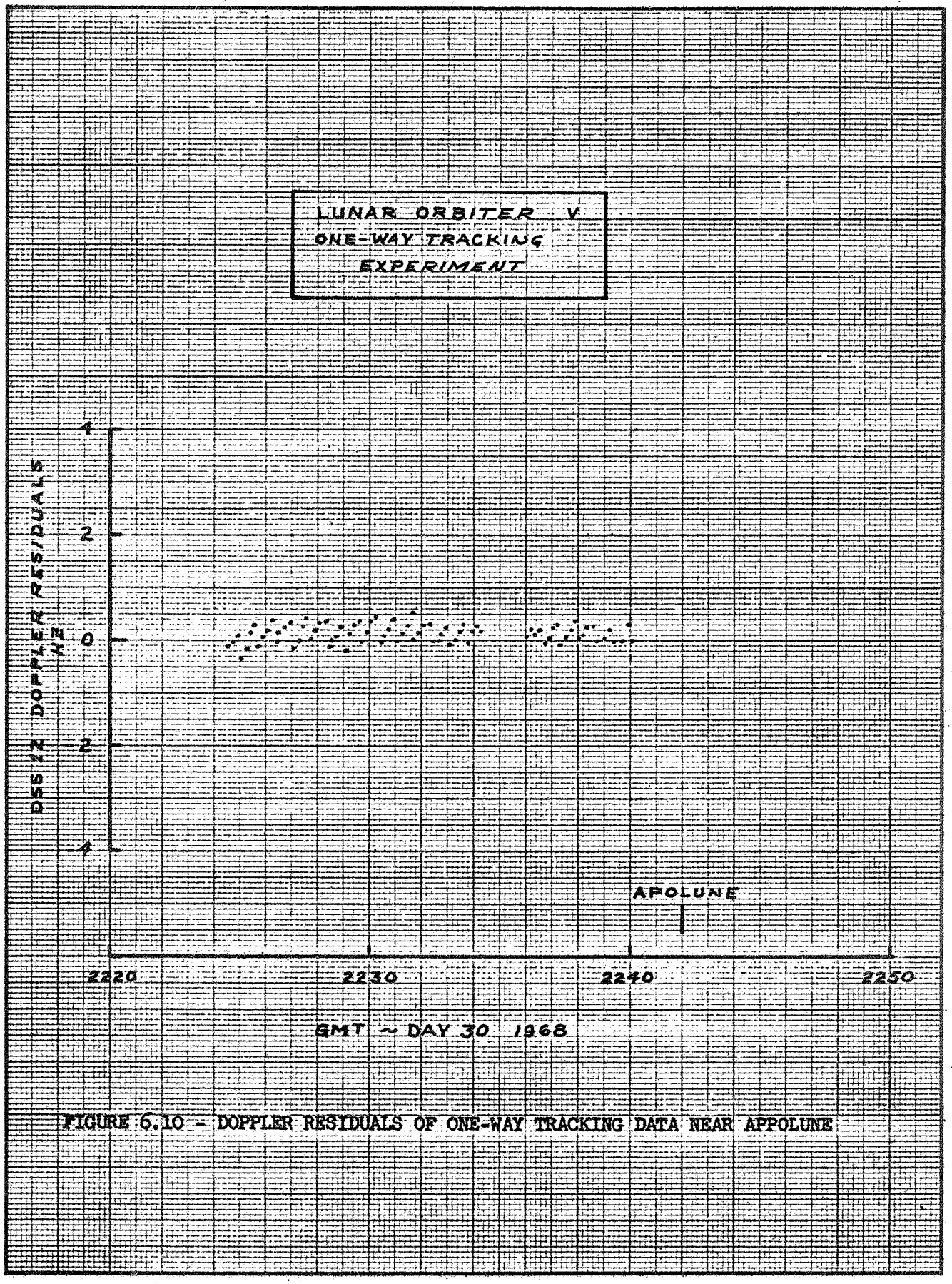

FIGURE 6.10 - DOPPLER RESIDUALS OF ONE-WAY TRACKING DATA NEAR APPOLUNE

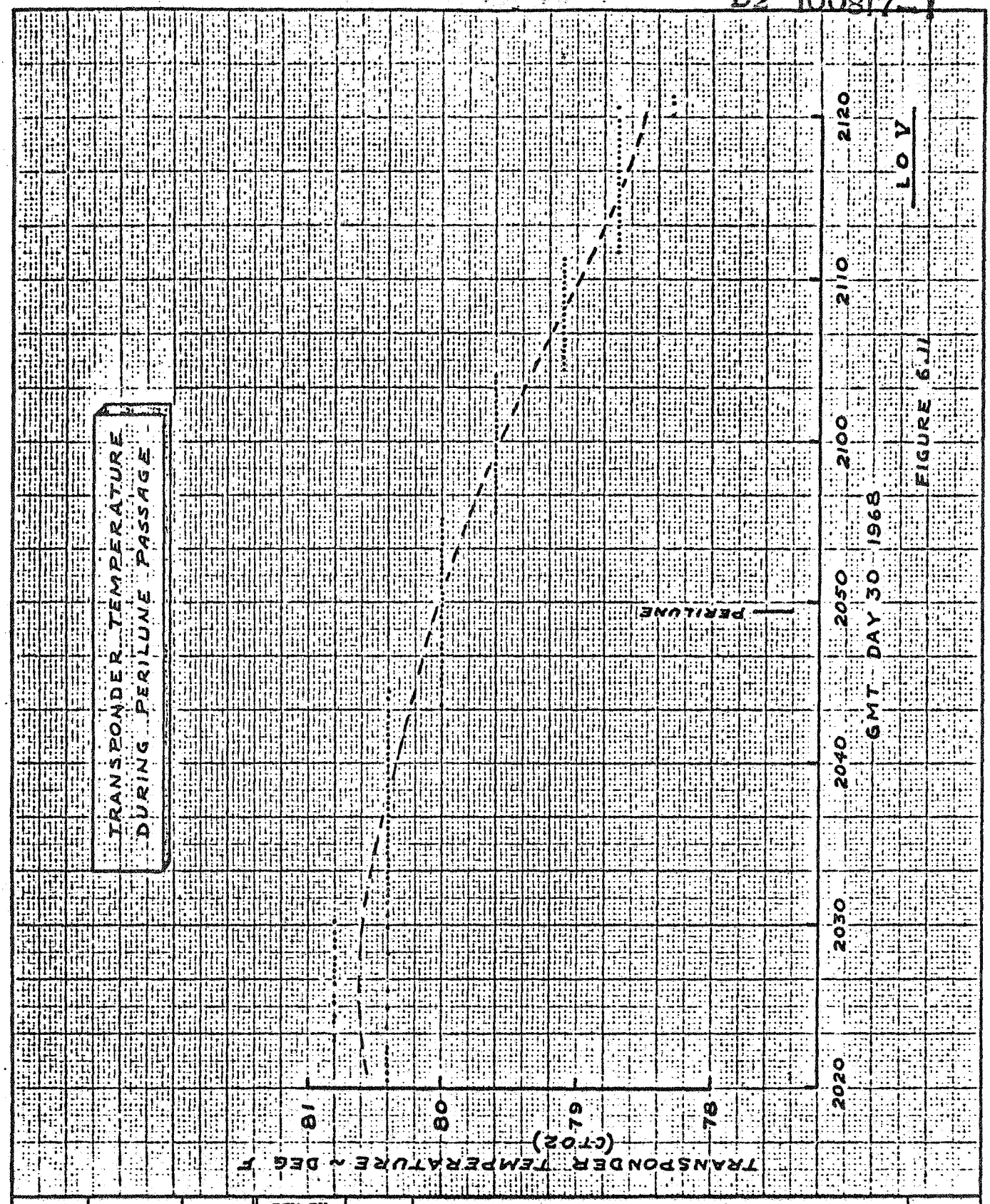

	INITIALS	DATE	REV BY INITIAL	DATE	TITLE	MODEL
CALC	UB	3-12-68				FIG 6.11
CHECK						
APPD.						
APPD.						

U3 4013 8000 REV. 1/66

REV LTR

BOEING NO.

SH. 73

FIGURE 6.12

	INITIALS	DATE	REV BY INITIAL	DATE	TITLE	MODEL
CALC	MB	3-14-68				FIG 6.12
CHECK						
APPD.						
APPD.						

U3 4013 8000 REV. 1/66

REV LTR

BOEING NO.

SH.

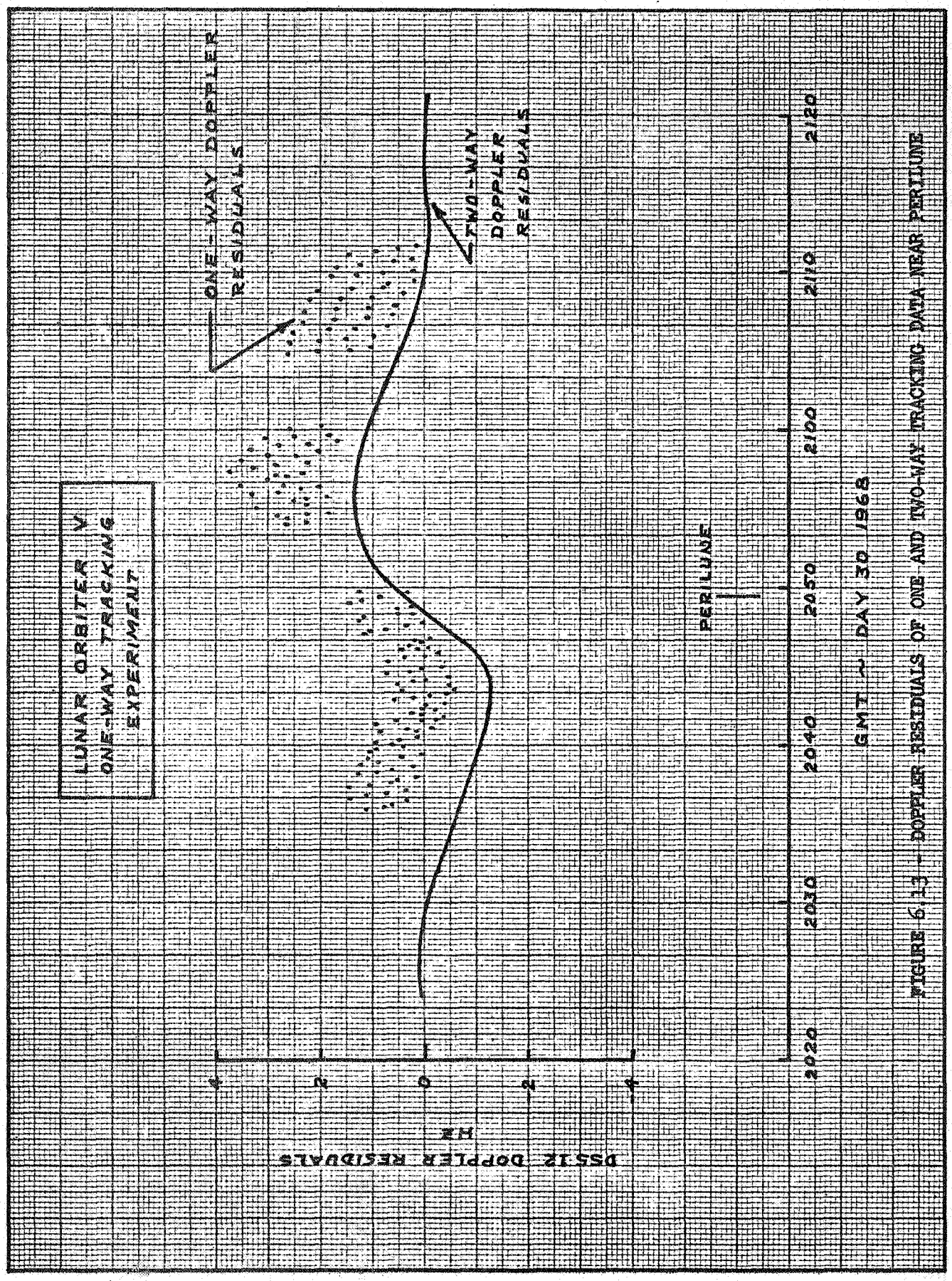

FIGURE 6.1-3 - DOPPLER RESIDUALS OF ONE AND TWO-WAY TRACKING DATA NEAR PERILUNE

7.0 LUNAR ATMOSPHERE

7.1 INTRODUCTION

The possibility that the presence of a residual atmosphere due to a cometary impact could contribute to the residual phenomenon was investigated. It is possible that the least-squares fitting procedure can lead to misleading results when an incorrect model is used. The effect of an unmodeled parameter can be hidden by variations in other parameters (in the fit) with which it is correlated. The presence of an atmosphere would necessarily cause a delay in the orbital period of the spacecraft but the fact that drag was not modeled in the orbit determination program makes it possible that a secular decoy in orbital period could be hidden in the least-squares fitting procedure. A direct measurement of the orbital period of the spacecraft would resolve the question.

7.2 METHOD OF ATTACK

An experiment conducted with Lunar Orbiter V made it possible to directly measure the orbital period of the spacecraft. The experiment involved the recording of spacecraft sun occultation times to an accuracy of 0.1 seconds. The recordings were accomplished over a time period of 35 days which allowed a study of any secular trend in the spacecraft orbital period.

7.3 ANALYSIS

The time period between two successive sun occultations is not a direct measure of the orbital period. The fact that the angle between the sun line and the orbit normal is changing at the rate of approximately one degree a day indicates that the occultations take place at a different lunar position each orbit. This implies that the time between successive sun occultations must be modified to account for this rotation in order to obtain the true orbital period. The data acquired during the experiment is shown in Figure 7.1.

7.4 RESULTS

The data obtained during the experiment was modified to obtain the true orbital period. A plot of the results are shown in Figure 7.2.

A preliminary analysis was performed to determine if an atmosphere could cause residuals of the proper magnitude. As a sample case the Lunar Orbiter III Apollo type orbit (perilune altitude = 150 km, apolune altitude = 350 km) was chosen for comparison. This orbit was selected because of the relatively low altitude during the whole orbital period.

USE FOR TYPEWRITTEN MATERIAL ONLY

US 4802 1434 REV. 8-65

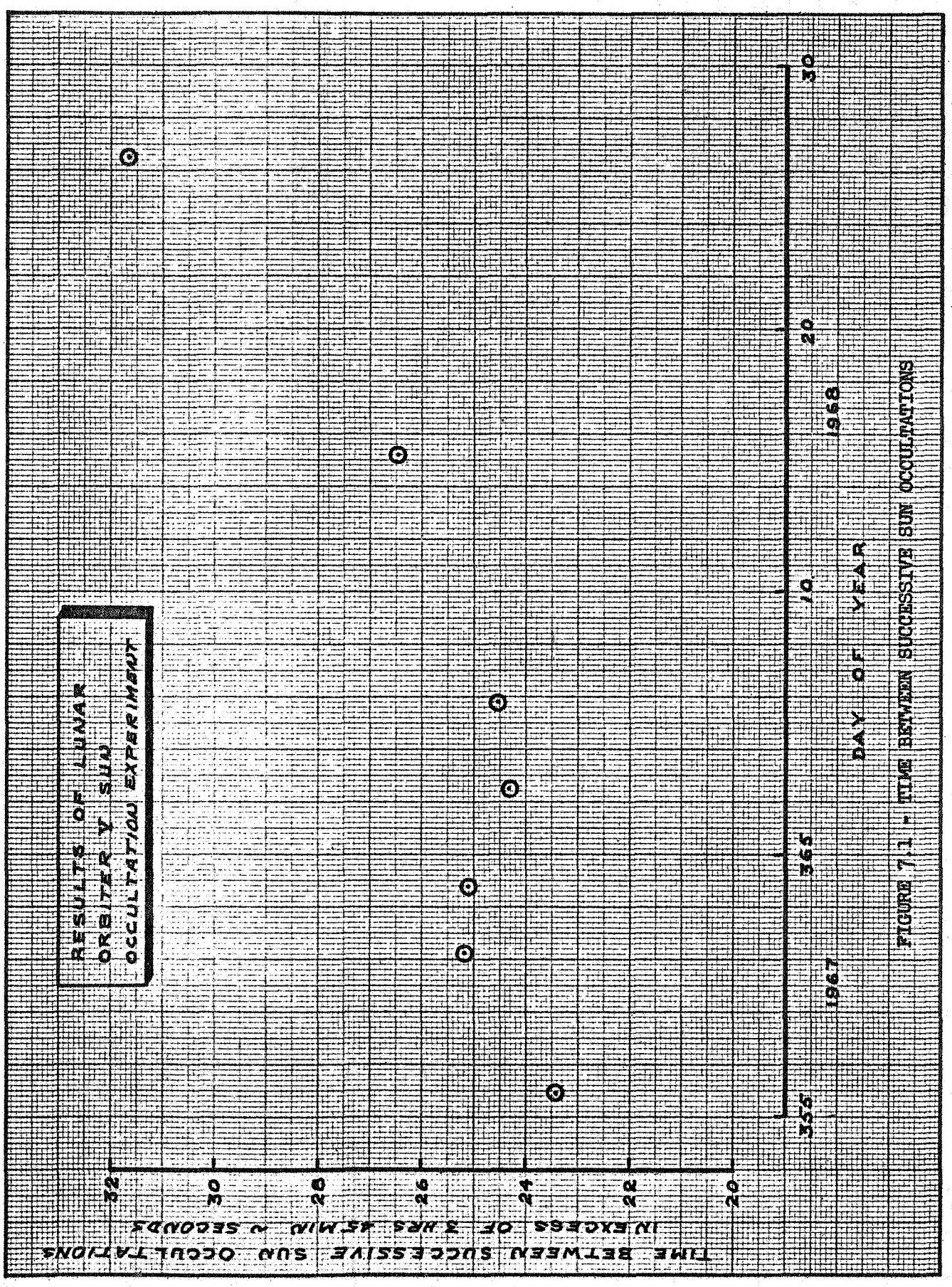

FIGURE 7.1 - TIME BETWEEN SUCCESSIVE SUN OCCULTATIONS

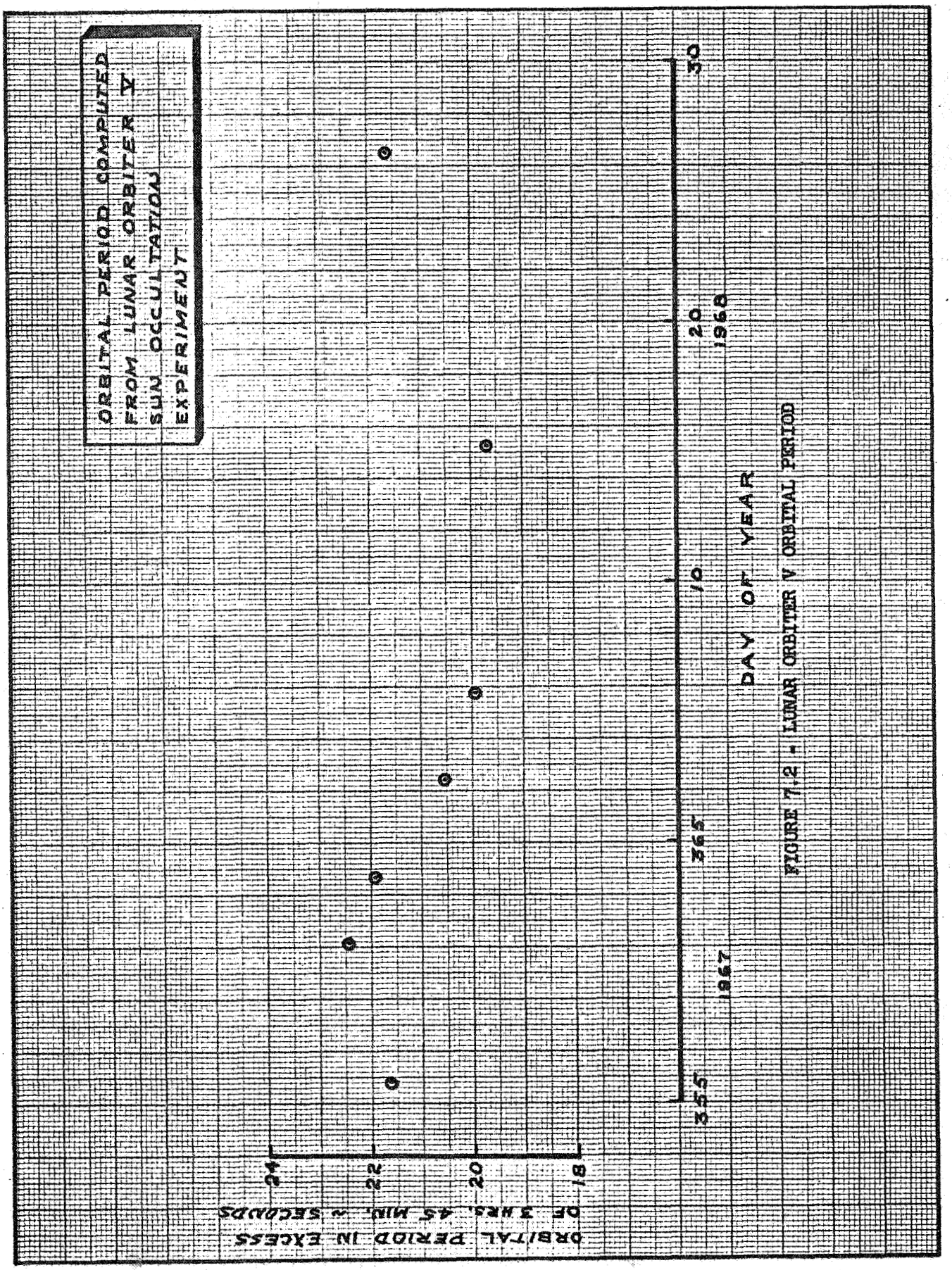

FIGURE 7.2 - LUNAR ORBITER V ORBITAL PERIOD

The radial velocity equation was used to compute doppler residuals from deviations of orbital elements :

$$\text{Radial Velocity} = \sqrt{\frac{\mu}{a(1-e^2)}} \sin i \left[e \cos\omega + \cos(\vartheta + \omega) \right]$$

a = semi-major axis

e = eccentricity

i = plane-of-sky inclination

ω = plane-of-sky argument of perilune

ϑ = true anomaly

μ = lunar gravitational constant

Doppler shift (Hz) = radial velocity (km/sec.) x 15,300

Doppler Residual (Hz) = observed doppler (Hz) - predicted doppler (Hz)

By integrating the effects of suspected perturbing sources (e.g. lunar atmosphere) over one or more orbits, the characteristic residual signature of a given perturbation due to a lunar atmosphere is shown in Table 7.1.

Nominal Selenographic Orbital Elements:

Semi-major axis	=	1968.1 km
Eccentricity	=	0.0435
Inclination	=	20.88 deg.
Argument of periapsis	=	-5.69 deg.
Longitude of ascending node	=	60.36 deg.

Perturbations at End of 2 Orbits Due to Drag:

Semi-major axis	=	-0.16 km
Eccentricity,	=	-0.00002

Atmosphere Definition:

Base density at 50 km	=	0.35 kg/km^3
Scale height	=	226 km

TABLE 7.1
ORBITAL ELEMENT PERTURBATIONS DUE TO SELECTED LUNAR ATMOSPHERE

USE FOR TYPEWRITTEN MATERIAL ONLY

The corresponding residuals are compared to the actual orbit determination residuals in Figure 7.3. It should be noted that the effects of perturbations on the orbit are cumulative; hence, the residuals will increase in size as time progresses. However, the actual residuals are computed by the orbit determination program such that any cumulative efforts have been averaged out.

7.5 CONCLUSIONS

In order for an atmosphere to be the cause of the residuals experienced in Lunar Orbit the density would have to be of a magnitude large enough to cause a significant decoy in orbital period. For the sample case investigated the decoy was an the order of 0.5 minutes per day. The results of the sun occultation data indicated that a decrease in period (in excess of 2 seconds) did not occur in the 35 days considered. It is obvious from this study that the existance of a significant lunar atmosphere is unlikely above the altitude of 100 km (perilune altitude of the Lunar Orbiter V orbit).

USE FOR TYPEWRITTEN MATERIAL ONLY

U3 4802 1434 REV. 8-65

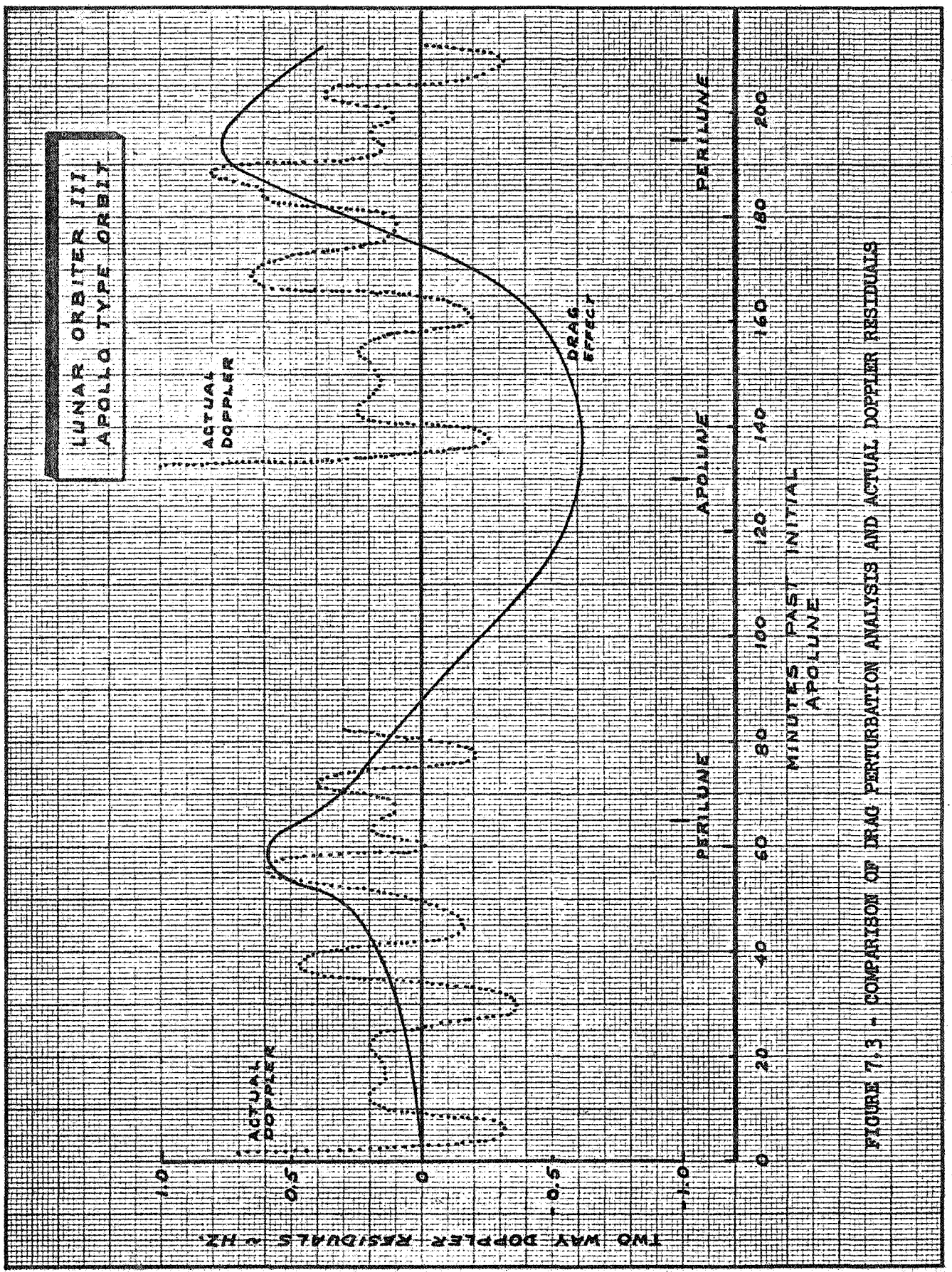

FIGURE 7.3 - COMPARISON OF DRAG PERTURBATION ANALYSIS AND ACTUAL DOPPLER RESIDUALS

8.0 SURFACE TERRAIN CORRELATION

8.1 INTRODUCTION

An investigation was performed to determine if irregular surface features in the form of highlands and lowlands could cause gravitational perturbations accounting for the residual phenomenon. These surface features could not be modeled by the relatively low order (fourth or seventh) lunar harmonic gravitational models used in the orbit determination program.

It was determined that Lunar Orbiter spacecraft flying over the same terrain had similar residual patterns. Figure 8.1 shows the residual pattern for Lunar Orbiters II and III passing over the same area. There are very distinct similarities in the two curves. The same two spacecraft passing over different lunar terrain again show similarities in their residual patterns. There are significant differences between this latter set of curves (Figure 8.2) and the previous set (Figure 8.1) indicating some correlation between doppler residuals and the spacecraft ground track.

8.2 METHOD OF ATTACK

An analysis similar to that described in Section 7.4 was used to determine if realistic surface features could cause residuals of the magnitude experienced during the Lunar Orbiter missions. For the example case used (Lunar Orbiter III Apollo type orbit) the spacecraft passed over a highland region at a relatively low altitude. This region was in the vicinity of the crater Longrenus and was simulated by a point mass perturbation located at the center of the crater.

A correlation of residual patterns resulting from single orbit OD fits to the surface terrain beneath the spacecraft was also attempted. The relative surface profile was obtained from the Lunar charts published by the Aeronautical Chart and Information Center (LAC).

8.3 ANALYSIS

The Lunar Orbiter III Apollo type orbit was used in this study since in the nearly circular orbit the effect of surface terrain (if improtant) would manifest itself in the doppler residuals throughout the whole orbit. The Lunar Orbiter II and III photographic orbits were also investigated since each spacecraft passed over similar lunar terrain at equivalent altitudes.

8.4 RESULTS

A comparison of residuals obtained from Lunar Orbiter data and those obtained from perturbation analysis (Section 7.4) due to surface irregularities is shown in Figure 8.3.

USE FOR TYPEWRITTEN MATERIAL ONLY

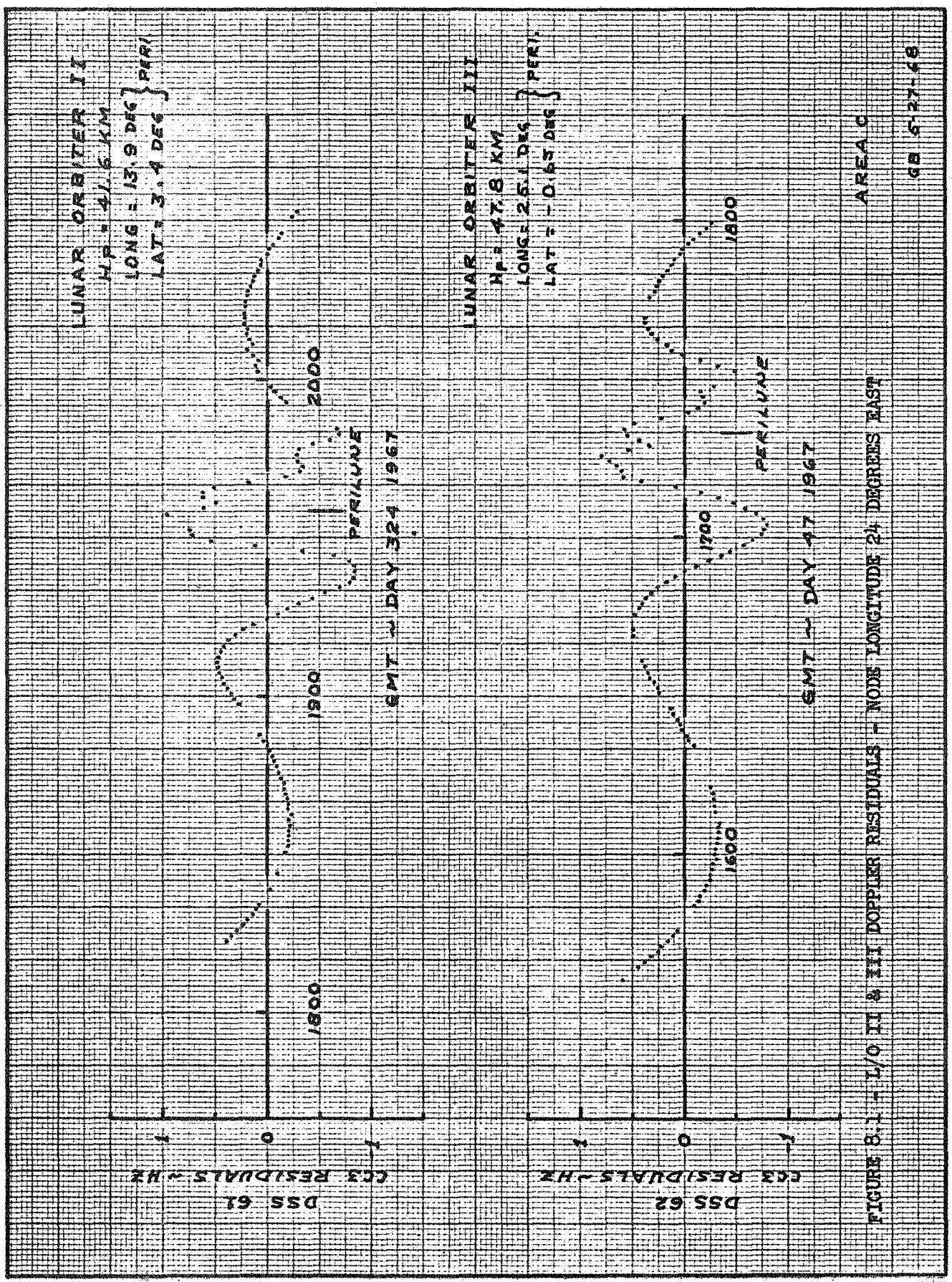

FIGURE 8.1 - L/O II & III DOPPLER RESIDUALS - NODE LONGITUDE 24 DEGREES EAST

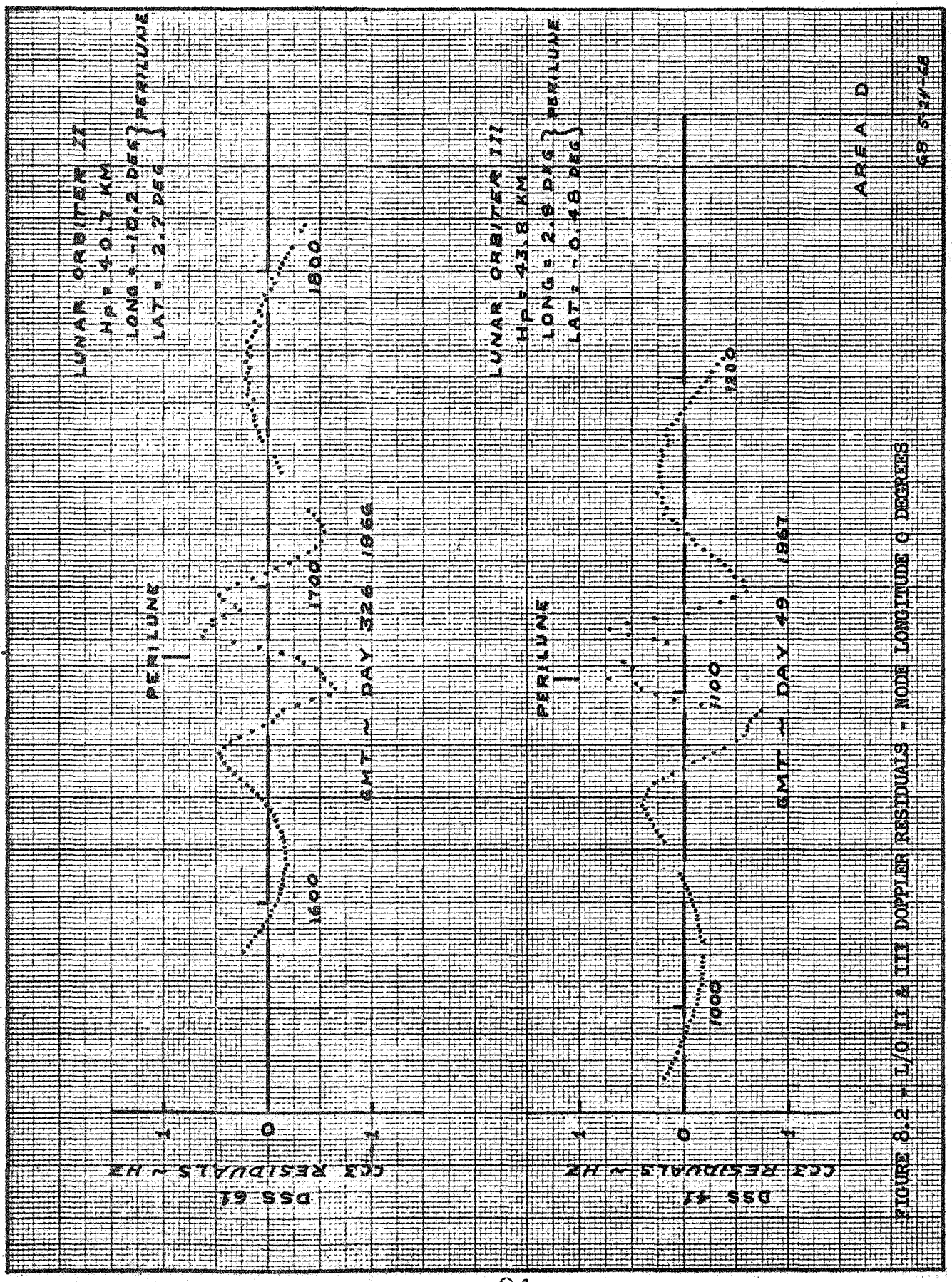

FIGURE 8.2 - L/O II & III DOPPLER RESIDUALS - NODE LONGITUDE 0 DEGREES

The point mass perturbation used for this study was located at the site of the crater Langrenus (longitude = 61° E, latitude = 9° S) at a radius of 1739 km. A gravitational constant of 0.005 km ^{3}/sec^2 was assigned to the point mass to simulate a mountain with an altitude of 3.6 km and a base diameter of 150 km.

At the completion of two orbits with only the presence of the point mass perturbing the flight path the following orbital elements were perturbed by the amount shown:

inclination = -0.001 degrees
time of periapsis passage = -0.04 seconds

all other elements remaining unchanged.

It is obvious from Figure 8.3 that the general shapes of the two residual curves do not agree but the maximum magnitude of the residuals do correspond.

Figure 8.4 indicates the residual pattern exhibited by the doppler data as the spacecraft passes over the surface terrain shown. Sharp spikes in the residuals are present when there is a drastic change in surface elevation beneath the spacecraft. Also the oscillations in the residuals correspond closely to the terrain changes.

8.5 CONCLUSIONS

It has been shown that doppler residuals of the magnitude experienced during the Lunar Orbiter missions can be simulated with perturbations caused by realistic lunar surface features. Other studies have also verified this result (References 9 and 10).

Correlations between residual patterns and the ground track of the spacecraft have been established by the investigation of residuals from different spacecraft passing over the same lunar terrain.

The low altitude, nearly circular orbit of Lunar Orbiter III exhibited a different trend in residuals than the other orbits. Normally the peak doppler residuals were in the region of the orbit periapsis but in the low orbit the maximum residuals occurred in various positions along the orbit. These peak residuals have been correlated to visible surface features in some cases and to masses buried beneath the lunar surface in other cases (Reference 11).

USE FOR TYPEWRITTEN MATERIAL ONLY

D3 4802 1434 REV. 8-65

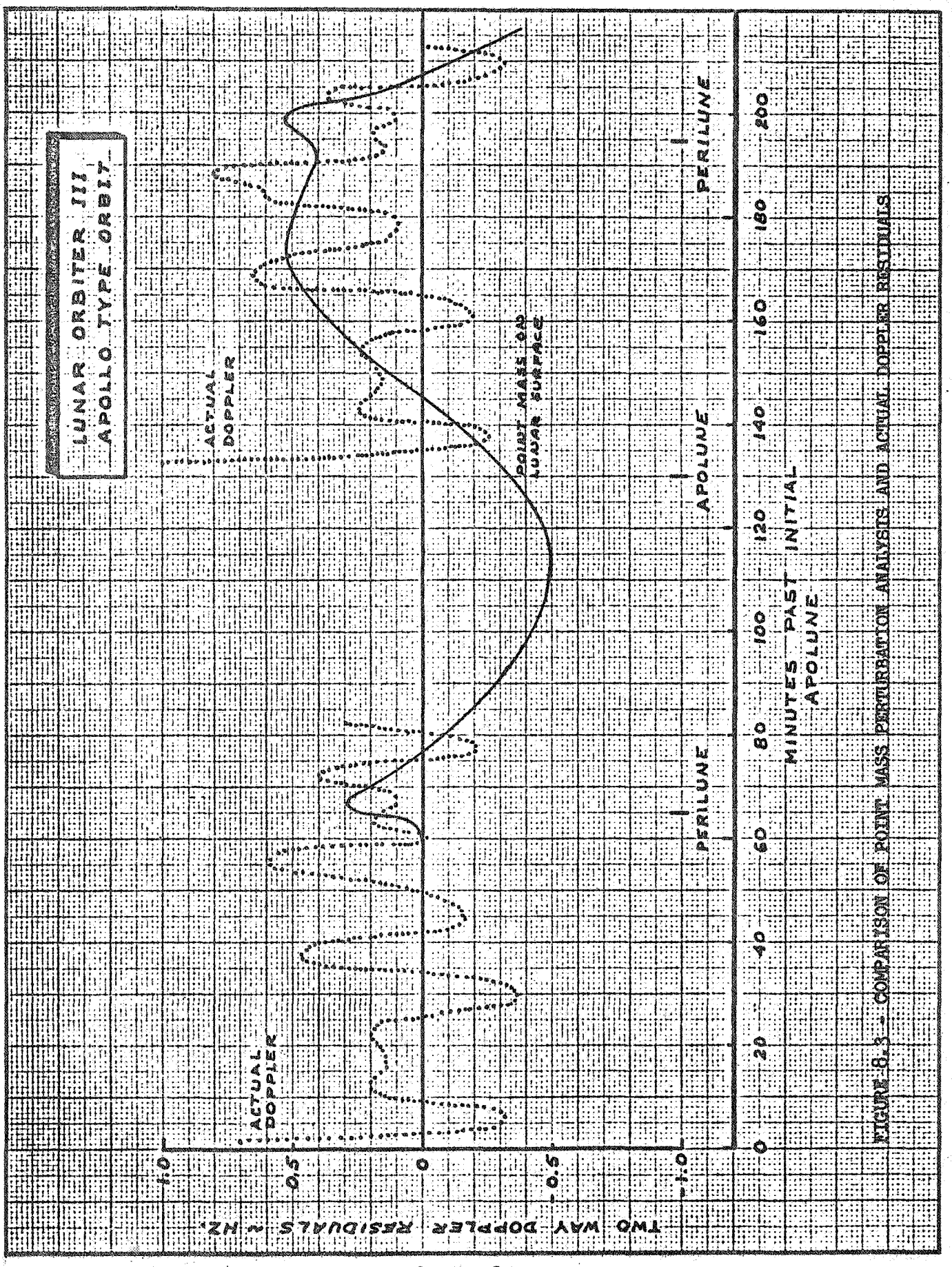

FIGURE 8.3 — COMPARISON OF POINT MASS PERTURBATION ANALYSIS AND ACTUAL DOPPLER RESIDUALS

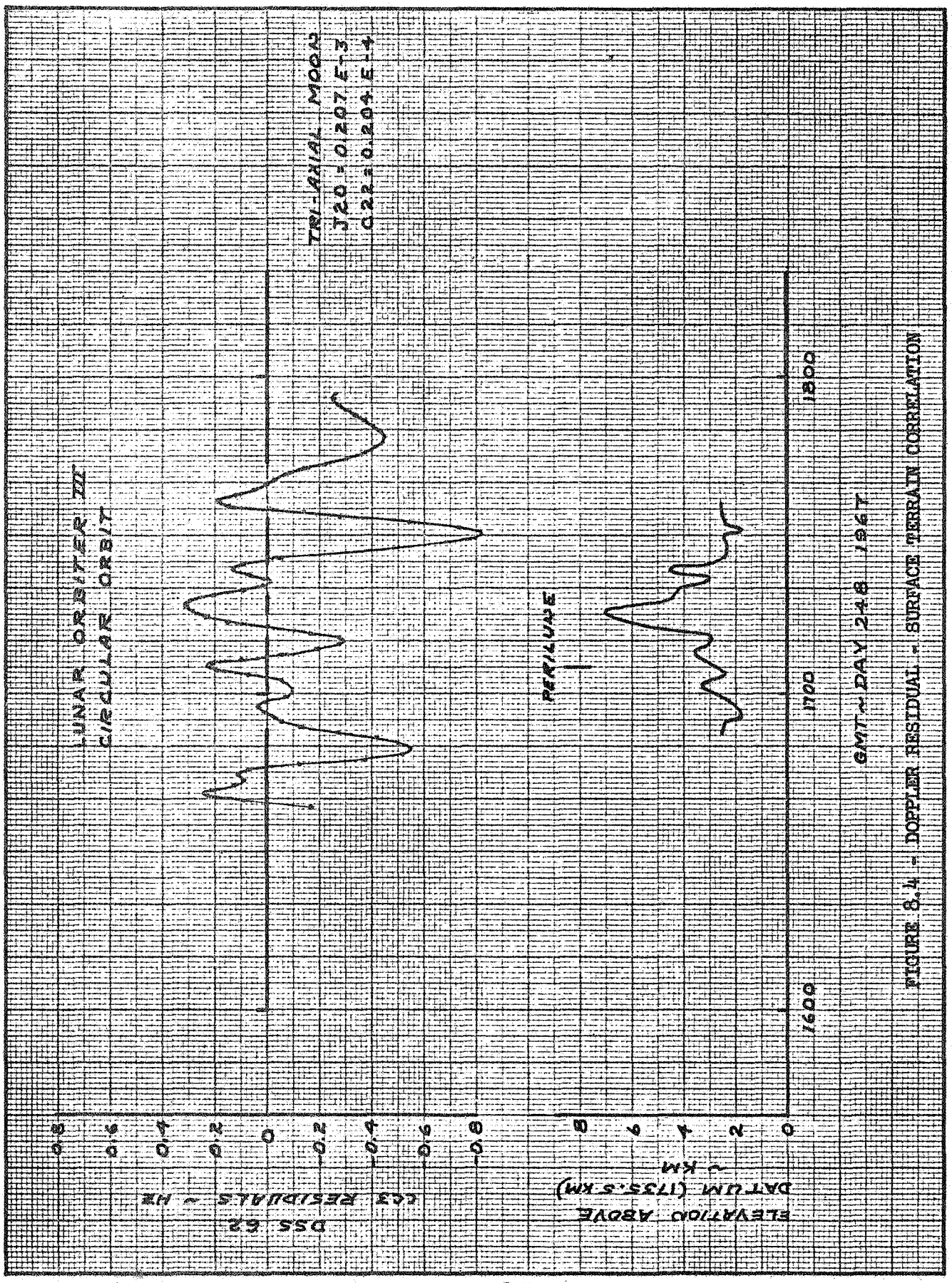

FIGURE 8.4 - DOPPLER RESIDUAL - SURFACE TERRAIN CORRELATION

9.0 REFERENCES

1. J. W. Cooley, J. W. Turey, "An Algorithm for the Machine Calculation of Complex Fourier Series," Mathematics of Computation, Vol. 19, 1965, pp. 297-301.

2. R. W. Sanneman, J. R. Rowbotham, "Unlock Characteristics of the Optimum Type II Phase-Locked Loop," IEEE Transactions on Aerospace and Navigational Electronics, March 1964.

3. R. Tansworthe, D. Sanger, "Experimental Study of the First-Slip Statistics of the Second-Order Phase-Locked Loop," JPL Space Program Summary 37-43, Vol. III, November 1 to December 31, 1966.

4. R. C. Tausworthe, "Cycle Slipping in Phase-Locked Loops," JPL Space Program Summary 37-42, Vol. IV, October 1 to November 30, 1966.

5. J. Lorell, W. L. Sjogren, "Lunar Orbiter Data Analysis," JPL Technical Report 32-1220, November 15, 1967.

6. Functional Specification, DFR-1001-FNC, "DSIF Tracking and Communication System, GSDS 1964 Model Receiver Subsystem," June 9, 1965, Jet Propulsion Laboratory.

7. M. F. Easterline, "Time-Synchronization System," Section 3, System Analysis, JPL Space Program Summary 37-42, Vol. IV, November 1 to December 31, 1966.

8. Kopak, Zdenek, "Physics and Astronomy of the Moon," Academic Press, New York and London, 1962.

9. J. P. Gapcynski, W. T. Blackshear, H. R. Compton, "The Lunar Gravitational Field As Determined From the Tracking Data of the Lunar Orbiter Series of Spacecraft," Paper presented at AAS/AIAA Astrodynamics Specialist Conference (Jackson, Wyoming), September 3-5, 1968.

10. P. M. Muller, "Consistency of Lunar Orbiter Residuals with Trajectory and Local Gravity Effects," Paper presented at AAS/AIAA Astrodynamics Specialist Conference (Jackson, Wyoming), September 3-5, 1968.

11. P.M. Muller, W. L. Sjogren, "Mascons: Lunar Mass Concentrations," Science, Vol. 161, No. 3842, August 16, 1968, pp 680-684.

USE FOR TYPEWRITTEN MATERIAL ONLY

U3 4802 1434 REV. 8-65

USE FOR TYPEWRITTEN MATERIAL ONLY

DISTRIBUTION LIST

NAS1-7954

	Copies each
NASA Langley Research Center Langley Station Hampton, Virginia 23365	
Attention: Research Program Records Unit, Mail Stop 122	1
Raymond L. Zavasky, Mail Stop 117	1
Wilbur L. Mayo, Mail Stop 159	1
I. G. Recant, Mail Stop 159	1
William H. Michael, Jr., Mail Stop 152A	1
Albert A. Schy, Mail Stop 152B	1
NASA Ames Research Center Moffett Field, California 94035 Attention: Library, Stop 202-3	1
NASA Flight Research Center P.O. Box 273 Edwards, California 93523	1
Jet Propulsion Laboratory 4800 Oak Grove Drive Pasadena, California 91103 Attention: Library, Mail 111-113	1
NASA Manned Spacecraft Center 2101 Webster Seabrook Road Houston, Texas 77058 Attention: Library, Code BM6	1
NASA Marshall Space Flight Center Huntsville, Alabama 35812 Attention: Library	1
NASA Wallops Station Wallops Island, Virginia 23337 Attention: Library	1
NASA Electronics Research Center 575 Technology Square Cambridge, Massachusetts 02139 Attention: Library	1
NASA Lewis Research Center 21000 Brookpark Road Cleveland, Ohio 44135 Attention: Library, Mail Stop 60-3	1

USE FOR TYPEWRITTEN MATERIAL ONLY

DISTRIBUTION LIST

NAS1-7954

	Copies each
NASA Goddard Space Flight Center Greenbelt, Maryland 20771 Attention: Library	1
NASA John F. Kennedy Space Center Kennedy Space Center, Florida 32899 Attention: Library, Code IS-CAS-42B	1
National Aeronautics and Space Administration Washington, D. C. 20546 Attention: Library, Code USS-10 L. Kosofsky, Code MAL	1 1
NASA Manned Spacecraft Center 2101 Webster Seabrook Raod Houston, Texas 77058 Attention: J. Sasser, Code TH3 W. R. Wollenhaupt, Code FM4	3 1
Army Map Service 6500 Brooks Lane Washington, D. C. 20315 Attention: D. Light, Code 12440 C. MacAfoos, Code 11910	1 1
Aeronautical Chart and Information Center 2nd and Arsenal Street St. Louis, Missouri 63118 Attention: C. F. Martin, ACDEG-2 R. Carder, ACO	1 1
National Space Science Data Cenyer Goddard Space Flight Center Greenbelt, Maryland 20771 Attention: K. Michlovitz, Code 601	50 plus reproducibles
Bellcomm, Inc. 995 L'Enfant Plaza North S.W. Washington, D. C. 20024 Attention: D. B. James	1
U. S. Geological Survey 345 Middlefield Road Menlo Park, California 94025 Attention: H. Masursky	2

DISTRIBUTION LIST

NAS1-7954

	Copies each
Dr. Donald Wise Department Department of Geology Franklin Marshall College Lancaster, Pennsylvania 17604	1
University of Arizona Tucson, Arizona 85721 Attention: Dr. G. P. Kuiper	1
Professor E. A. Whitaker	1
University of California P. O. Box 109 LaJolla, California 92037 Attention: Dr. H. C. Urey	1
NASA Scientific and Technical Information Facility P. O. Box 33 College Park, Maryland 20740	17

USE FOR TYPEWRITTEN MATERIAL ONLY